AD-A032 272 DAVID W TAYLOR NAVAL SHIP RESEARCH AND DEVELOPMENT CE--ETC F/G 13/10
LIFT AND DRAG CHARACTERISTICS OF NACA 16-309 AND NACA 64A309 HY--ETC(U)
OCT 76 D E LAYNE

UNCLASSIFIED SPD-326-07 NL

1 OF 2
AD A032 272

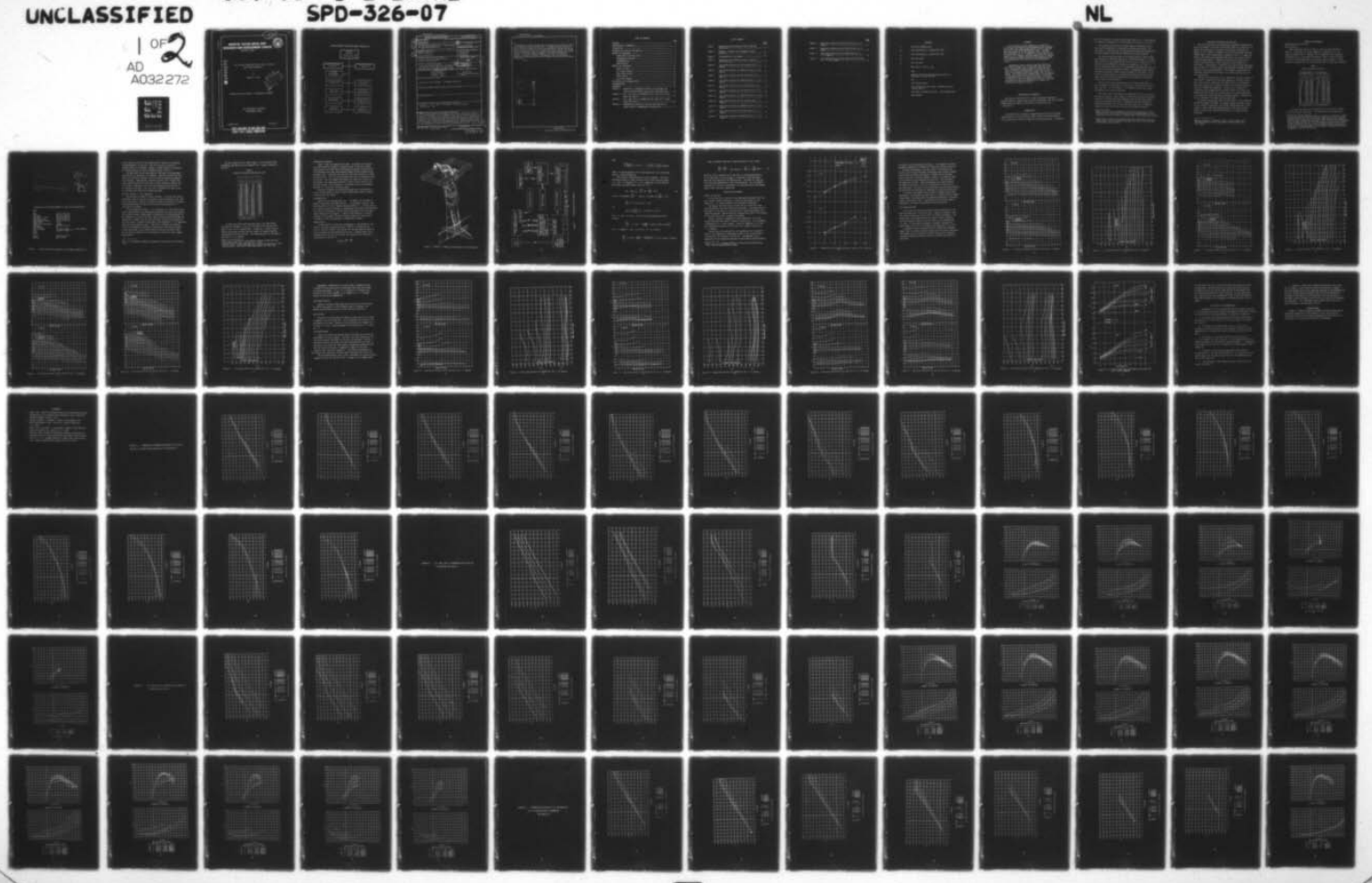

DAVID W. TAYLOR NAVAL SHIP RESEARCH AND DEVELOPMENT CENTER

Bethesda, Md. 20084

LIFT AND DRAG CHARACTERISTICS OF NACA 16-309 AND NACA 64A309 HYDROFOILS

by

Douglas E. Layne

SHIP PERFORMANCE DEPARTMENT

DEPARTMENTAL REPORT

OCTOBER 1976 SPD-326-07

SPD-326-07

LIFT AND DRAG CHARACTERISTICS OF NACA 16-309 AND NACA 64A309 HYDROFOILS

MAJOR DTNSRDC ORGANIZATIONAL COMPONENTS

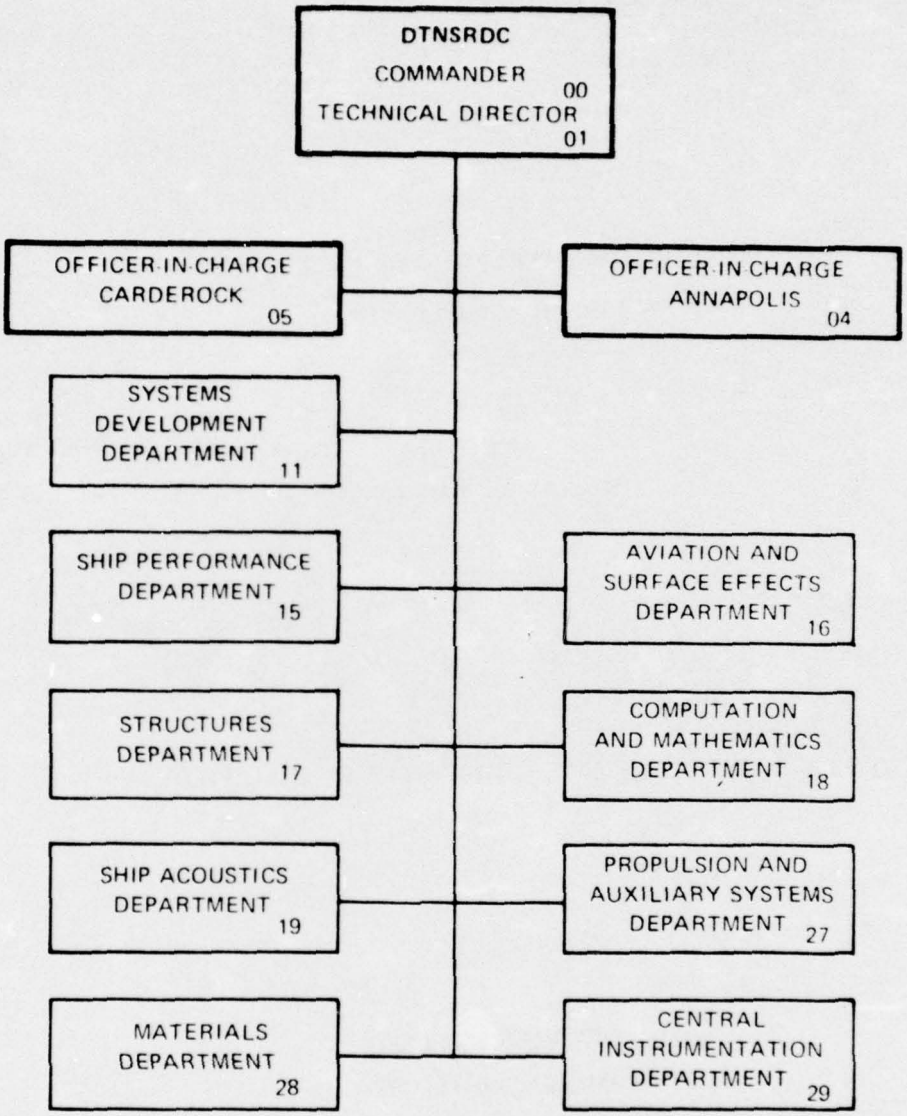

UNCLASSIFIED

SECURITY CLASSIFICATION OF THIS PAGE (When Data Entered)

REPORT DOCUMENTATION PAGE

READ INSTRUCTIONS BEFORE COMPLETING FORM

1. REPORT NUMBER: SPD-326-07	2. GOVT ACCESSION NO.
3. RECIPIENT'S CATALOG NUMBER	
4. TITLE (and Subtitle): LIFT AND DRAG CHARACTERISTICS OF NACA 16-309 AND NACA 64A309 HYDROFOILS.	5. TYPE OF REPORT & PERIOD COVERED: Final rept.,
	6. PERFORMING ORG. REPORT NUMBER
7. AUTHOR(s): Douglas E. Layne	8. CONTRACT OR GRANT NUMBER(s): 1-1153-503-30, 1-1153-603-33, 1-1153-603-34
9. PERFORMING ORGANIZATION NAME AND ADDRESS: David W. Taylor Naval Ship R&D Center, Bethesda, Maryland 20084	10. PROGRAM ELEMENT, PROJECT, TASK AREA & WORK UNIT NUMBERS: Task Area SSH6001
11. CONTROLLING OFFICE NAME AND ADDRESS: Systems Development Department, Advanced Hydrofoil Systems, Office, David W. Taylor Naval Ship R&D Center, Bethesda, Maryland 20084	12. REPORT DATE: October 1976
	13. NUMBER OF PAGES: 91
14. MONITORING AGENCY NAME & ADDRESS(if different from Controlling Office) 98 p.	15. SECURITY CLASS. (of this report): UNCLASSIFIED
	15a. DECLASSIFICATION DOWNGRADING SCHEDULE

16. DISTRIBUTION STATEMENT (of this Report)

APPROVED FOR PUBLIC RELEASE: DISTRIBUTION UNLIMITED

17. DISTRIBUTION STATEMENT (of the abstract entered in Block 20, if different from Report)

18. SUPPLEMENTARY NOTES

19. KEY WORDS (Continue on reverse side if necessary and identify by block number)

Hydrofoil, Lift, Drag, Cavitation, Flap Effectiveness, NACA Section, PCH

20. ABSTRACT (Continue on reverse side if necessary and identify by block number)

Lift and drag data were obtained by the David W. Taylor Naval Ship Research and Development Center (DTNSRDC) for two NACA foil shapes geometrically similar to the forward foil system of the PCH hydrofoil craft. The NACA foil shapes were the 16-309 (presently used on PCH) and a modified 64A309 section. Information was obtained for flap angles up to 17.5 degrees and pitch angles up to 12 degrees. There was good agreement between similar measurements made in the High-Speed Tow Facility and in the Rotating Arm Facility.

DD FORM 1 JAN 73 1473 EDITION OF 1 NOV 65 IS OBSOLETE S/N 0102-014-6601

UNCLASSIFIED

SECURITY CLASSIFICATION OF THIS PAGE (When Data Entered)

Experimental results indicate that the 64A309 foil can achieve a higher lift-to-drag ratio than the 16-309 foil. Although the angle of pitch at which cavitation inception occurred was approximately the same for the two foils, the inception occurred at a higher lift for the 64A309. The 64A309 section produced more lift with changes in flap angles than did the 16-309 section. Flap effectiveness decreases at the larger flap angles as velocity is increased. Depth of submergence of the foils noticeably influenced lift and drag, particularly at depths less than one chord length of the foil.

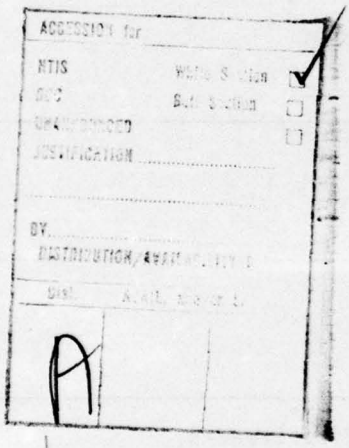

TABLE OF CONTENTS

LIST OF FIGURES

NOTATION

A	Total foil planform area
C_D	Drag coefficient $C_D = (\text{drag})/(\frac{1}{2}\rho V^2 A)$
C_L	Lift coefficient $C_L = (\text{lift})/(\frac{1}{2}\rho V^2 A)$
C_R	Foil root chord
C_T	Foil tip chord
c	Mean chord $= (\frac{1}{2})(C_T + C_R)$
D	Drag
h	Depth of foil below undisturbed free surface at one-fourth of chord for foil
L	Lift
V	Free-stream velocity
α	Foil incidence or pitch angle in degrees (positive - leading edge up)
δ	Flap angle in degrees (positive - trailing edge down)
ρ	Water density

ABSTRACT

Lift and drag data were obtained by the David W. Taylor Naval Ship Research and Development Center (DTNSRDC) for two NACA foil shapes geometrically similar to the forward foil system of the PCH hydrofoil craft. The NACA foil shapes were the 16-309 (presently used on PCH) and a modified 64A309 section. Information was obtained for flap angles up to 17.5 degrees and pitch angles up to 12 degrees. There was good agreement between similar measurements made in the High-Speed Tow Facility and in the Rotating Arm Facility.

Experimental results indicate that the 64A309 foil can achieve a higher lift-to-drag ratio than the 16-309 foil. Although the angle of pitch at which cavitation inception occurred was approximately the same for the two foils, the inception occurred at a higher lift for the 64A309. The 64A309 section produced more lift with changes in flap angles than did the 16-309 section. Flap effectiveness decreases at the larger flap angles as velocity is increased. Depth of submergence of the foils noticeably influenced lift and drag, particularly at depths less than one chord length of the foil.

ADMINISTRATIVE INFORMATION

This work was sponsored by the Systems Development Department, Advanced Hydrofoil Systems Office, and was funded under Task Area SS H6001, DTNSRDC Work Unit Numbers 1-1153-503-30, 1-1153-603-33, and 1-1153-603-34.

INTRODUCTION

The objective was to obtain a large data base on the lift and drag characteristics of the forward foil (NACA 16-309) of the PCH hydrofoil craft, particularly from the standpoint of flap effectiveness. Information

was to be obtained at a depth-to-chord (h/c) ratio of 1.0. This amounted to a depth of submergence of 125 millimeters to the center of the foil.

The original plan had been to obtain data at velocities up to 50 knots and flap angles up to 20 degrees at various pitch angles. Unfortunately, it was impossible to meet this goal because of limitations in the existing model of the PCH foil employed in the investigation.

The existing 1/8-scale model of the forward PCH foil (NACA 16-309) was designed for conducting experiments with Froude scaling (i.e., experimental velocities were approximately one-third of full scale), and it had originally been intended for evaluation at speeds up to 25 knots. A problem immediately arose when it was determined that model velocities for the present study would approach 50 knots. A subsequent stress analysis showed that the model strength would be marginal at that speed. In the interest of time, however, it was decided to proceed with the existing model, and restrictions were imposed on the flap angle to be used for various speeds and pitch angles.

Since the data base would obviously be less broad than hoped, it was also decided to complement the information it provided by constructing a new foil. The NACA 64A309, a = 8 (modified) section was chosen and adapted to the existing PCH strut.

Both foils were investigated in the High-Speed Tow Facility and the Rotating Arm Facility. When a model is towed in a circular path through calm water, noticeable waves are produced after the model has traveled through its own wake a few times. Although this was not expected to significantly affect* the lift and drag characteristics, it seemed advisable to obtain data in both facilities for comparison purposes.

---

* Nelka[1] had found little difference in side force characteristics when a NACA 16-012 foil was towed in calm water in a straight channel of the High-Speed Tow Facility and in a circular path at the Rotating Arm Facility.

[1] Nelka, John., "Effects of Mid-Chord Flaps on the Ventilation and Force Characteristics of a Surface-Piercing Hydrofoil Strut," Naval Ship R&D Center Report 4508 (Nov 1974).

RATIONALE FOR CHOICE OF THE NEW FOIL

The 16-309 wing section has unfavorable separation characteristics which are inherent in the NACA 1-Series from which it was derived.[2] At design lift coefficient, the suction side pressure distribution of members of the 1-Series is intended to be as flat as possible from the leading edge to the trailing edge, as implied by the a = 1.0 mean line. Ideally, this pressure distribution would result in the most lift for a given minimum pressure. Therefore, the cavitation inception and critical speeds would be as high as possible at the design lift coefficient. Unfortunately, in practice, the large trailing edge angle used to achieve the required pressure distribution encourages premature turbulent trailing edge separation. This tendence is aggravated for off-design conditions which creates a very narrow operating range of lift coefficients.

Because of the likelihood of tail separation, the effectiveness of flaps would be expected to be poor when applied to 1-Series sections. Use of the 6-Series, typified by the 64A309 section, is considered preferable because of its greater tolerance for off-design conditions with less tendency for separation. In part, this is achieved by concentrating the minimum pressure further forward; this allows the pressure recovery of the tail to take place over a greater proportion of the chord and lessens the adverse pressure gradient. Geometrically, this is reflected in a sharper trailing edge angle.

The larger leading edge radius of the 6-Series is also related to the greater design lift range. The larger leading edge radii typical of the 6-Series in contrast to the smaller leading edge radii of the 1-Series, creates less sharp pressure peaks at smaller off-design angles of attack; this decreases susceptibility to separation and cavitation.

---

[2] Hoerner, Sighard, F. and Henry V. Borst, "Fluid Dynamic Lift," published privately by Mrs. Liselotte A. Hoerner, Brick Town, N.J. (1975).

METHOD AND PROCEDURES

DESCRIPTION OF THE TWO FOILS

NACA 16-309 Foil

Model dimensions for the 16-309 foil and strut are presented in Figure 1. The 16-309 section was adapted to a meanline a=1.0. The angle of incidence was 1.3 degrees, but (as explained later) data were corrected to give a zero angle of incidence. Table 1 contains offsets for the foil, and definitions of X and Y are given in Figure 1. These values were obtained from the existing model since no plans were available.

TABLE 1

Offsets for NACA 16-309 Foil

ROOT CHORD OFFSETS			TIP CHORD OFFSETS		
X (% c)	Y_u (% c)	Y_L (% c)	X (% c)	Y_u (% c)	Y_L (% c)
0	0	0	0	0	0
0.5	0.76	-0.58	0.5	0.76	-0.61
1.25	1.13	-0.81	1.25	1.12	-0.81
2.5	1.64	-1.08	2.5	1.62	-1.07
5.0	2.36	-1.41	5.0	2.34	-1.42
7.5	2.91	-1.64	7.5	2.90	-1.62
10	3.36	-1.82	10	3.35	-1.83
15	4.11	-2.10	15	4.11	-2.08
20	4.69	-2.30	20	4.67	-2.28
25	5.16	-2.46	25	5.13	-2.49
30	5.52	-2.60	30	5.54	-2.59
40	5.99	-2.78	40	5.99	-2.79
50	6.16	-2.84	50	6.14	-2.84
60	5.98	-2.77	60	5.99	-2.79
70	5.41	-2.49	70	5.38	-2.49
80	4.34	-1.96	80	4.32	-1.93
90	2.67	-1.12	90	2.64	-1.12
95	1.54	-0.58	95	1.52	-0.56
100	0.09	-0.09	100	0.10	-0.10
L.E. radius:0.39 % c			L.E. radius:0.41 %c		

The model flap mechanism was modified* to give a positive locking system for discrete flap angles. The wooden pod at the intersection

*The existing locking mechanism relied on friction and although it seemed to work satisfactorily for low (20 knot) velocities and low (8 degrees) angle of pitch, it was unable to hold the flap angle for the velocities and pitch angles planned for the present study. During earlier experiments in the Rotating Arm Facility, the foil separated from the strut on two occasions, and the series was cancelled without yielding reliable data. On the basis of that experience, it was decided to redesign the method of attachment of the foil to the strut.

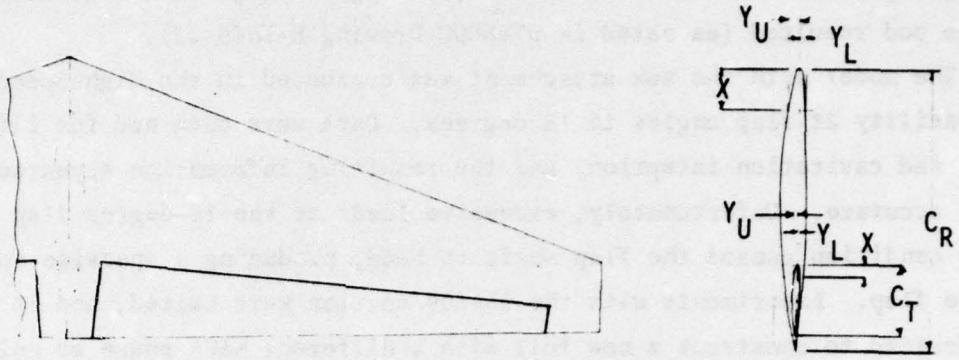

Dimensions of 16-309 and 64A309 Foil and Strut Configurations

Foil

Span	762 mm (2.50 ft)
1/2 Span	381 mm (1.25 ft)
Root Chord (C_R)	200 mm (0.656 ft)
Tip Chord (C_T)	50 mm (0.164 ft)
Mean Geometric Chord	125 mm (0.410 ft)
Taper Ratio	0.25
Sweep of 1/4 Chordline	15 deg
Flap Span	648 mm (2.125 ft)
Percent Flap	25
Foil incidence	1.3 deg (16309) 0 deg (64A309)
Area	0.095 m^2 (1.025 ft^2)

Strut

Chord	162 mm (0.53 ft)
Section	NACA 16-012

Figure 1 - Sketch and Overall Dimensions for 16-309 and 64A309 Foils

of the strut with the foil was replaced with a larger one of aluminum fixed permanently to the strut. The net effect was to provide a stronger point for attachment; however, a slight change in the geometry of the pod resulted (as noted in DTNSRDC Drawing E-1646-22).

The model with the new attachment was evaluated in the High-Speed Tow Facility at flap angles to 15 degrees. Data were obtained for lift, drag, and cavitation inception, and the resulting information appeared to be accurate. Unfortunately, excessive loads at the 15-degree flap angle condition caused the flap shaft to bend, producing a spanwise bow in the flap. Experiments with the 16-309 section were halted, and it was decided to construct a new foil with a different NACA shape as well as to devise a new method for setting flap angle.

NACA FOIL 64A309, a = 0.8 (modified)

The new model was made of 7075-T6 aluminum. It has the same overall dimensions as the 16-309 foil (see Figure 1) and was attached to the strut by the same method. Because the 64A309 foil had a zero angle of incidence, data presented herein for the 16-309 foil have been corrected to a zero angle of incidence.

In the designation 64A309, a = 0.8 (modified), the first digit is the series identification, the second digit represents the distance (in tenths) of the chord from the leading edge to the position of minimum pressure for the symmetrical section at zero lift, the third digit gives the design lift coefficient in tenths, and the final two digits indicate the thickness of the wing section in percent of the chord. The designation a = 0.8 (modified) shows the type of meanline used.* The letter A indicates (1) that the section is substantially straight on both surfaces from about 80 percent of the chord length to the trailing edge for the basic thickness form, and (2) that the cusped tail of the section is filled up so that a wedge shape results.

---

*The a = 0.8 (modified) meanline is designed to be used with the 6A-Series foil.

The foil offsets for the 64A309 (Table 2) were obtained using information from Abbott and Von Doenhoff[3] and a computer program by Brockett.[4]

TABLE 2

Offsets for NACA 64A309 Modified Foil

X_u (% c)	Y_u (% c)	X_L (% c)	Y_L (% c)
0	0	0	0
0.40	0.816	.60	-0.647
0.63	1.003	.87	-0.766
1.12	1.301	1.38	-0.939
2.35	1.842	2.65	-1.209
4.83	2.643	5.17	-1.561
7.32	3.266	7.68	-1.807
9.82	3.787	10.18	-1.998
14.83	4.630	15.17	-2.272
19.84	5.273	20.16	-2.456
24.86	5.745	25.14	-2.591
29.89	6.094	30.11	-2.649
34.91	6.314	35.09	-2.642
39.94	6.408	40.06	-2.571
44.97	6.335	45.04	-2.393
49.99	6.131	50.01	-2.141
55.02	5.815	54.98	-1.837
60.04	5.404	59.96	-1.499
65.05	4.908	64.95	-1.143
70.07	4.334	69.93	-0.786
75.07	3.688	74.92	-0.447
80.08	2.964	79.92	-0.160
85.08	2.148	84.92	0.016
90.04	1.345	89.96	0.126
95.02	0.594	94.98	0.141
100.00	0	100.00	0
L.E. radius: 0.55 percent c			

To reduce the load on the flap pivot point, the flap-locking mechanism was designed as a pin lock anchored in the flap trailing edge as well as to its leading edge. In addition, a center hinge was added to help carry the flap load and prevent the spanwise bending experienced with the 16-309 foil. This mechanism provided flap angles from zero to 17 1/2 degrees.

---

[3] Abbot, Ira H. and Albert E. Von Doenhoff, "Theory of Wing Sections," Dover Publications, Inc., New York, N.Y. (1959).

[4] Brockett, Terry, "Steady Two-Dimensional Pressure Distributions on Arbitrary Profiles," David Taylor Model Basin Report 1821 (Oct 1965).

EXPERIMENTAL APPARATUS

Figure 2 shows the experimental setups. The models were attached to a pitch mechanism designed to remotely sweep or step pitch angles. A BLH angulator provided digital monitoring and readout of pitch angle. Two 2000-pound force gages were mounted between the pitch mechanism and the model strut. Since the strut and foil were thus treated as a system, the data contain lift (if any) and drag of the strut in addition to that of the foil. The force gages were mounted in a plane that varied with pitch angle, thus requiring resolution of force to give values of lift and drag relative to the horizontal. The design of the pitch mechanism resulted in a varying h/c with pitch angle.

Cavitation inception was monitored through video instrumentation. A split screen method was used to obtain correlations between incipient cavitation and pitch angle.

INSTRUMENTATION

Digitized force gage and angle indicator signals were recorded on magnetic tape along with model velocity. Data recorded on magnetic tape were processed on-line by computer (Interdata Model 70). The scan rate of the analog to digital converted was approximately 100 samples/second/channel. The forces were averaged to obtain discrete data points while the model swept through the pitch angles. A check of data obtained at discrete intervals (static angles of pitch) yielded virtually the same results. A schematic of the instrumentation is presented in Figure 3.

ERROR ANALYSIS

An error analysis of the force coefficients is now presented. The error in lift due to calibration error is $\frac{dL}{L}$ of 0.5 percent and the error in velocity is $\frac{dV}{V}$ of 0.625 percent for the High-Speed Tow Facility and 1.25 percent for the Rotating Arm Facility. Assuming density and planform area of the foil to be exact, the expression for error due to calibration and velocity is:

$$d(C_L)_{\alpha=0} = \frac{dL}{L} - \frac{2dV}{V} \qquad [1]$$

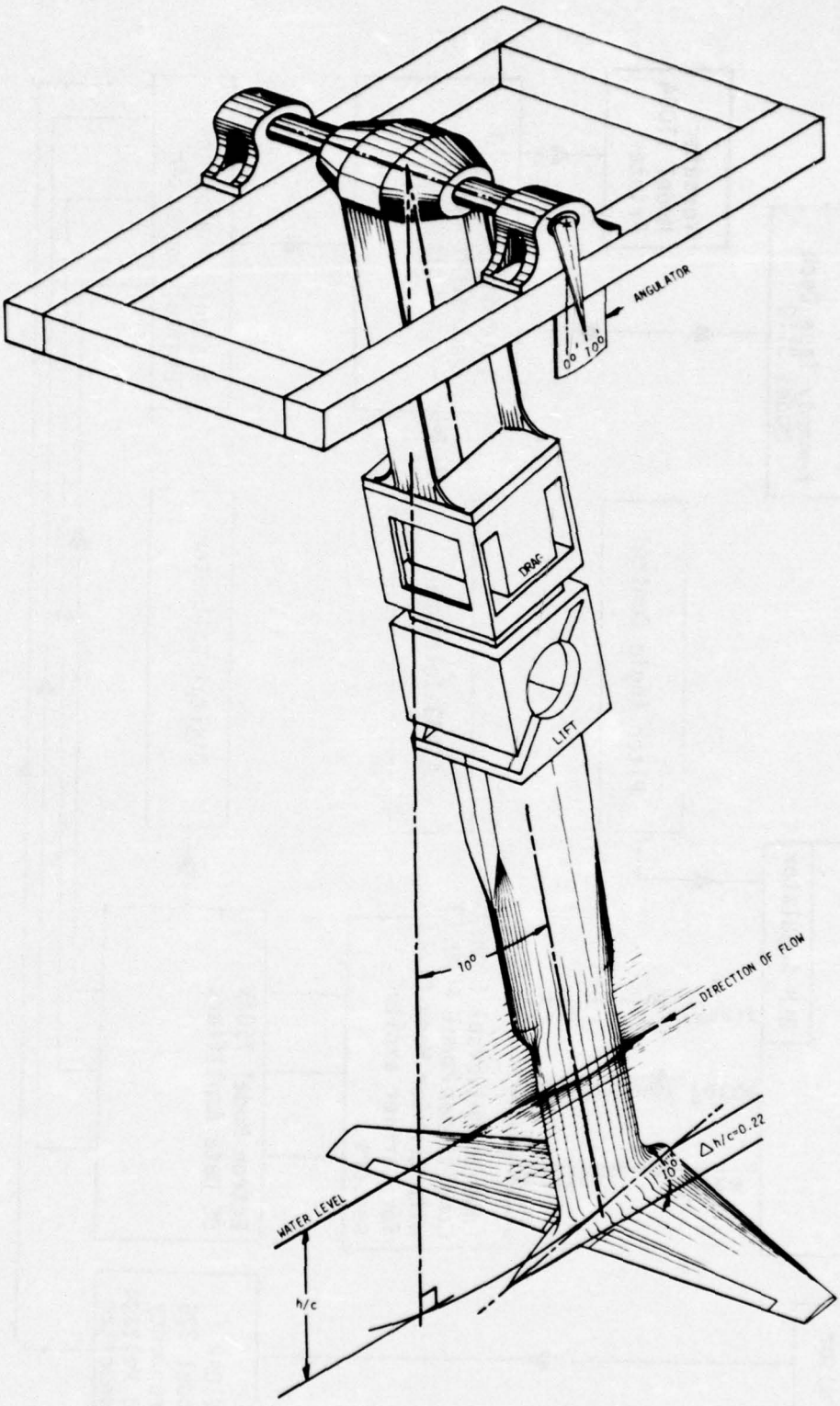

Figure 2 - Schematic of Model with Attachment to Pitch Mechanism

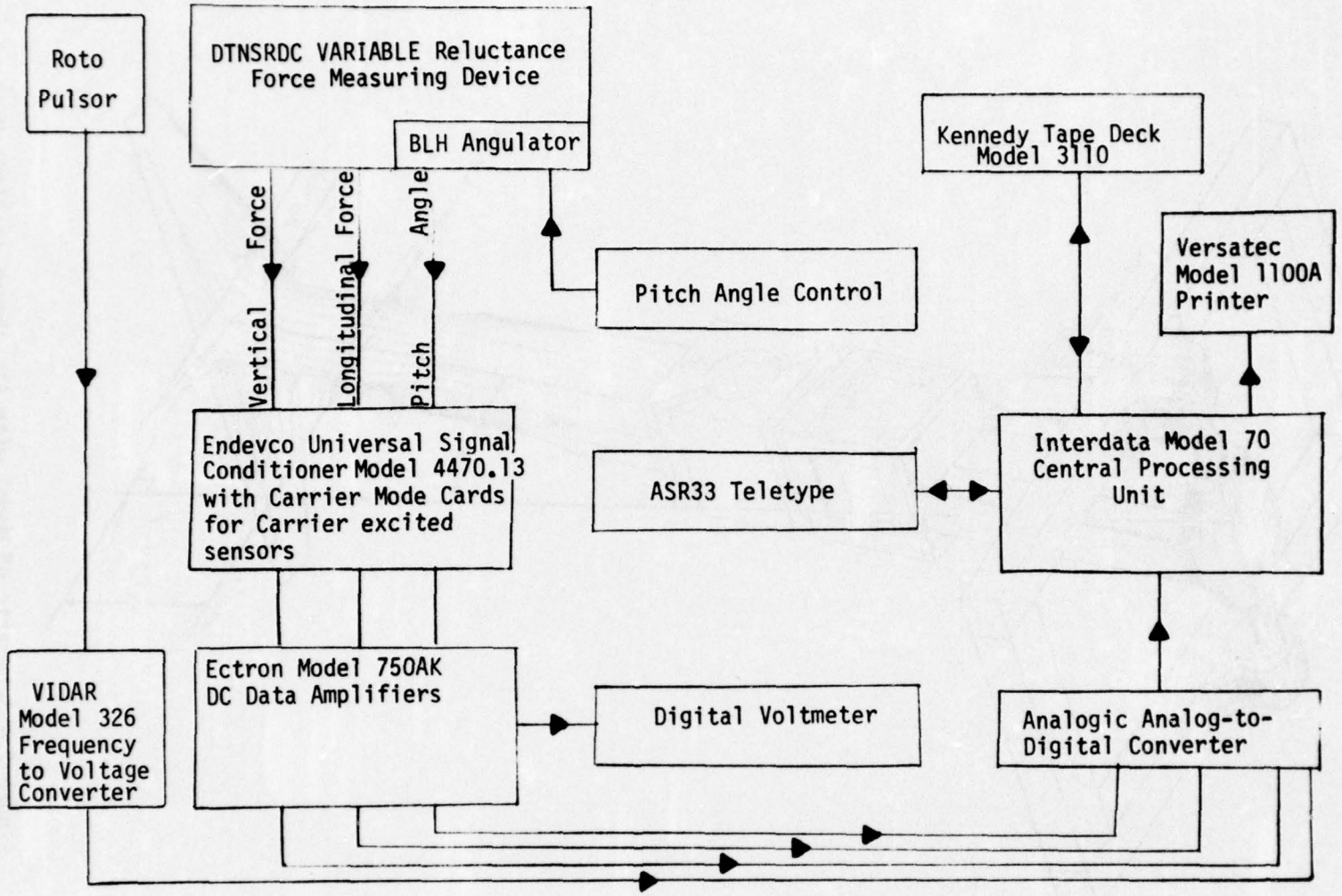

Figure 3 - Instrumentation Flow Diagram

then

$$\left|\frac{d(C_L)_{\alpha=0}}{C_L}\right| \leq \left|0.05\right| + 2\left|\begin{matrix}0.625\\1.25\end{matrix}\right| = \left|\begin{matrix}1.75\\3.00\end{matrix}\right| \text{ percent}$$

where 1.75 percent pertains to the High-Speed Basin and 3.00 percent pertains to the Rotating Arm.

Pitch angles α were measured within ± 0.05 degrees. The pitch mechanism produced a slight variation in h/c ratio with pitch angle; i.e., for α = 10 degrees, h/c = 0.22. Combining (1) with terms for pitch angle and depth change yields for lift:

$$dC_L = d(C_L)_{\alpha=0} + \frac{\partial C_L}{\partial \alpha}\, d\alpha + \frac{\partial C_L}{\partial h/c}\, d\, h/c \qquad [2]$$

For $d\alpha$ = 0.05 degrees, $\frac{\partial C_L}{\partial \alpha} \simeq 2\pi$/rad or $\simeq$ 0.1/deg, and $\frac{\partial C_L}{\partial h/c} \simeq 0.01$,

$$\frac{\partial C_L}{\partial \alpha}\, d\alpha \simeq (0.1)\ (0.05) \simeq 0.005$$

and

$$\left|dC_L\right| \leq \begin{matrix}0.0175\\0.0300\end{matrix} \left|C_L\right| + \left|0.005\right| + \left|0.01\ \Delta h/c\right|$$

For α = 0, $\Delta h/c$ = 0 and C_L + 0.122 in the High Speed Basin and at 15 knots,

$$\frac{\left|dC_L\right|}{C_L} \leq 0.0175 + \frac{0.005}{0.122} = 0.0585 \text{ or about 6 percent}$$

For α = 10 degrees, $\Delta h/c$ = 0.22 for C_L = 0.7 at 25 knots

$$\frac{\left|dC_L\right|}{C_L} = 0.0175 + \frac{0.005}{0.7} + \frac{(0.01)\ 0.22}{0.7} = 0.0277 \text{ or about 3 percent}$$

Drag is primarily made up of induced drag due to lift so that

$$\frac{dC_D}{C_D} \simeq \frac{2dC_L}{C_L} = \frac{2}{C_L}\left[d(C_L)_{\alpha=0} + \frac{\partial C_L}{\partial \alpha}\, d\alpha + \frac{\partial C_L}{\partial h/c}\, dh/c\right] \qquad [3]$$

The first term in equation [3] is the error in the drag gage which is of the same order as the lift gage (1.75 percent for the High Speed Basin and 3.00 percent for the Rotating Arm). The other two terms are twice the error experienced in the lift measurement. For the examples presented for lift error calculations, the drag coefficient then becomes about 10 and 4 percent, respectively.

RESULTS AND DISCUSSION

QUALITY OF THE DATA

On the basis of an overview of the information obtained on the two foil sections, greater confidence is placed in the results for the 64A309 foil. It yielded smoother, more repeatable information.

The smaller confidence placed in data for the 16-309 foil stems from the problems that arose during the experiment, as mentioned earlier. The quality of the data for the 16-309 foil is considered adequate for comparison purposes, despite questions regarding the effect of the bending of the flap of that foil at higher pitch angles.

Figure 4 contains a comparison of data obtained for the 16-309 section with that from Jones[5] of data on a similar foil. The information is presented for $\alpha = 0$ and 2 degrees. From this comparison, it is felt that information obtained for the 16-309 foil is good at least up to $\delta = 10$ degrees.

Because data on the 64A309 foil are considered to be of superior quality, the comparison of measurements taken in the two facilities is discussed only with reference to that foil. See Appendix A for a comparison of the information obtained for the 64A309 in the High-Speed

[5] Jones, C.E., Jr., "Flapped Hydrofoils in Smooth Water Subcavitating Flow," General Dynamics/Convair Report

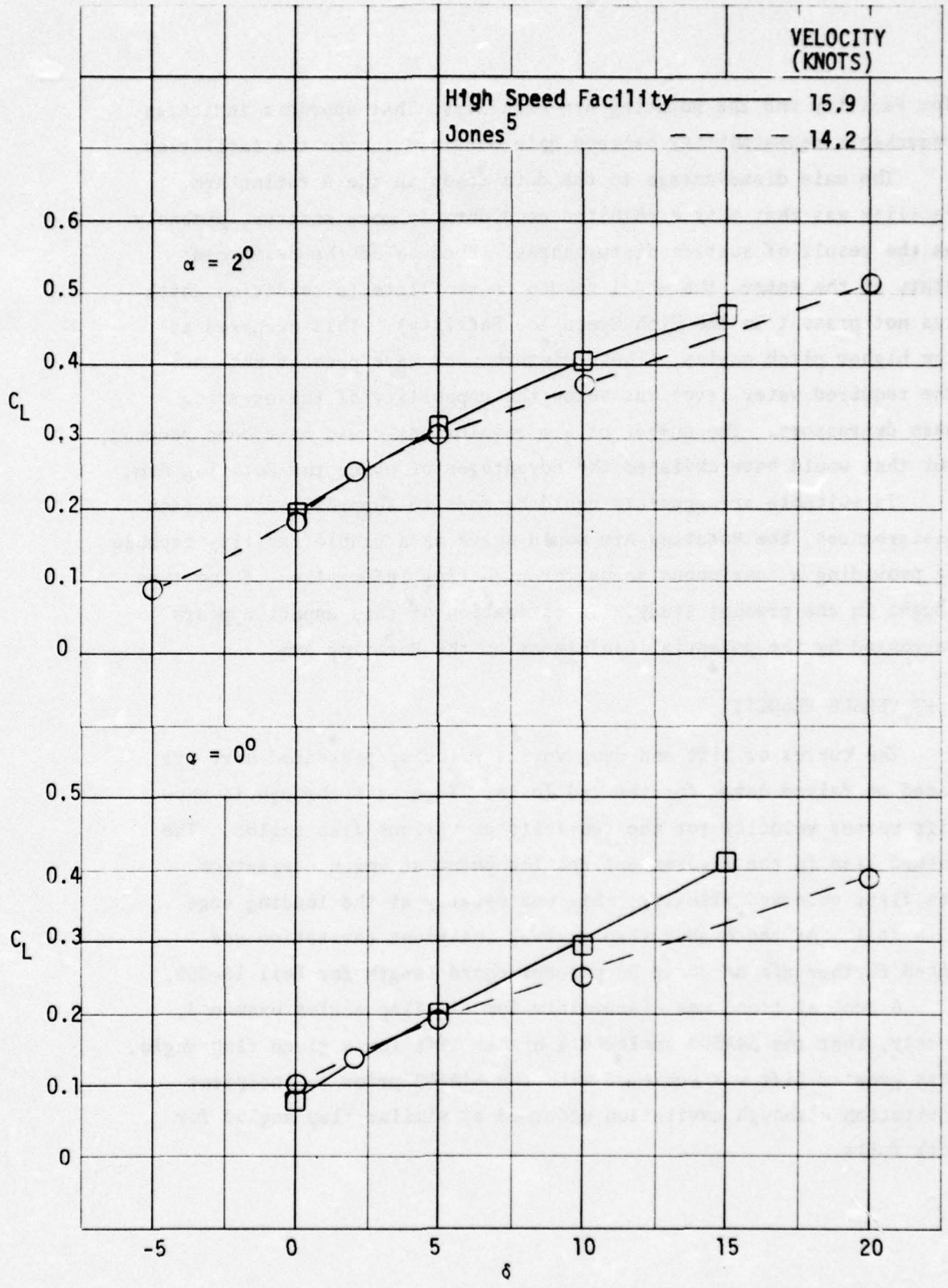

Figure 4 - Comparison of Two Sources of Data C_L versus δ for 16-309 Foil

Tow Facility and the Rotating Arm Facility. That appendix indicates remarkable repeatability between data obtained in the two facilities.

The main disadvantage to the data taken in the Rotating Arm Facility was that they exhibited considerably more scatter, probably as the result of surface disturbances. Because of the disturbed state of the water, the model tended to ventilate (a condition which was not present in the High-Speed Tow Facility). This occurred at the higher pitch angles. These disturbances were present because the required water level was below the capability of the existing wave depressors. The number of arm revolutions could have been reduced, but that would have obviated the advantages of using the Rotating Arm.

If suitable arrangements could be made to suppress such surface disturbances, the Rotating Arm would serve as a viable facility capable of providing a continuous means for gathering information of the type sought in the present study. Investigation of this aspect appears warranted by the potential usefulness of the Rotating Arm.

LIFT VERSUS VELOCITY

The curves of lift and drag versus velocity presented here are based on faired data for the two foils. Figures 5 through 11 show lift versus velocity for the two foils at various flap angles. The dashed line in the figures defines the point at which cavitation was first observed visually; this was usually at the leading edge of a foil. At the higher flap angles, incipient cavitation was noted further aft at 30 to 50 percent chord length for Foil 16-309.

A general trend was discernible for all flap angles examined, namely, that the 64A309 achieved a higher lift for a given flap angle. This greater lift was achieved with the 64A309 prior to incipient cavitation although cavitation occurred at similar flap angles for both foils.

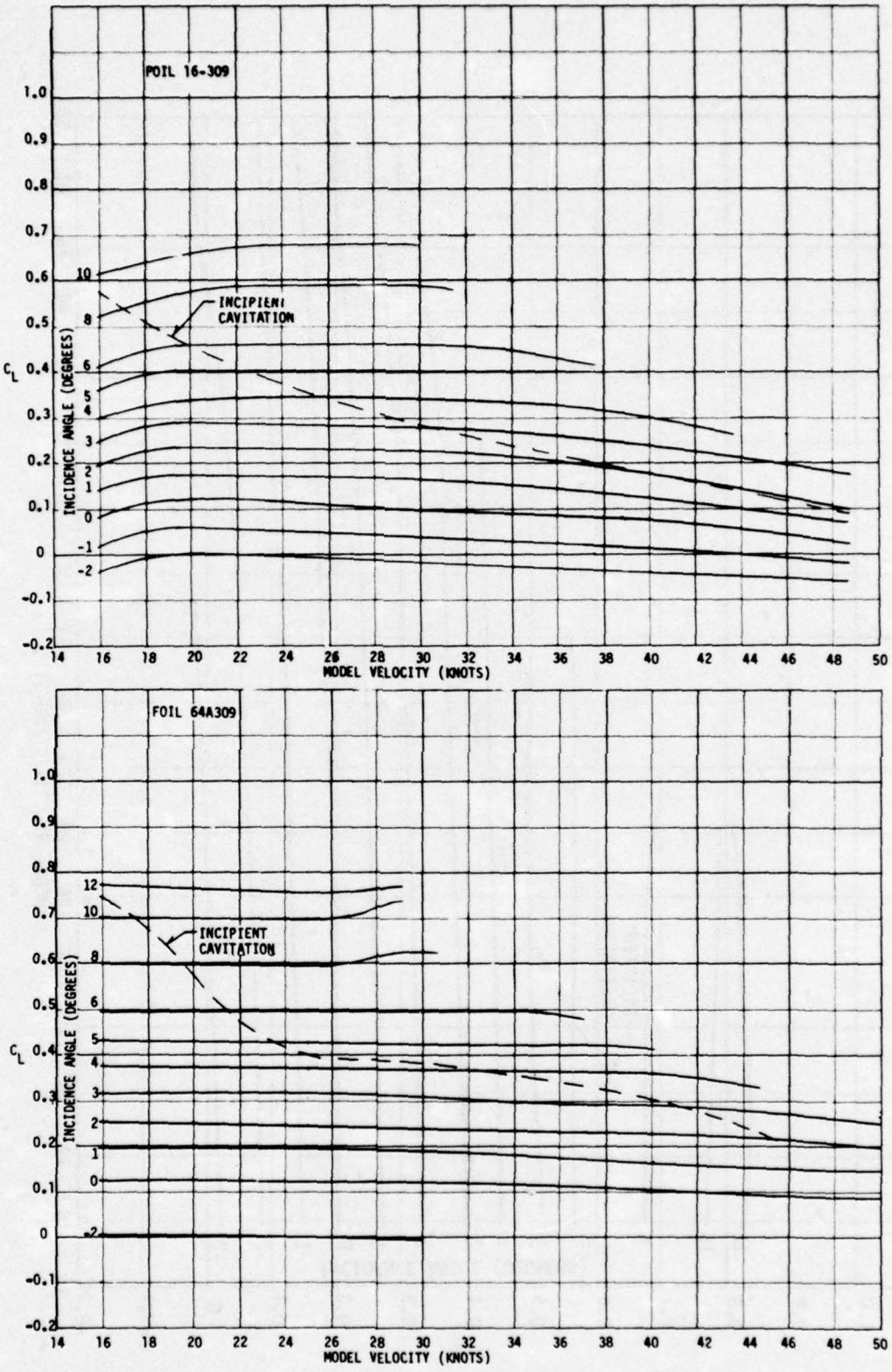

Figure 5 - Lift versus Velocity for the Two Foils for δ = 0 Degree

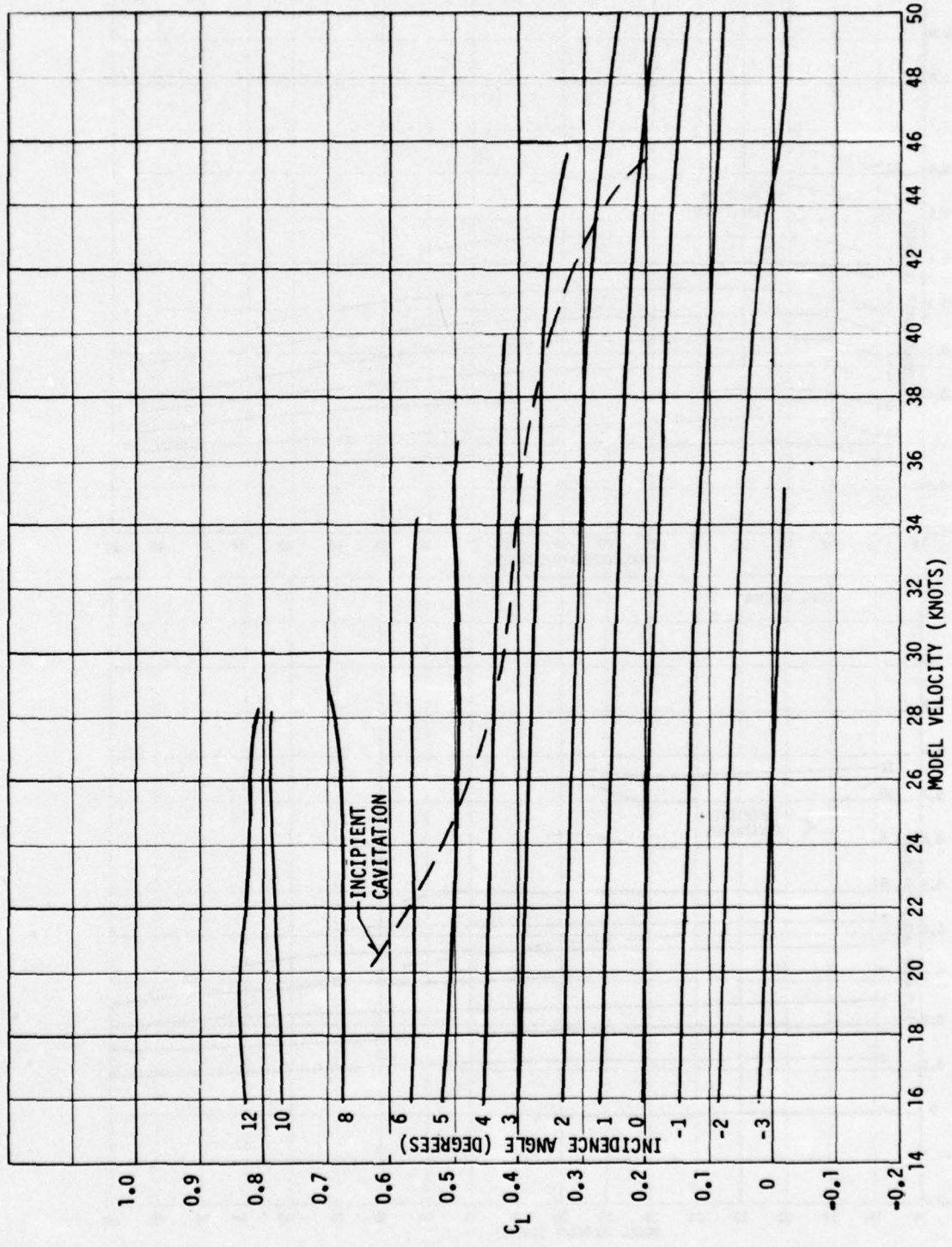

Figure 6 - Lift versus Velocity for 64A309 Foil for δ = 2½ Degrees

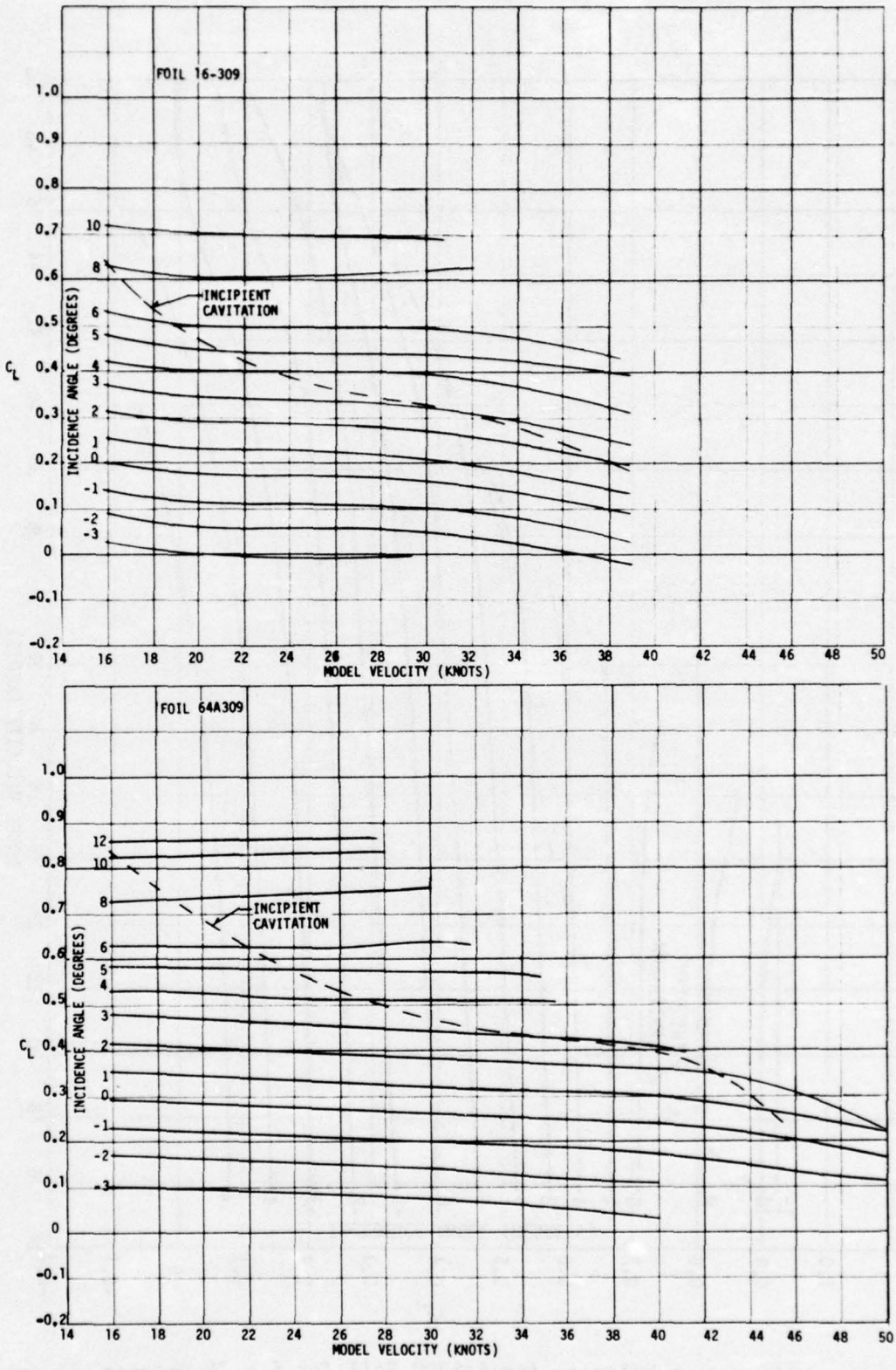

Figure 7 - Lift versus Velocity for the Two Foils for δ = 5 Degrees

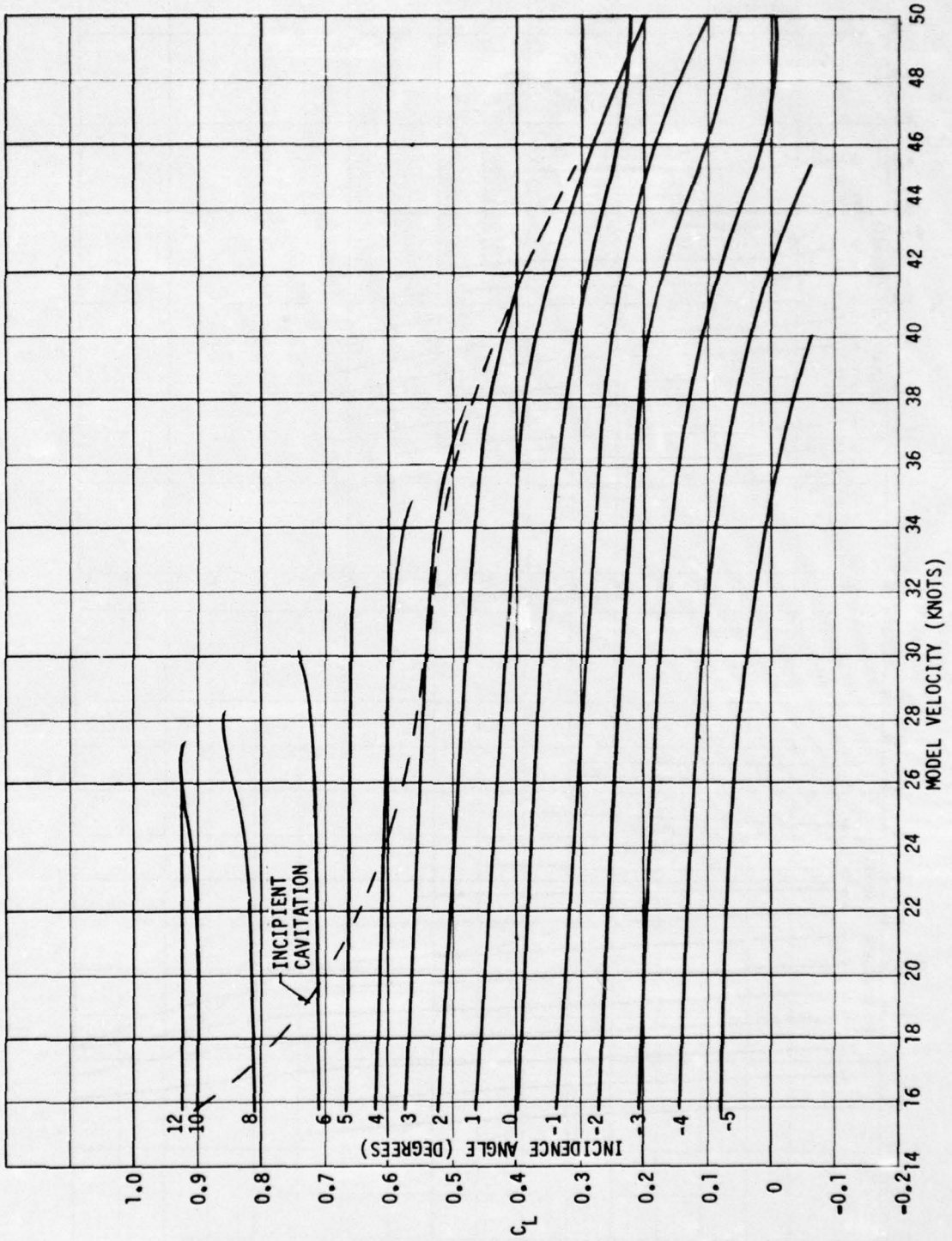

Figure 8 - Lift versus Velocity for 64A309 Foil for δ = 7½ Degrees

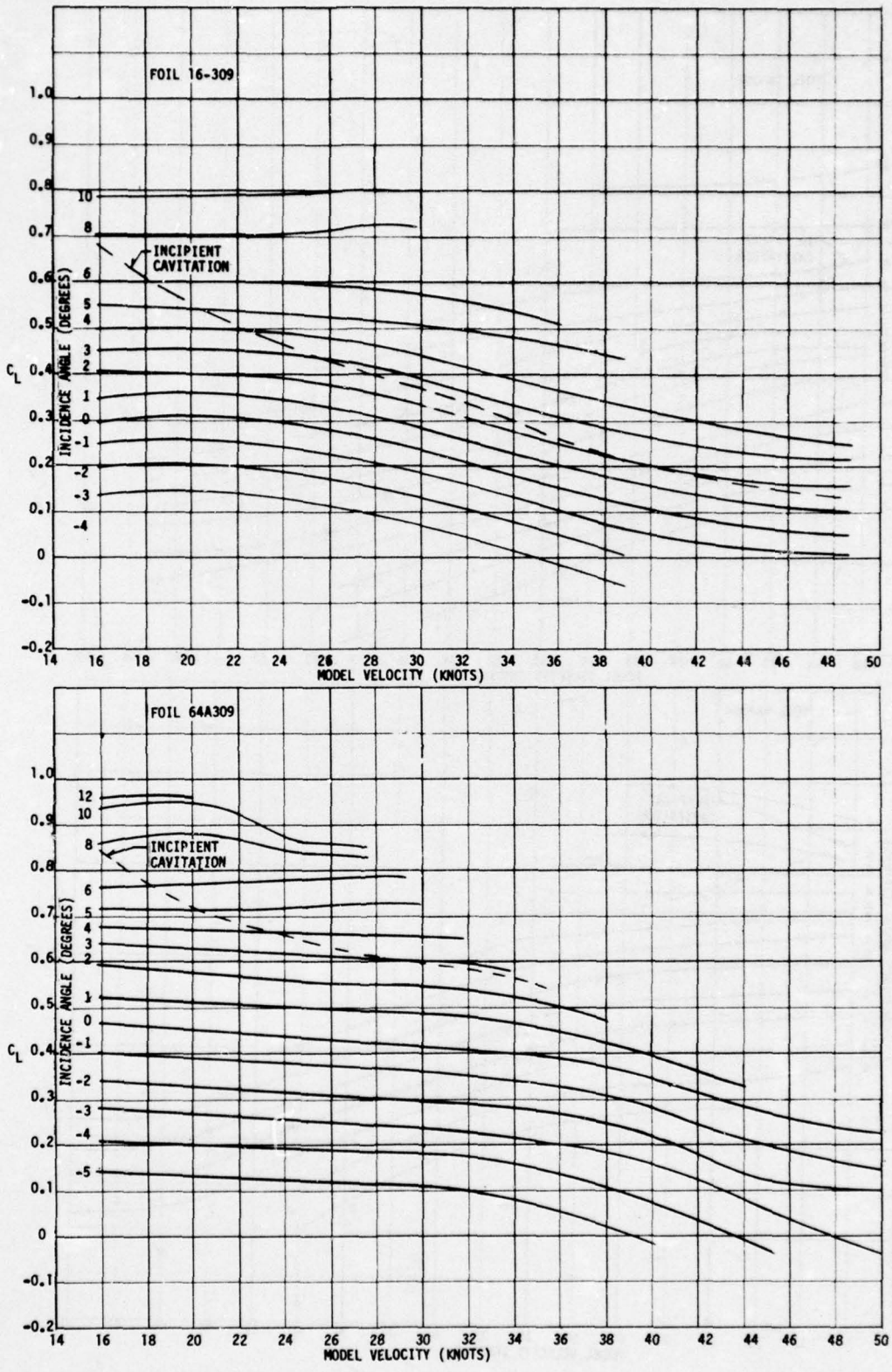

Figure 9 - Lift versus Velocity for the Two Foils for δ = 10 Degrees

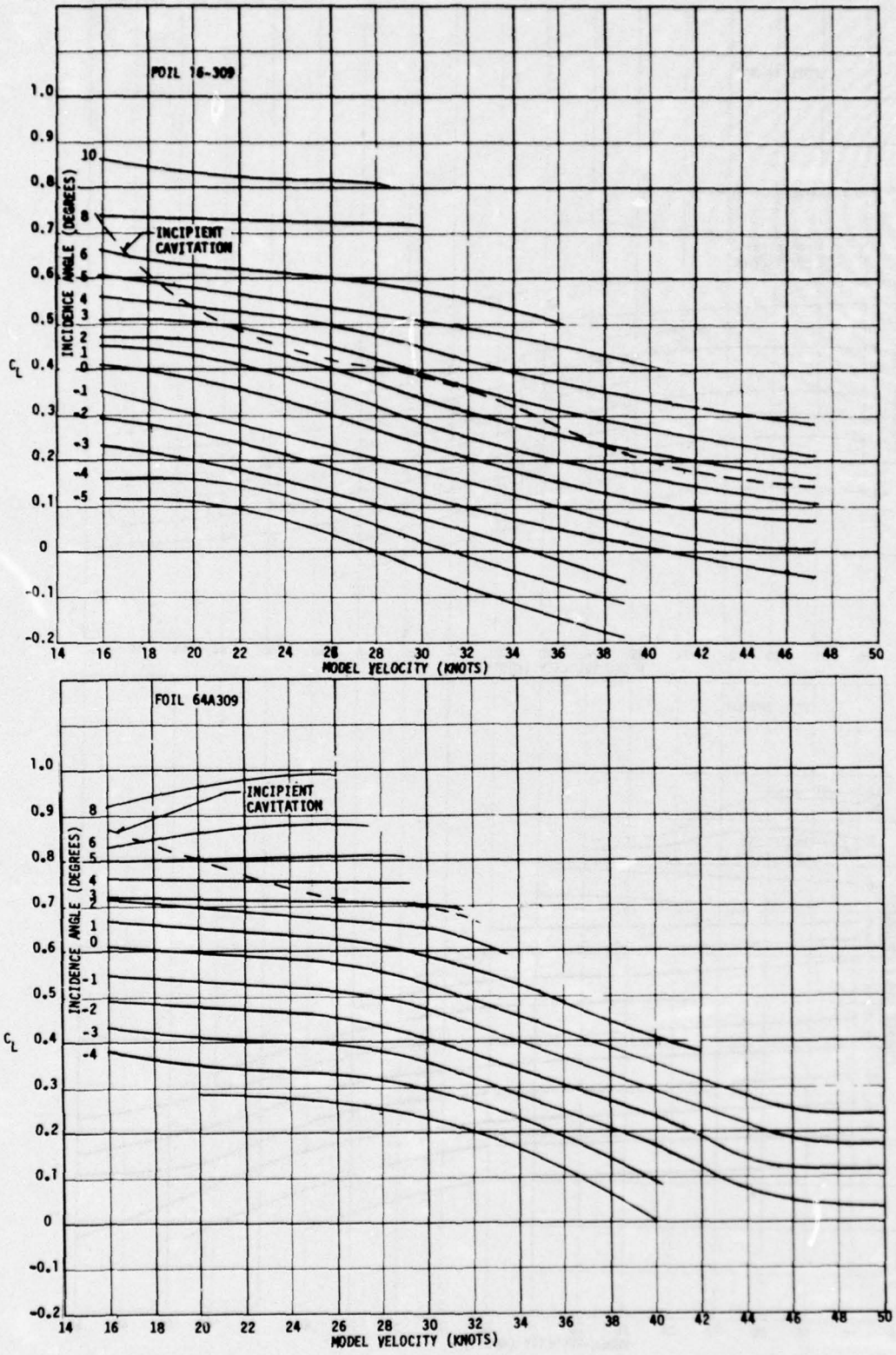

Figure 10 - Lift versus Velocity for the Two Foils for δ = 15 Degrees

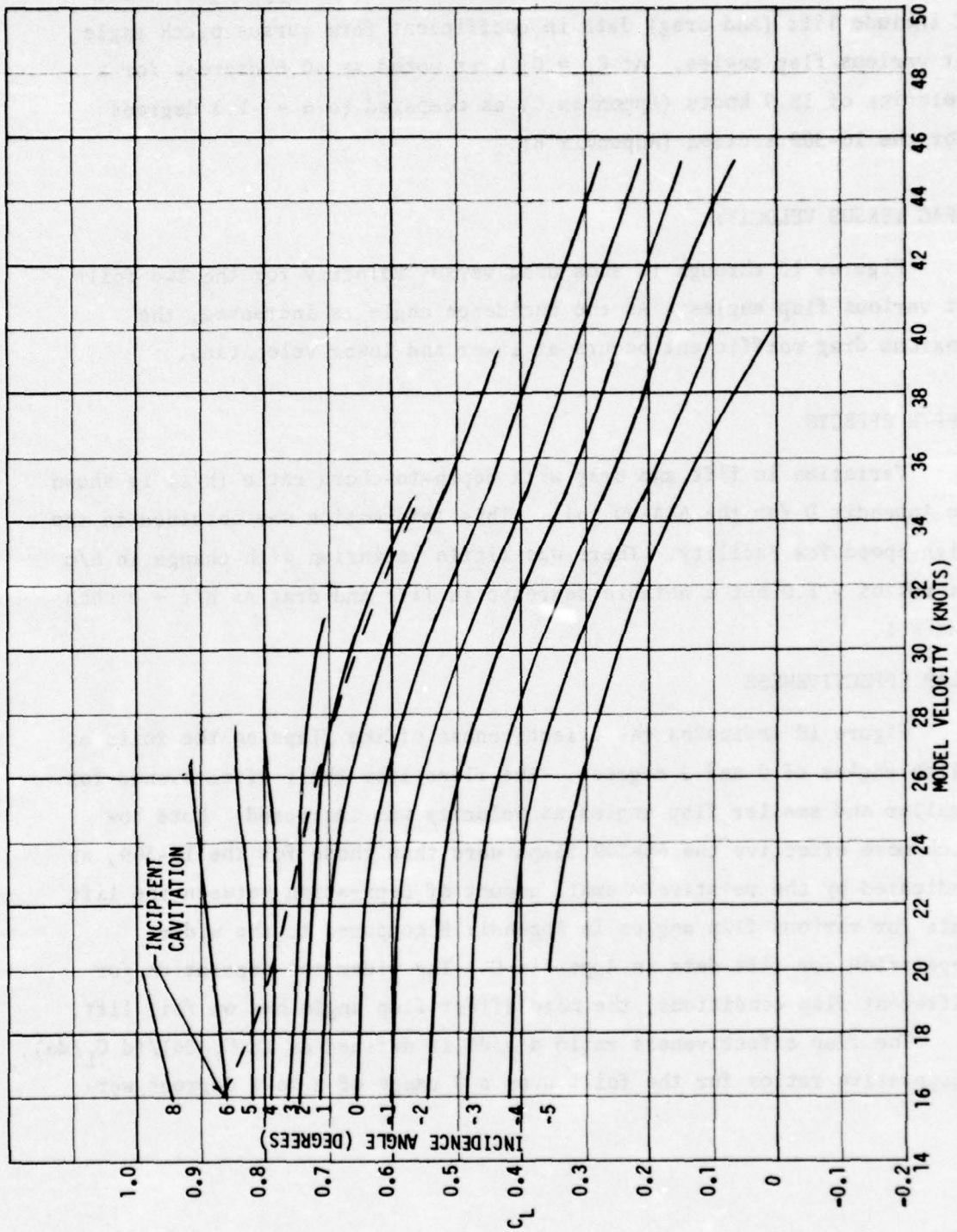

Figure 11 - Lift versus Velocity for 64A309 Foil for δ = 17½ Degrees

Supplemental information on the foils given in Appendices B and C include lift (and drag) data in coefficient form versus pitch angle at various flap angles. At $C_L = 0$, α is noted as -0.6 degrees for a velocity of 15.9 knots (Appendix C) as compared to $\alpha = -1.3$ degrees for the 16-309 section (Appendix B).

DRAG VERSUS VELOCITY

Figures 12 through 18 show drag versus velocity for the two foils at various flap angles. As the incidence angle is increased, the maximum drag coefficient occurs at lower and lower velocities.

DEPTH EFFECTS

Variation in lift and drag with depth-to-chord ratio (h/c) is shown in Appendix D for the 64A309 foil. This information was obtained in the High-Speed Tow Facility. There was little variation with change in h/c at ratios > 1.0 but a notable decrease in lift and drag as $h/c \rightarrow 0$ when $h/c < 1$.

FLAP EFFECTIVENESS

Figure 19 indicates the effectiveness of the flaps on the foils at pitch angles of 0 and 2 degrees. The flaps lose their effectivenss for smaller and smaller flap angles as velocity was increased. Note how much more effective the 64A309 flaps were than those for the 16-309, as indicated by the relatively small amount of separation between the lift data for various flap angles in Appendix B compared to the wider separation for lift data in Appendix C. The wider the separation for different flap conditions, the more effect flap angle has on foil lift.

The flap effectiveness ratio $d\alpha/d\delta$ is defined as $(d C_L/d\delta)/(d C_L/d\alpha)$. Comparative ratios for the foils over a δ range of 2 to 6 degrees were

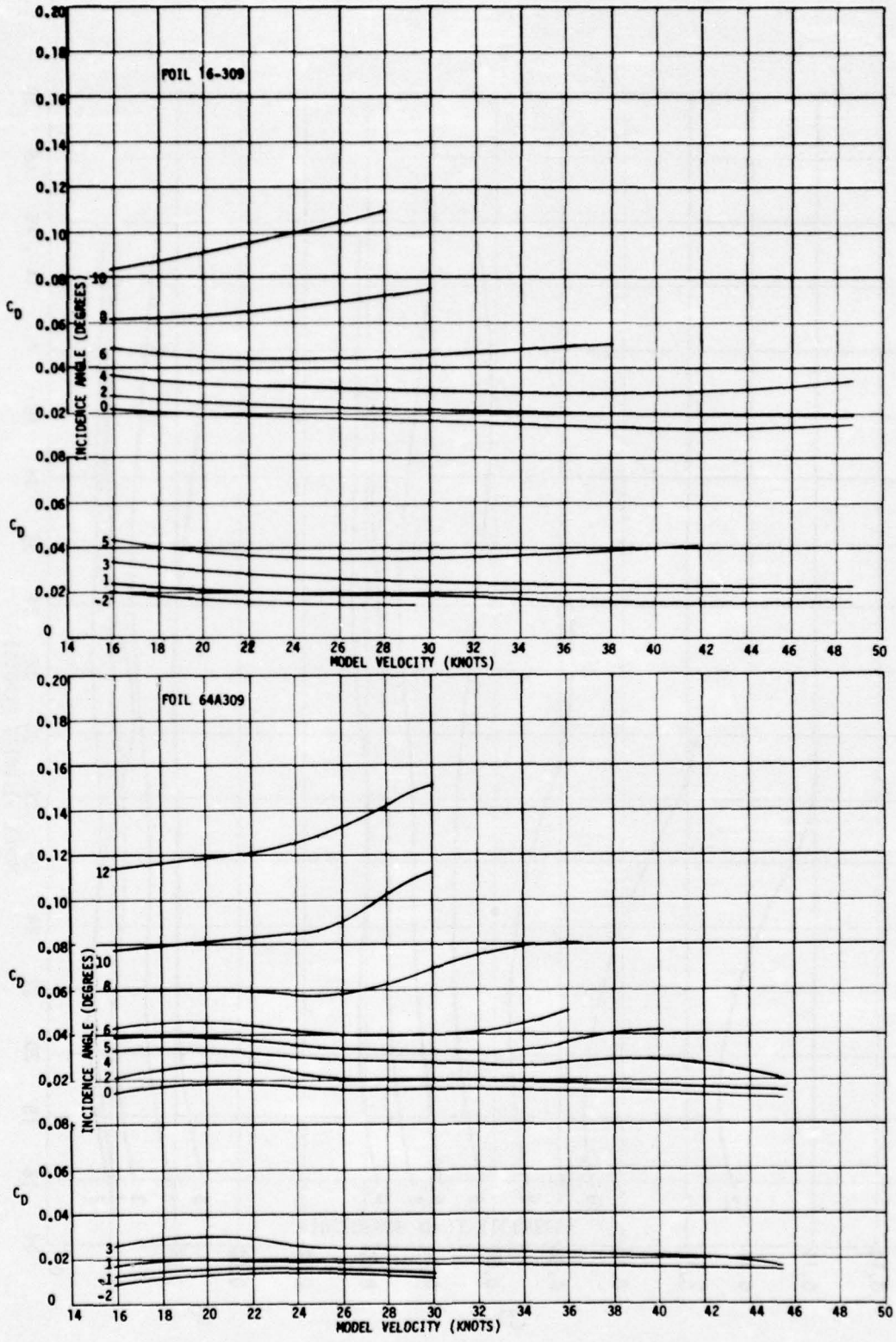

Figure 12 - Drag versus Velocity for the Two Foils for δ = 0 Degree

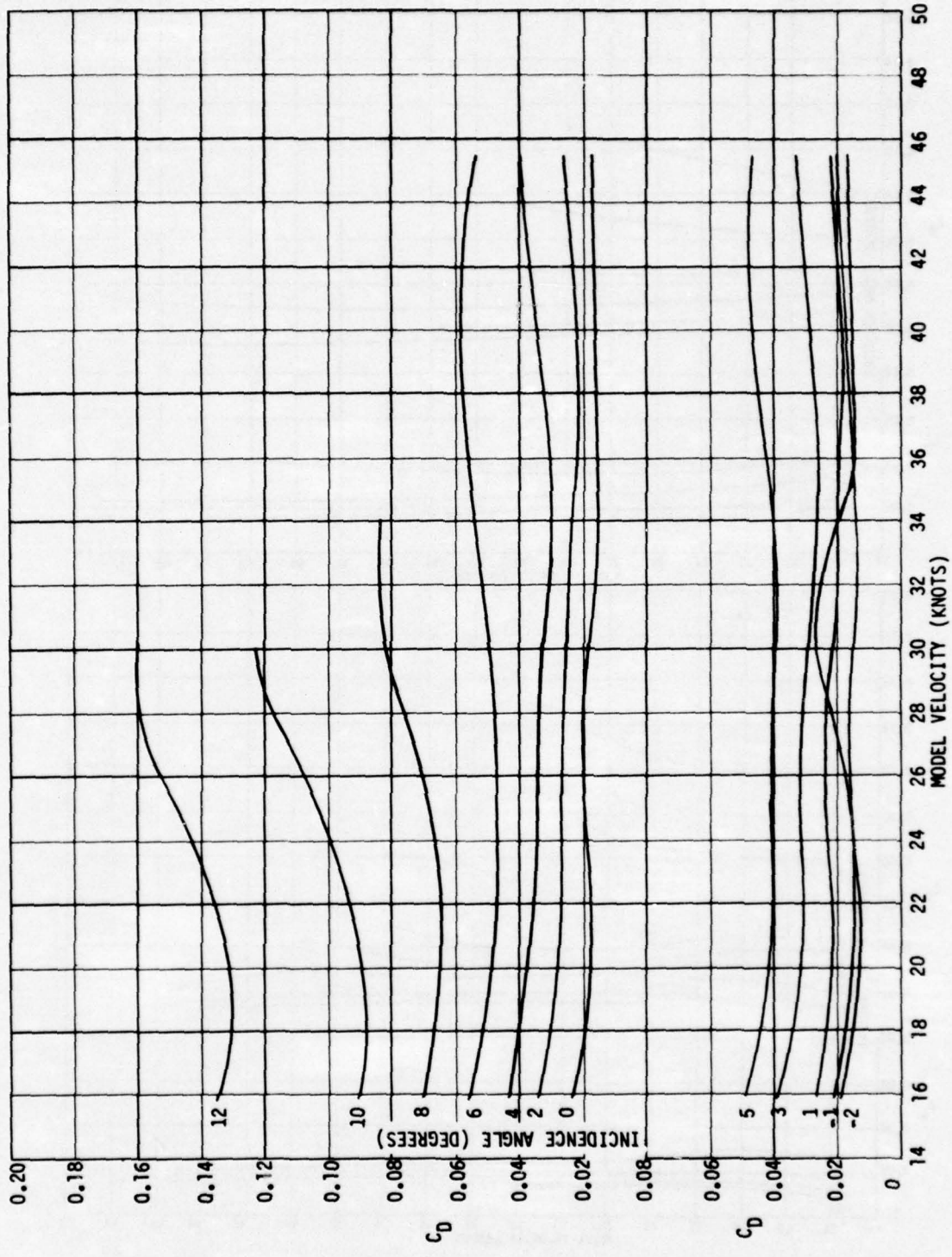

Figure 13 - Drag versus Velocity for 64A309 Foil for $\delta = 2\frac{1}{2}$ Degrees

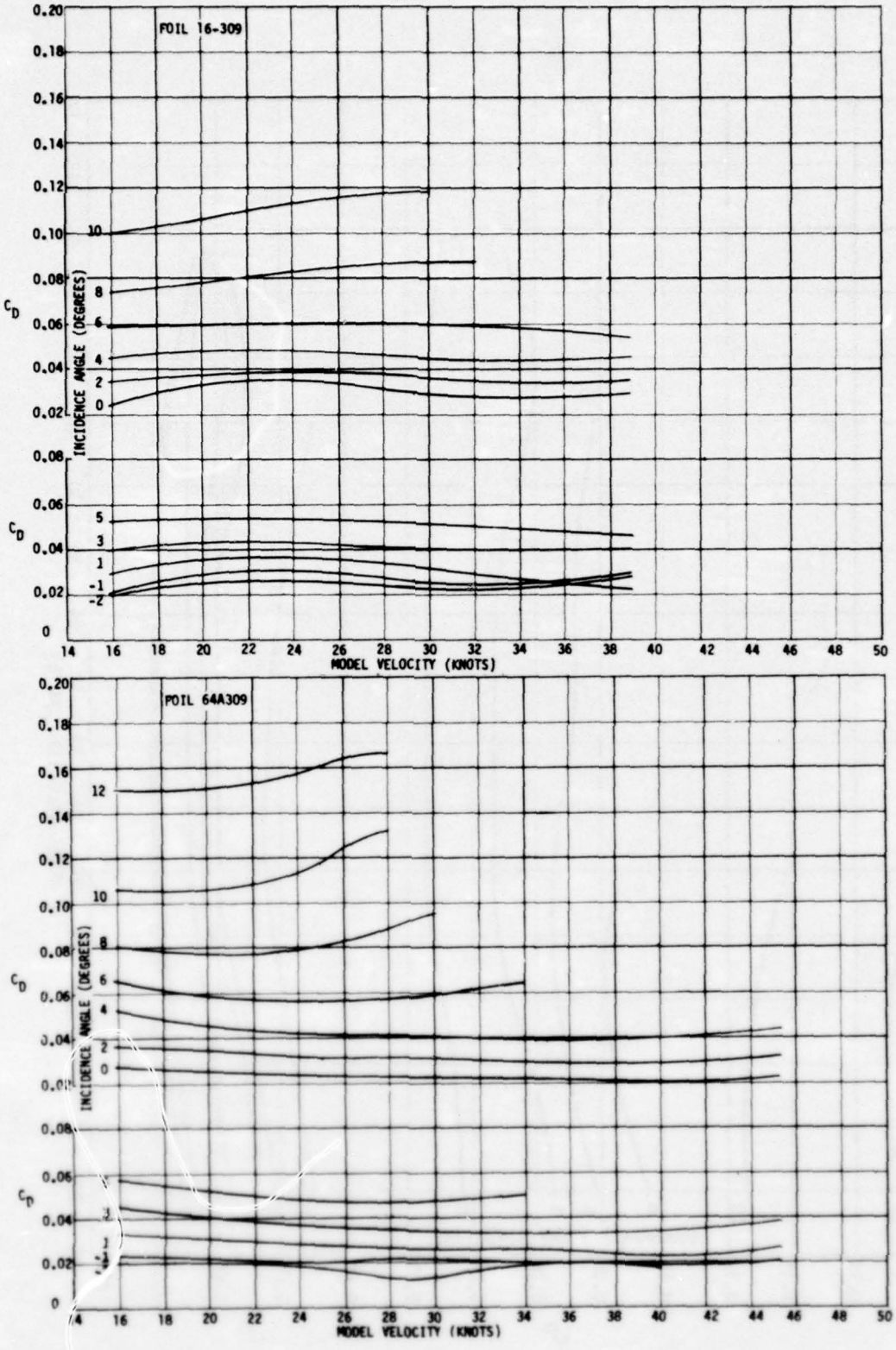

Figure 14 - Drag versus Velocity for the Two Foils for δ = 5 Degrees

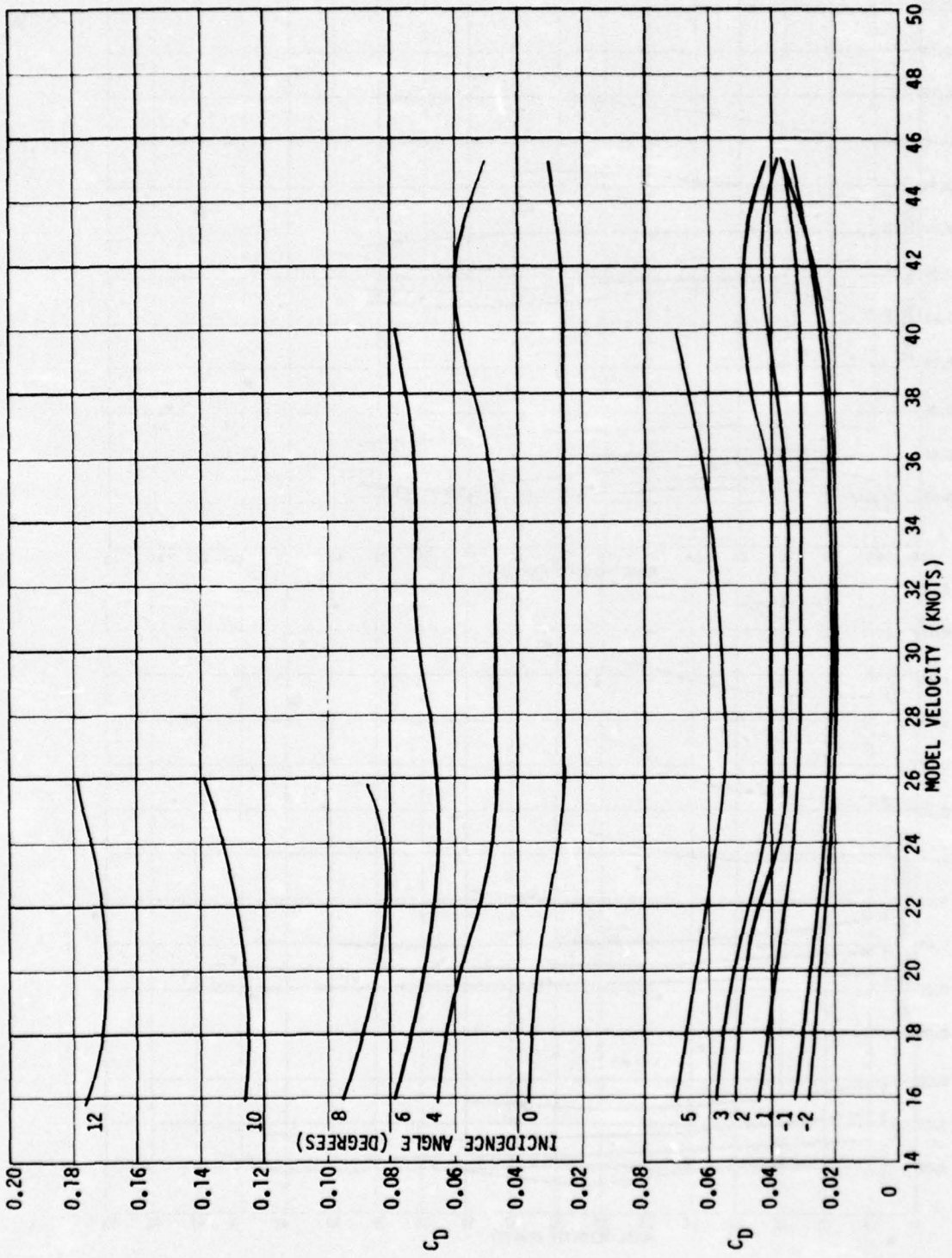

Figure 15 - Drag versus Velocity for 64A309 Foil for δ = 7½ Degrees

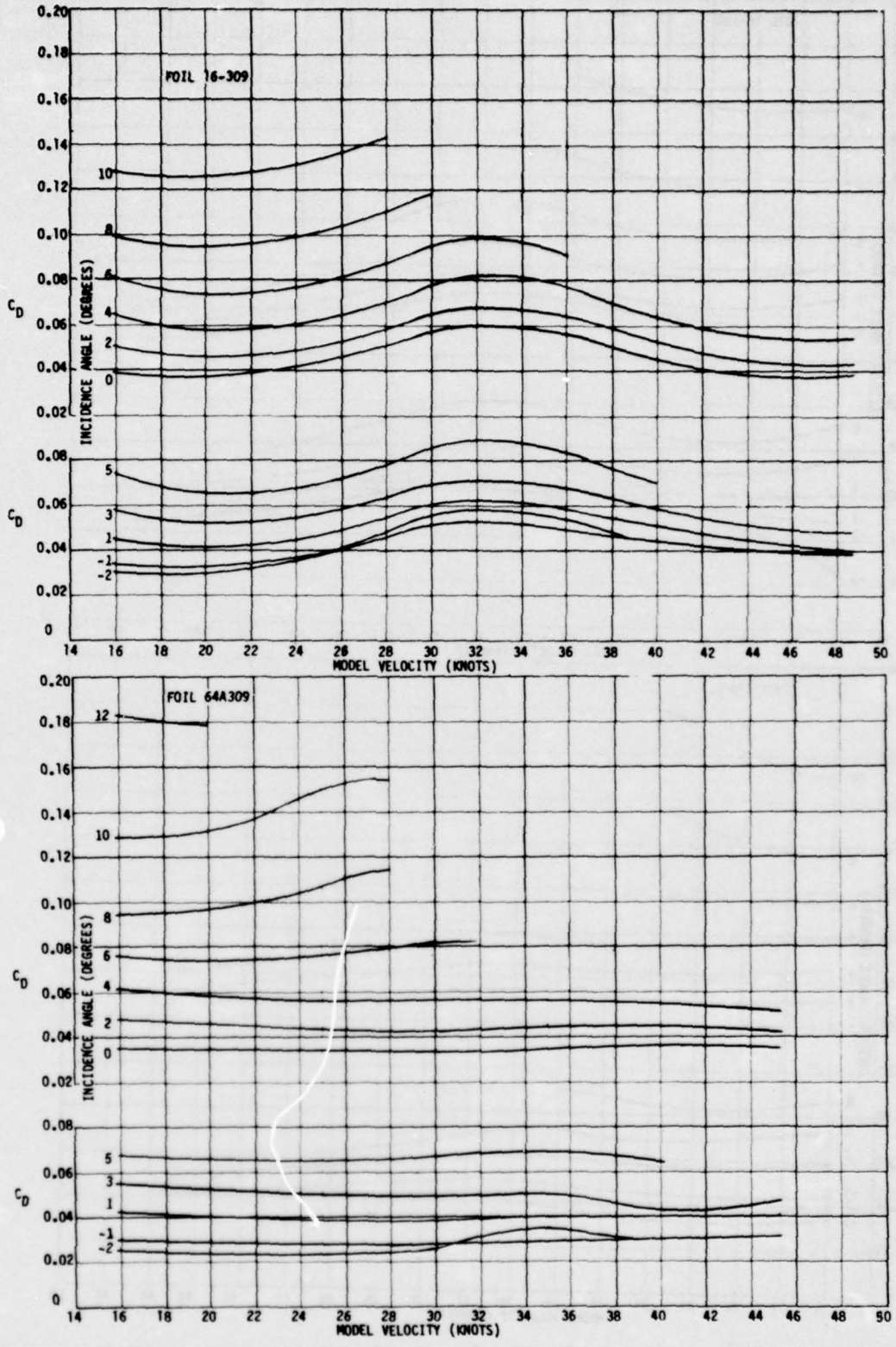

Figure 16 - Drag versus Velocity for the Two Foils for δ = 10 Degrees

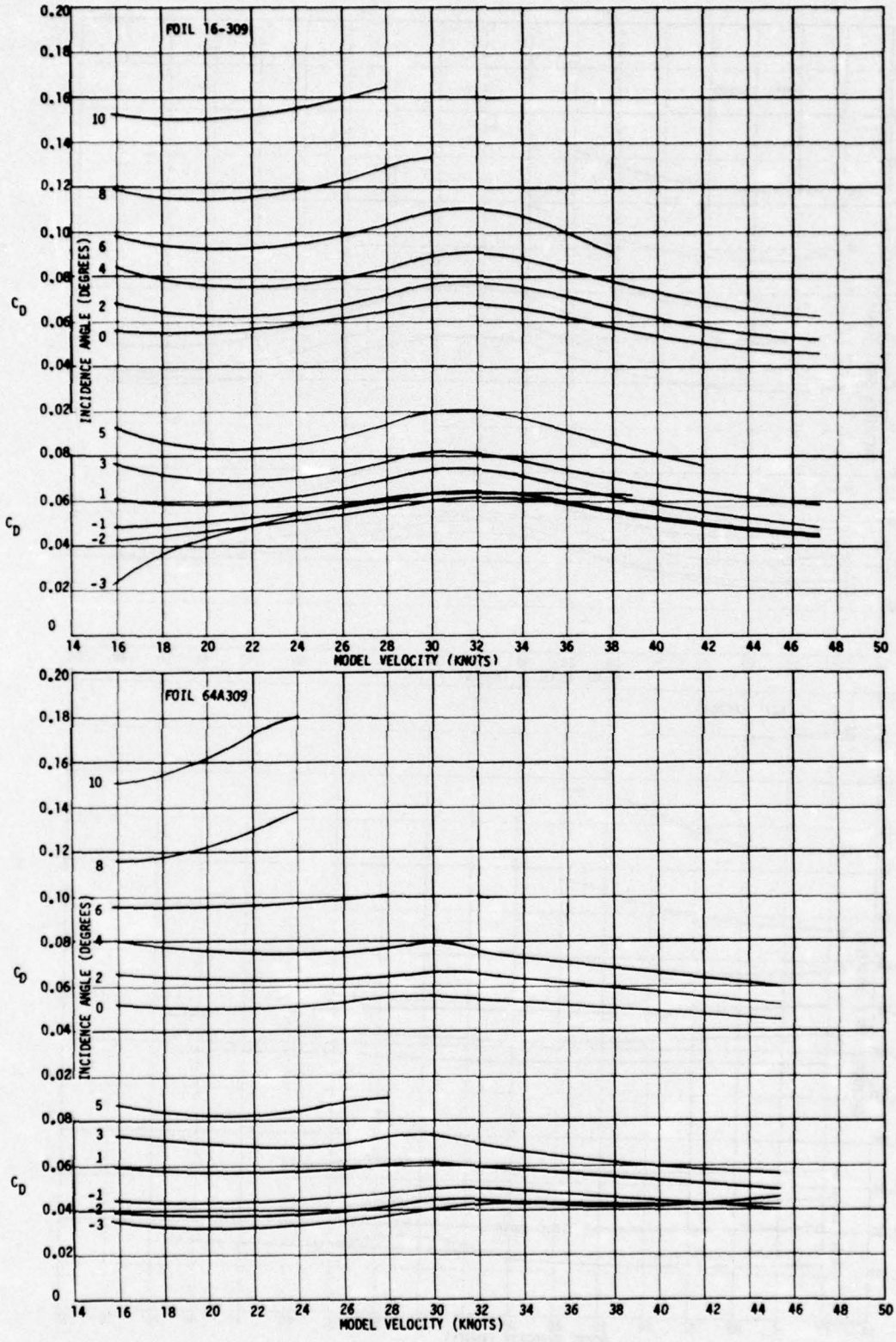

Figure 17 - Drag versus Velocity for the Two Foils for δ = 15 Degrees

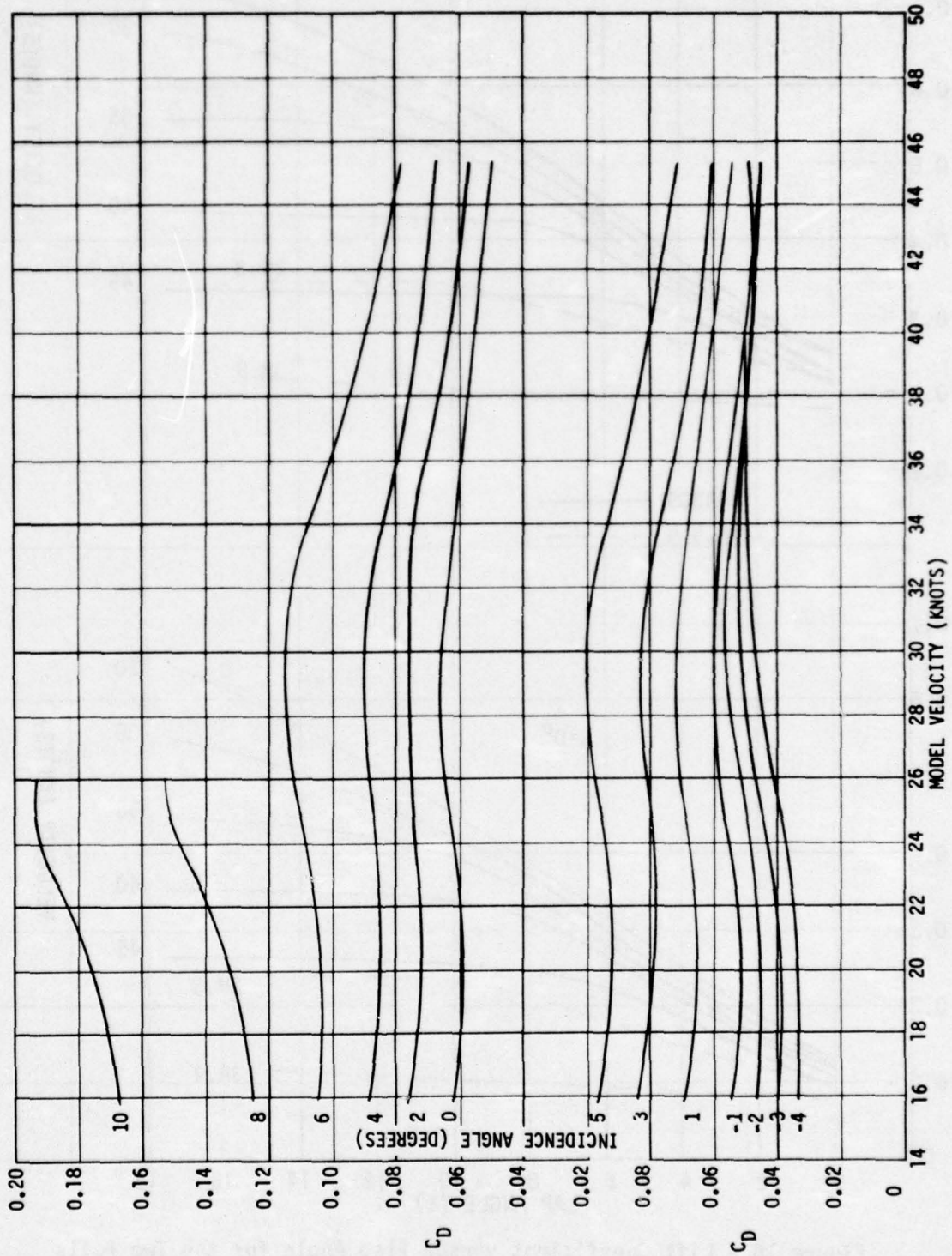

Figure 18 - Drag versus Velocity for the 64A309 Foil for $\delta = 17\frac{1}{2}$ Degrees

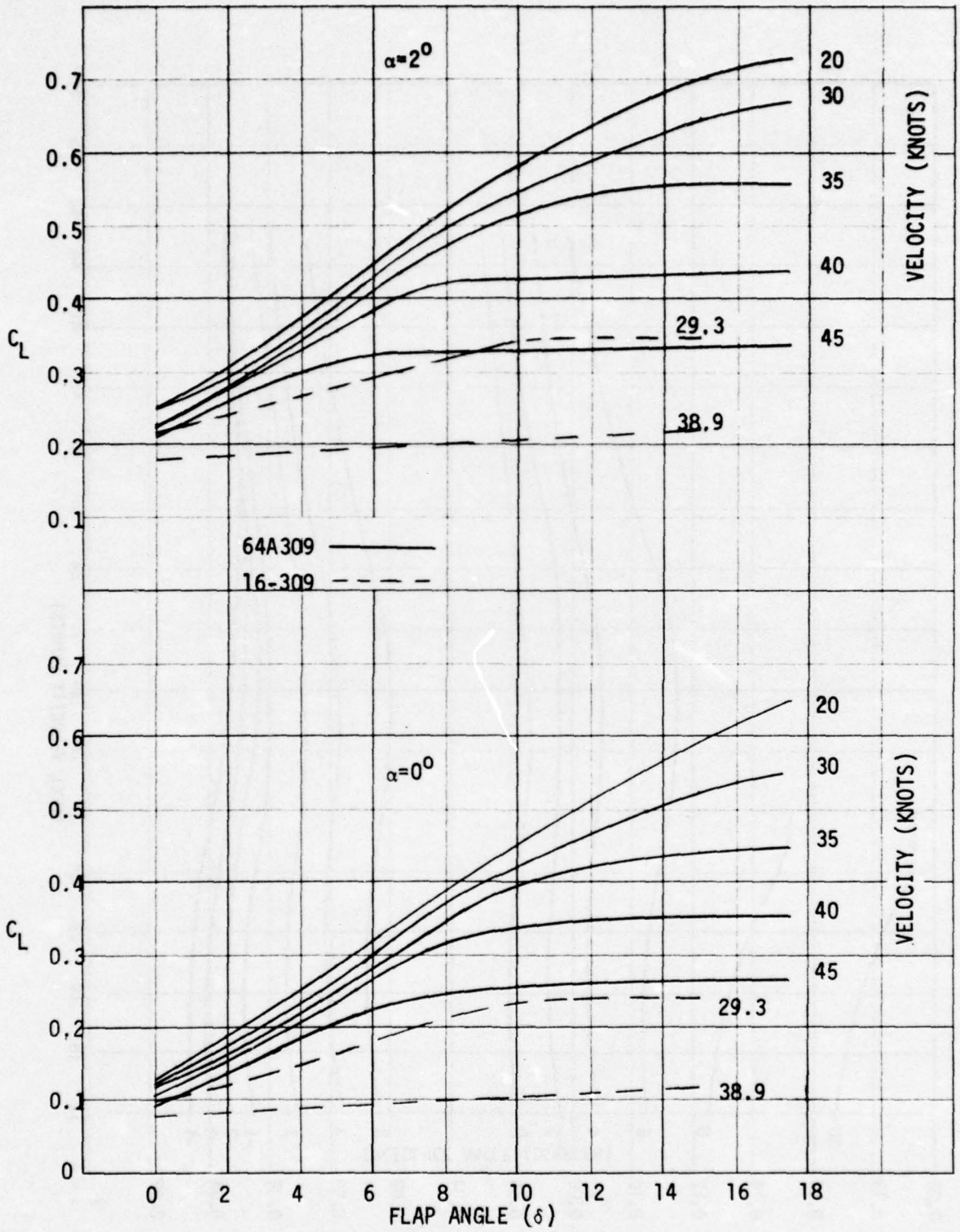

Figure 19 - Lift Coefficient versus Flap Angle for the Two Foils at α = 0 and 2 Degrees

0.24 for the 16-309 at 29.3 knots and 0.50 for the 64A309 at 30 knots. In other words, the flaps were twice as effective for the new foil. It should be noted also that the value for the 16-309 compares very well with that obtained on the full-scale PCH. For this same range of δ, when velocities were increased to 40 knots, the $d\alpha/d\delta$ ratio for the 16-309 decreased to 0.05 compared to a decrease to only 0.46 for 64A309.

CONCLUSIONS AND RECOMMENDATIONS

1. Measurements of lift and drag were taken with greater precision in the High-Speed Tow Facility than in the Rotating Arm Facility, although the latter data are considered adequate for purposes of comparison.

2. The 64A309 foil exhibited higher lift-to-drag characteristics than those of the 16-309 section for a given pitch angle, flap angle, and velocity.

3. The 64A309 foil attained higher values of lift prior to incipient cavitation than did the 16-309 although cavitation occurred approximately at the same pitch angle for the same velocity for both foils.

4. The 64A309 foil maintained effective flap control up to δ = 17 1/2 degrees for lower velocities. At the higher velocities and higher flap angles, the effectiveness decreased markedly. In comparison, the 16-309 foil exhibited only a fraction of the effectiveness of the 64A309 foil.

5. Variation in flap angle had considerably more effect on increasing lift in the case of the 64A309 foil. For velocities in the 30-knot range, the flap effectiveness ratio for the 64A309 was twice that of the 16-309 foil.

6. Lift decreased as water depth decreased, espectially at h/c ratios lower than 1.0.

7. Inasmuch as some of the information pertaining to the 16-309 foil is suspect, a new 16-309 foil should be constructed to replace the existing model and then the experiment repeated in the High-Speed Tow Facility. Before further experiments are run in the Rotating Arm, a new method of attaching the pitch mechanism to the carriage must be developed to enable the water surface to be at the level of the existing wave depressors. This improvement should produce smooth data of the quality obtained in the High-Speed Facility.

ACKNOWLEDGEMENT

Michael F. Jeffers developed the computer software package used to produce the graphs given in the appendices of this report and was responsible for the on-line computer programming and data analysis for this project. His assistance is gratefully acknowledged.

REFERENCES

1. Nelka, John, "Effects of Mid-Chord Flaps on the Ventilation and Force Characteristics of a Surface-Piercing Hydrofoil Strut," Naval Ship R&D Center Report 4508 (Nov 1974).
2. Hoerner, Sighard, F. and Henry V. Borst, "Fluid Dynamic Lift," published privately by Mrs. Liselotte A. Hoerner, Brick Town, N. J. (1975).
3. Abbot, Ira H. and Albert E. Von Doenhoff, "Theory of Wing Sections," Dover Publications, Inc., New York, N.Y. (1959).
4. Brockett, Terry, "Steady Two-Dimensional Pressure Distributions on Arbitrary Profiles," David Taylor Model Basin Report 1821 (Oct 1965).
5. Jones, C.E., Jr., "Flapped Hydrofoils in Smooth Water Subcavitating Flow," General Dynamics/Convair Report TZH-153 (Nov 1961).

APPENDIX A - COMPARISON OF INFORMATION OBTAINED IN HIGH-SPEED TOW FACILITY VERSUS ROTATING ARM FACILITY FOR 64A309 FOIL

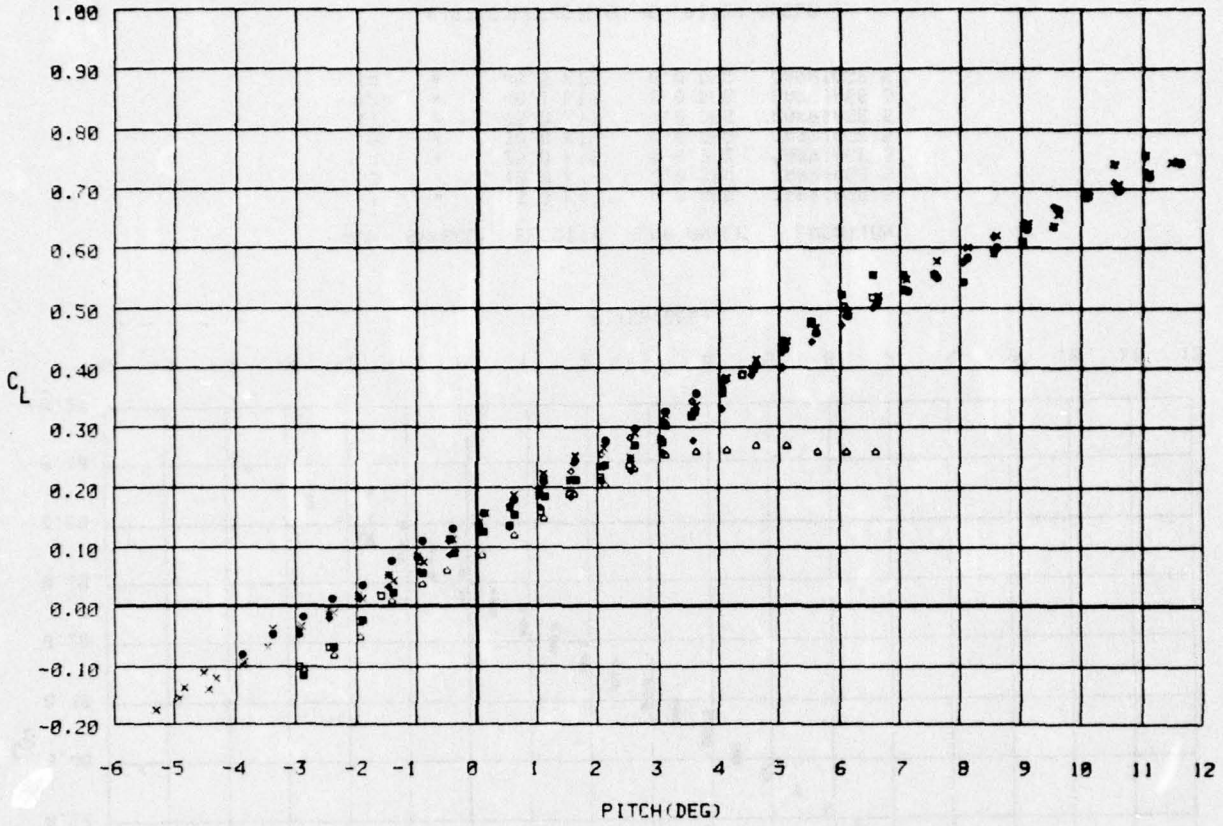

RUN	SYMBOL	VELOCITY	FLAP ANGLE	LOCATION
101	•	16.1 KTS	0.0 DEG	ROTATING ARM
102	×	20.1 KTS	0.0 DEG	ROTATING ARM
103	◦	25.0 KTS	0.0 DEG	ROTATING ARM
104	▪	30.0 KTS	0.0 DEG	ROTATING ARM
105	▫	35.1 KTS	0.0 DEG	ROTATING ARM
106	•	40.0 KTS	0.0 DEG	ROTATING ARM
107	▪	45.0 KTS	0.0 DEG	ROTATING ARM
108	▵	50.1 KTS	0.0 DEG	ROTATING ARM

LIFT COEFFICIENT VS. PITCH ANGLE

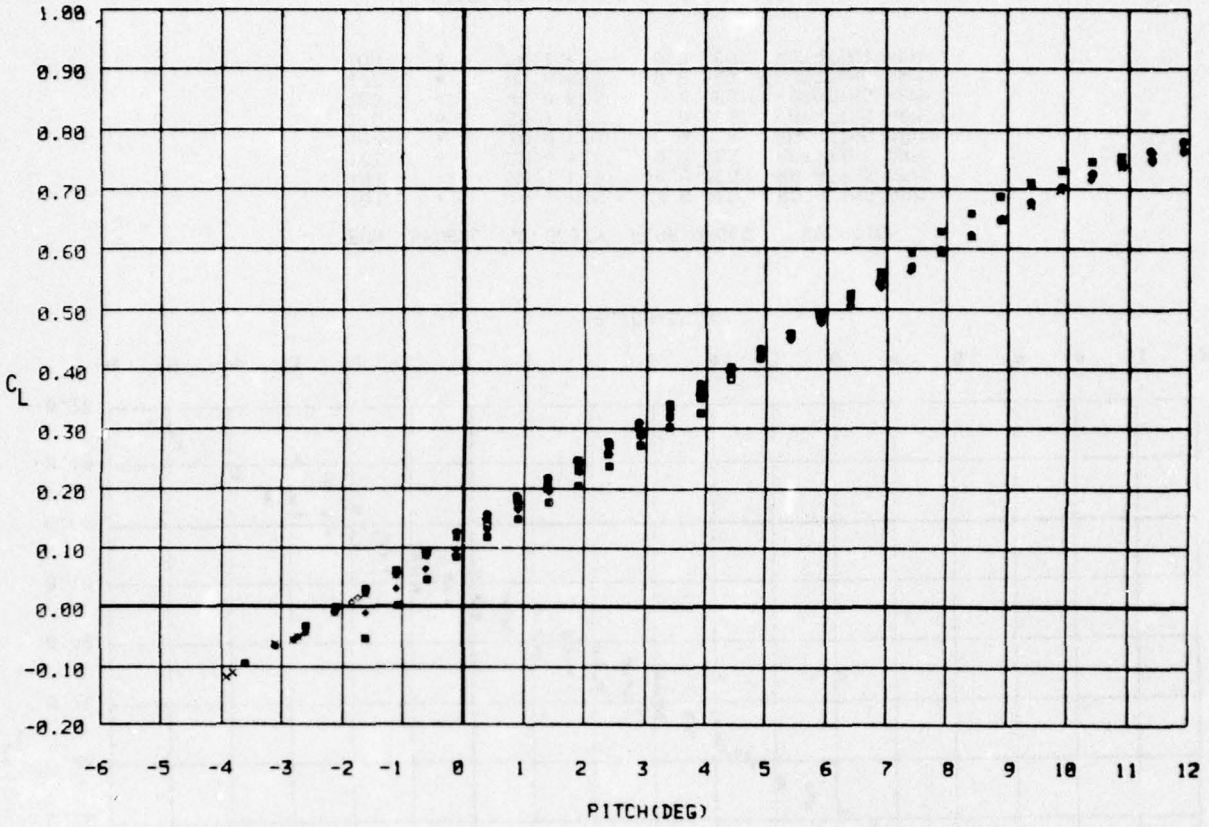

RUN	SYMBOL	VELOCITY	FLAP ANGLE	LOCATION
1	•	15.9 KTS	0.0 DEG	CARRIAGE 5
3	×	19.9 KTS	0.0 DEG	CARRIAGE 5
4	◦	25.0 KTS	0.0 DEG	CARRIAGE 5
9	▪	30.0 KTS	0.0 DEG	CARRIAGE 5
11	▫	35.0 KTS	0.0 DEG	CARRIAGE 5
12	•	40.1 KTS	0.0 DEG	CARRIAGE 5
14	▪	45.5 KTS	0.0 DEG	CARRIAGE 5

LIFT COEFFICIENT VS. PITCH ANGLE

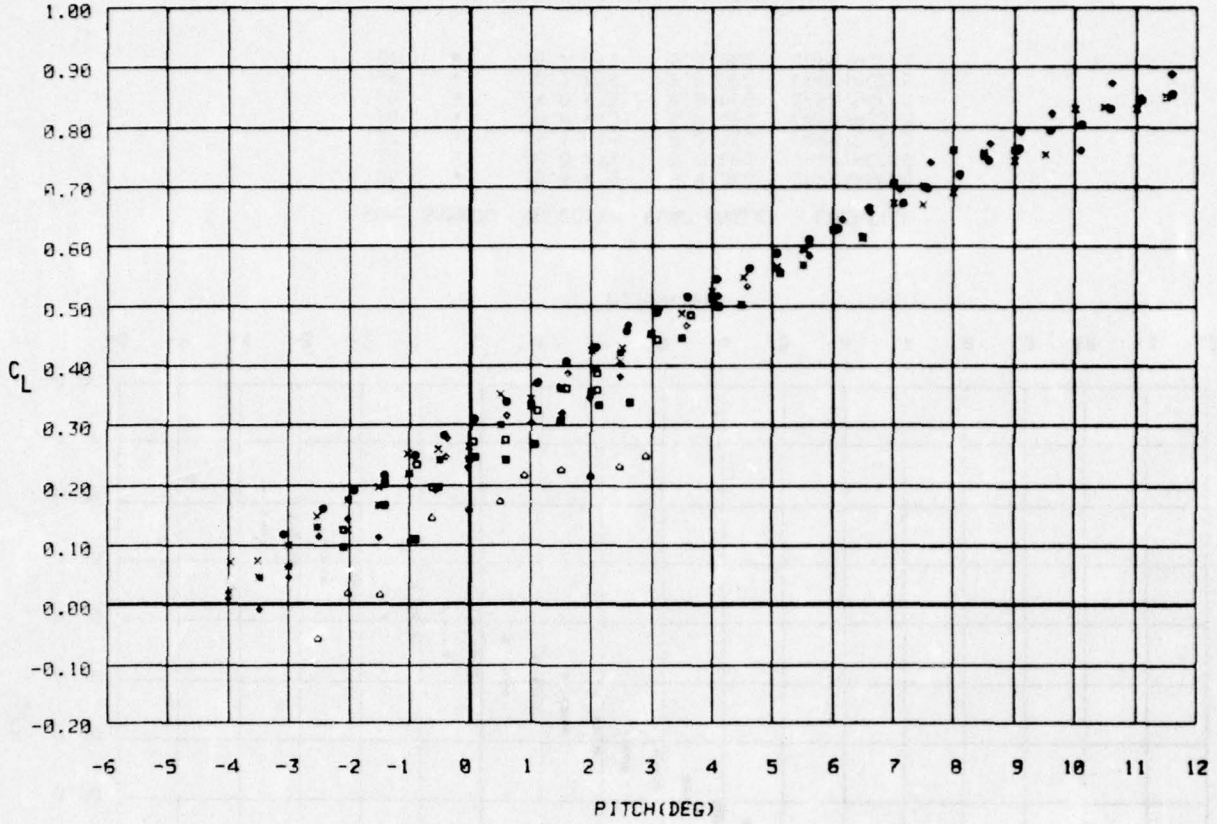

RUN	SYMBOL	VELOCITY	FLAP ANGLE	LOCATION
122	•	15.9 KTS	5.0 DEG	ROTATING ARM
126	×	20.2 KTS	5.0 DEG	ROTATING ARM
123	◦	25.0 KTS	5.0 DEG	ROTATING ARM
127	•	30.0 KTS	5.0 DEG	ROTATING ARM
124	□	35.0 KTS	5.0 DEG	ROTATING ARM
128	•	40.0 KTS	5.0 DEG	ROTATING ARM
125	■	45.2 KTS	5.0 DEG	ROTATING ARM
129	◦	50.1 KTS	5.0 DEG	ROTATING ARM

LIFT COEFFICIENT VS. PITCH ANGLE

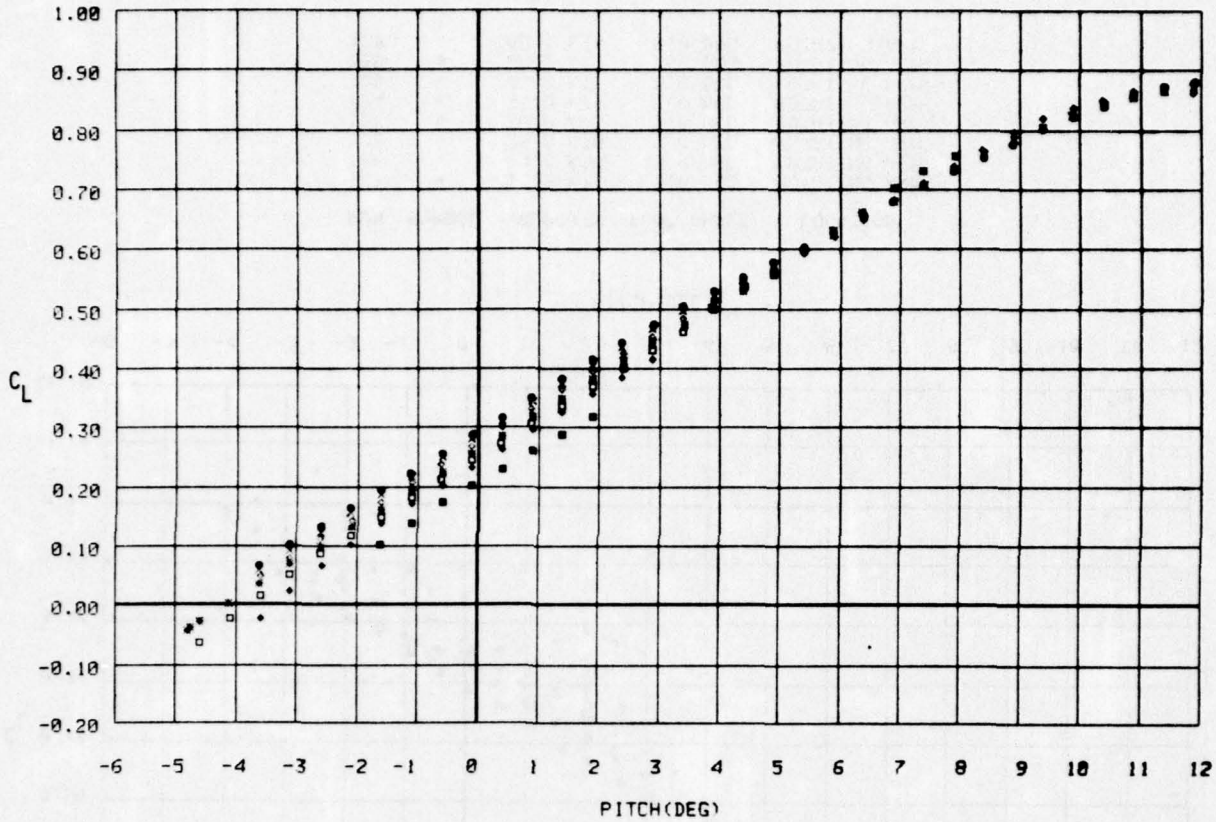

RUN	SYMBOL	VELOCITY	FLAP ANGLE	LOCATION
25	•	15.9 KTS	5.0 DEG	CARRIAGE 5
26	×	20.0 KTS	5.0 DEG	CARRIAGE 5
27	◇	25.1 KTS	5.0 DEG	CARRIAGE 5
28	▪	30.0 KTS	5.0 DEG	CARRIAGE 5
29	□	35.0 KTS	5.0 DEG	CARRIAGE 5
30	◆	40.1 KTS	5.0 DEG	CARRIAGE 5
31	■	45.4 KTS	5.0 DEG	CARRIAGE 5

LIFT COEFFICIENT VS. PITCH ANGLE

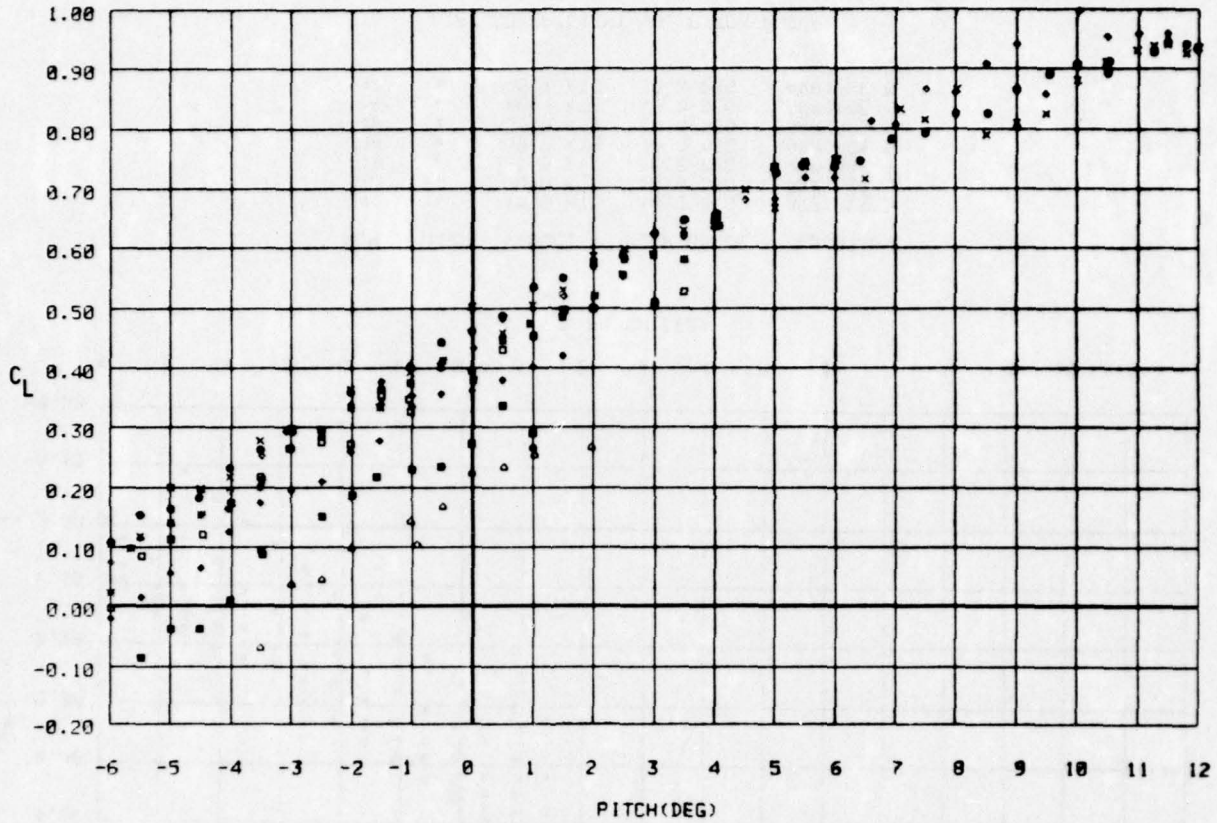

RUN	SYMBOL	VELOCITY	FLAP ANGLE	LOCATION
138	•	16.0 KTS	10.0 DEG	ROTATING ARM
142	×	20.2 KTS	10.0 DEG	ROTATING ARM
139	▵	25.1 KTS	10.0 DEG	ROTATING ARM
143	▪	30.1 KTS	10.0 DEG	ROTATING ARM
140	□	35.1 KTS	10.0 DEG	ROTATING ARM
144	•	40.1 KTS	10.0 DEG	ROTATING ARM
141	▪	45.1 KTS	10.0 DEG	ROTATING ARM
145	▵	50.2 KTS	10.0 DEG	ROTATING ARM

LIFT COEFFICIENT VS. PITCH ANGLE

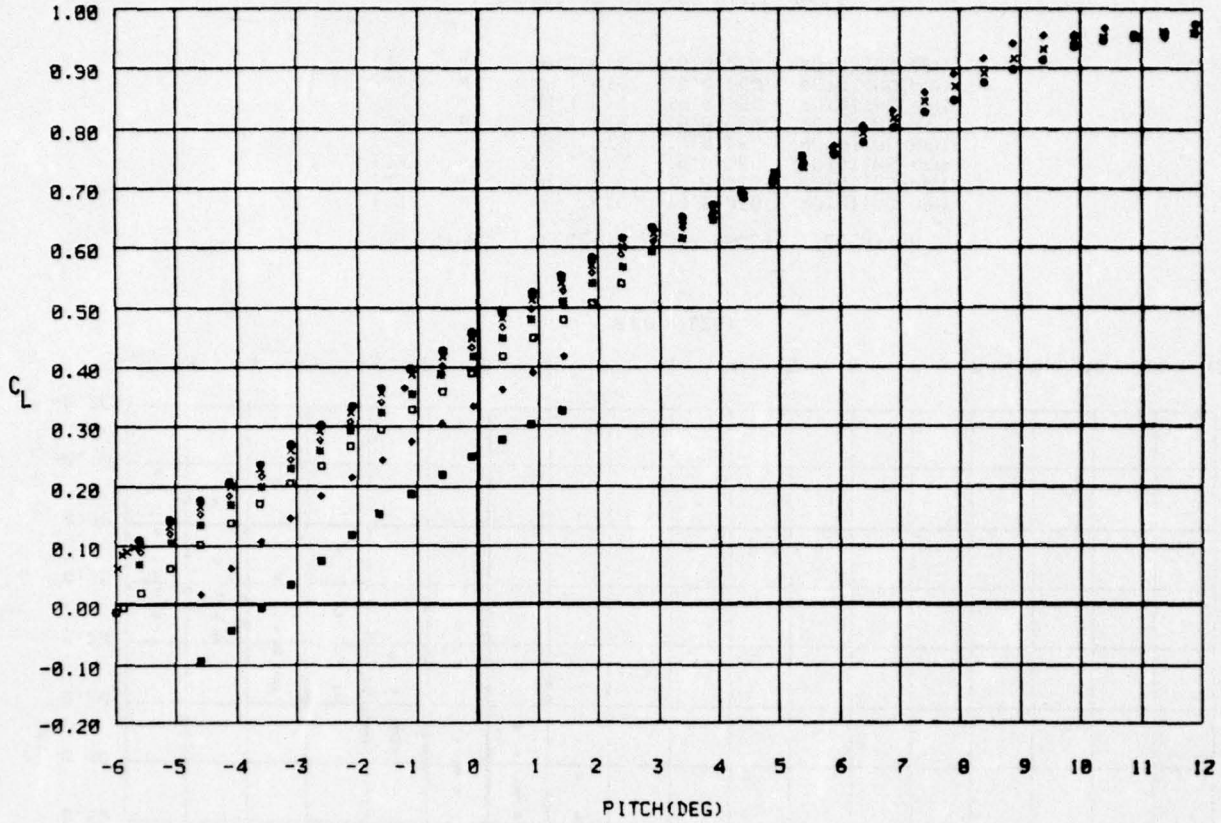

RUN	SYMBOL	VELOCITY	FLAP ANGLE	LOCATION
41	•	15.9 KTS	10.0 DEG	CARRIAGE 5
42	×	20.0 KTS	10.0 DEG	CARRIAGE 5
43	◇	25.0 KTS	10.0 DEG	CARRIAGE 5
44	■	30.0 KTS	10.0 DEG	CARRIAGE 5
45	□	35.0 KTS	10.0 DEG	CARRIAGE 5
46	◆	40.1 KTS	10.0 DEG.	CARRIAGE 5
47	■	45.3 KTS	10.0 DEG	CARRIAGE 5

LIFT COEFFICIENT VS. PITCH ANGLE

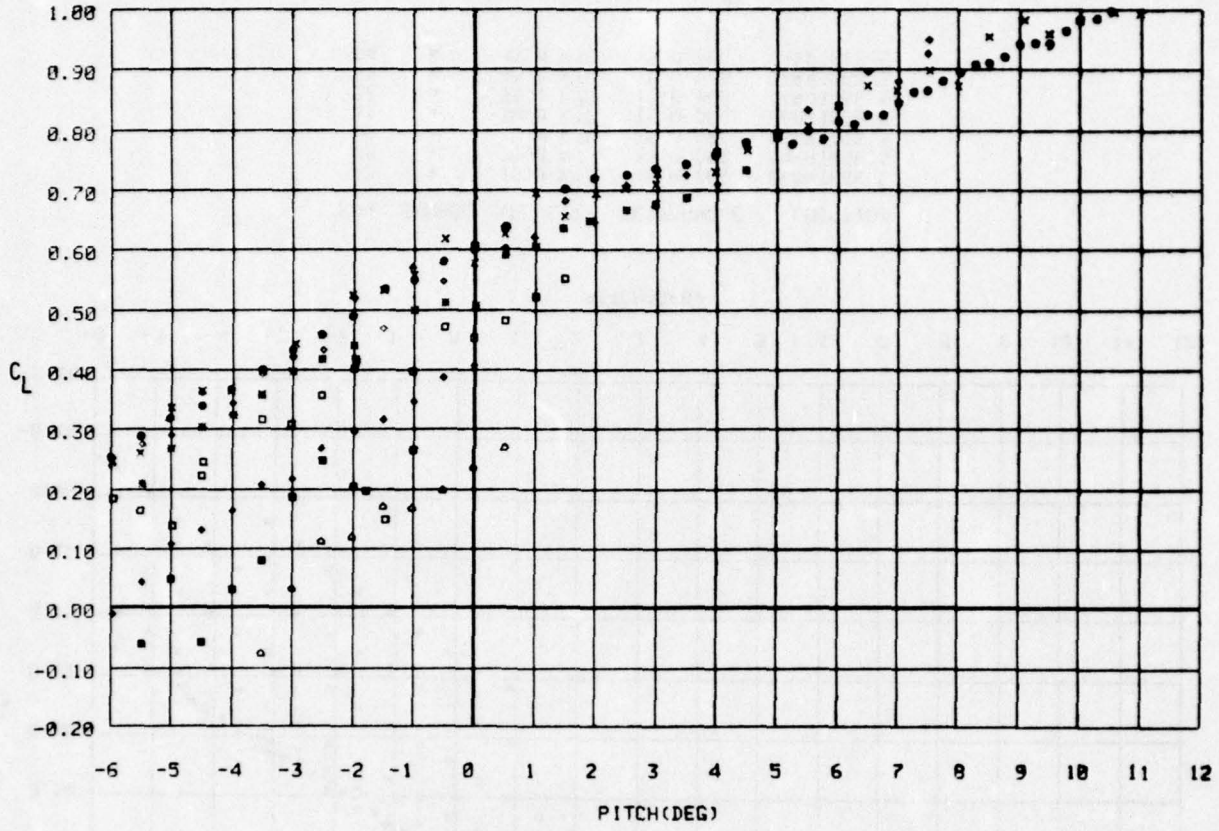

RUN	SYMBOL	VELOCITY	FLAP ANGLE	LOCATION
146	•	15.9 KTS	15.0 DEG	ROTATING ARM
150	×	20.2 KTS	15.0 DEG	ROTATING ARM
147	◇	25.1 KTS	15.0 DEG	ROTATING ARM
151	■	30.1 KTS	15.0 DEG	ROTATING ARM
148	□	35.1 KTS	15.0 DEG	ROTATING ARM
152	◆	40.0 KTS	15.0 DEG	ROTATING ARM
149	■	45.1 KTS	15.0 DEG	ROTATING ARM
153	◇	50.2 KTS	15.0 DEG	ROTATING ARM

LIFT COEFFICIENT VS. PITCH ANGLE

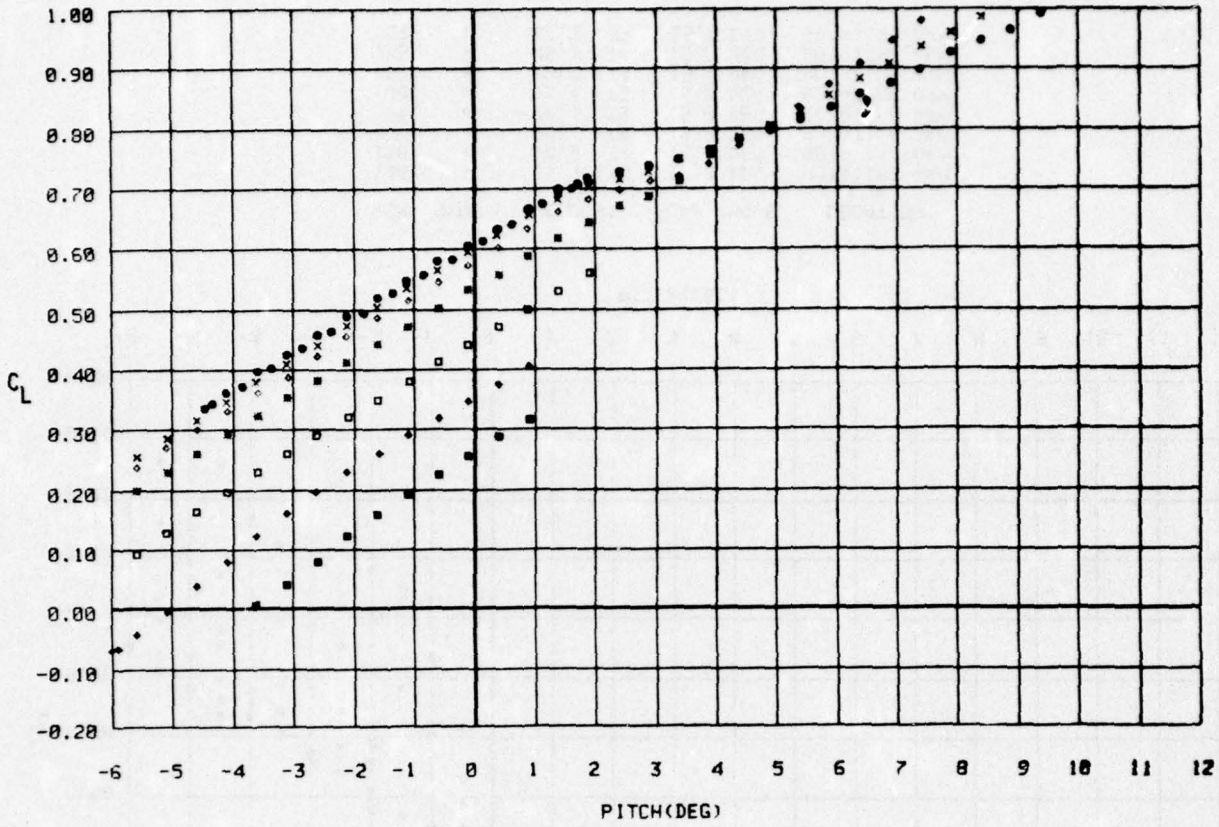

RUN	SYMBOL	VELOCITY	FLAP ANGLE	LOCATION
48	•	15.9 KTS	15.0 DEG	CARRIAGE 5
49	×	20.0 KTS	15.0 DEG	CARRIAGE 5
50	◇	25.0 KTS	15.0 DEG	CARRIAGE 5
51	■	30.0 KTS	15.0 DEG	CARRIAGE 5
52	□	35.1 KTS	15.0 DEG	CARRIAGE 5
53	◆	40.0 KTS	15.0 DEG	CARRIAGE 5
54	■	45.4 KTS	15.0 DEG	CARRIAGE 5

LIFT COEFFICIENT VS. PITCH ANGLE

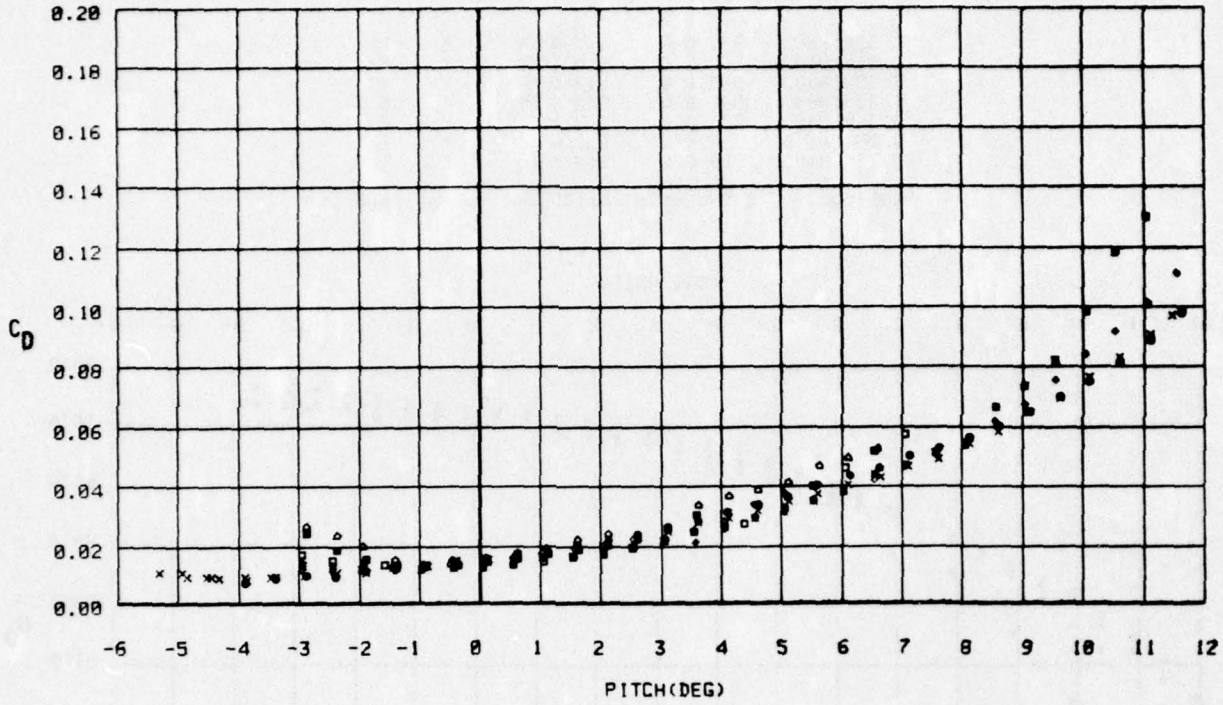

RUN	SYMBOL	VELOCITY	FLAP ANGLE	LOCATION
101	•	16.1 KTS	0.0 DEG	ROTATING ARM
102	×	20.1 KTS	0.0 DEG	ROTATING ARM
103	◇	25.0 KTS	0.0 DEG	ROTATING ARM
104	■	30.0 KTS	0.0 DEG	ROTATING ARM
105	□	35.1 KTS	0.0 DEG	ROTATING ARM
106	◆	40.0 KTS	0.0 DEG	ROTATING ARM
107	■	45.0 KTS	0.0 DEG	ROTATING ARM
108	△	50.1 KTS	0.0 DEG	ROTATING ARM

DRAG COEFFICIENT VS. PITCH ANGLE

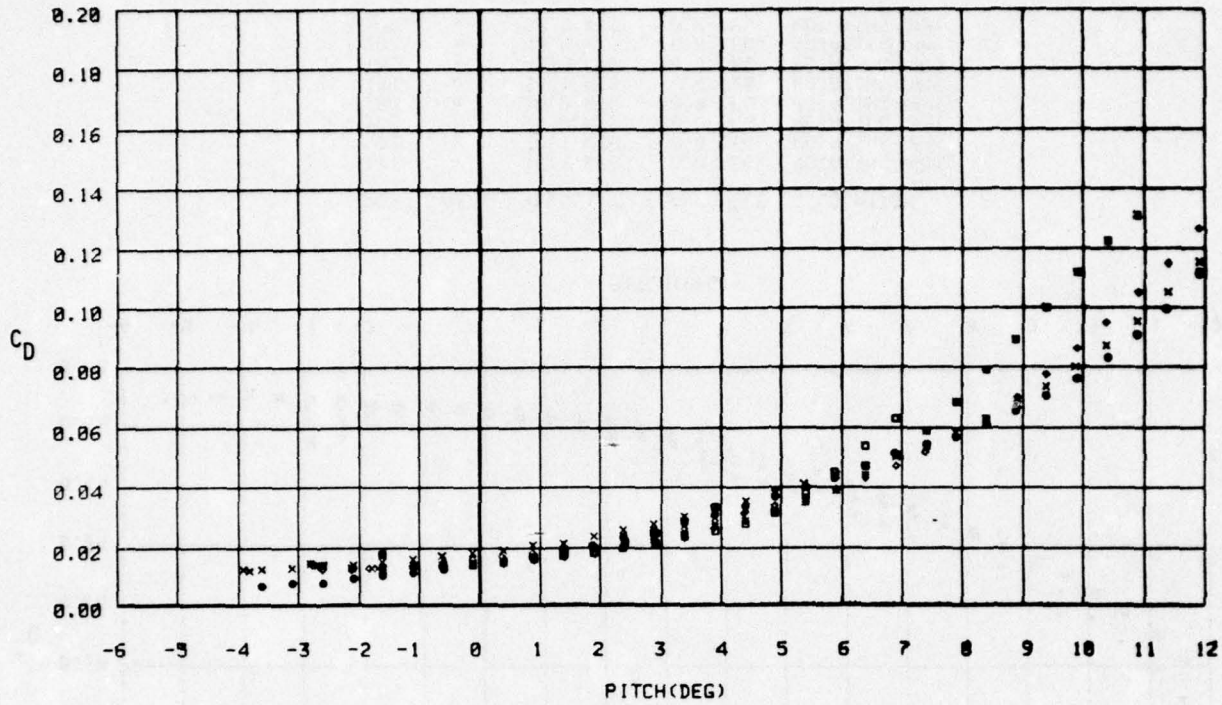

RUN	SYMBOL	VELOCITY	FLAP ANGLE	LOCATION
1	•	15.9 KTS	0.0 DEG	CARRIAGE 5
3	×	19.9 KTS	0.0 DEG	CARRIAGE 5
4	◇	25.0 KTS	0.0 DEG	CARRIAGE 5
9	■	30.0 KTS	0.0 DEG	CARRIAGE 5
11	□	35.0 KTS	0.0 DEG	CARRIAGE 5
12	◆	40.1 KTS	0.0 DEG	CARRIAGE 5
14	■	45.5 KTS	0.0 DEG	CARRIAGE 5

DRAG COEFFICIENT VS. PITCH ANGLE

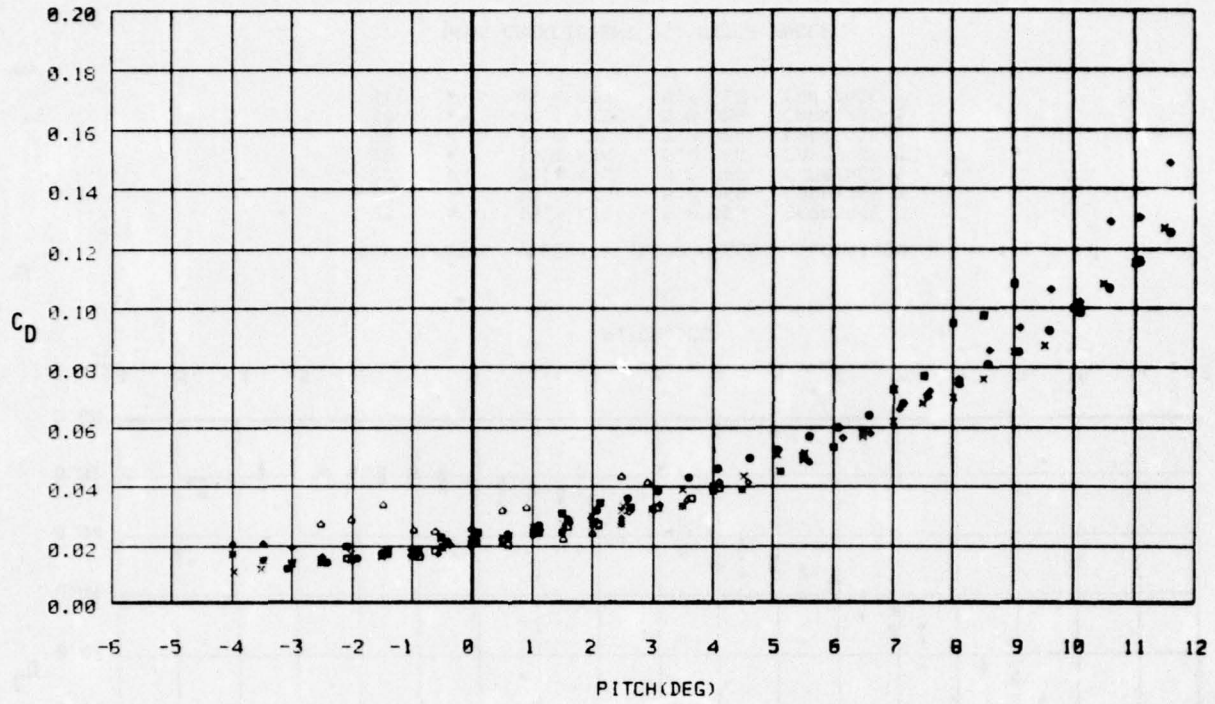

RUN	SYMBOL	VELOCITY	FLAP ANGLE	LOCATION
122	•	15.9 KTS	5.0 DEG	ROTATING ARM
126	×	20.2 KTS	5.0 DEG	ROTATING ARM
123	◦	25.0 KTS	5.0 DEG	ROTATING ARM
127	▪	30.0 KTS	5.0 DEG	ROTATING ARM
124	□	35.0 KTS	5.0 DEG	ROTATING ARM
128	▪	40.0 KTS	5.0 DEG	ROTATING ARM
125	■	45.2 KTS	5.0 DEG	ROTATING ARM
129	▫	50.1 KTS	5.0 DEG	ROTATING ARM

DRAG COEFFICIENT VS. PITCH ANGLE

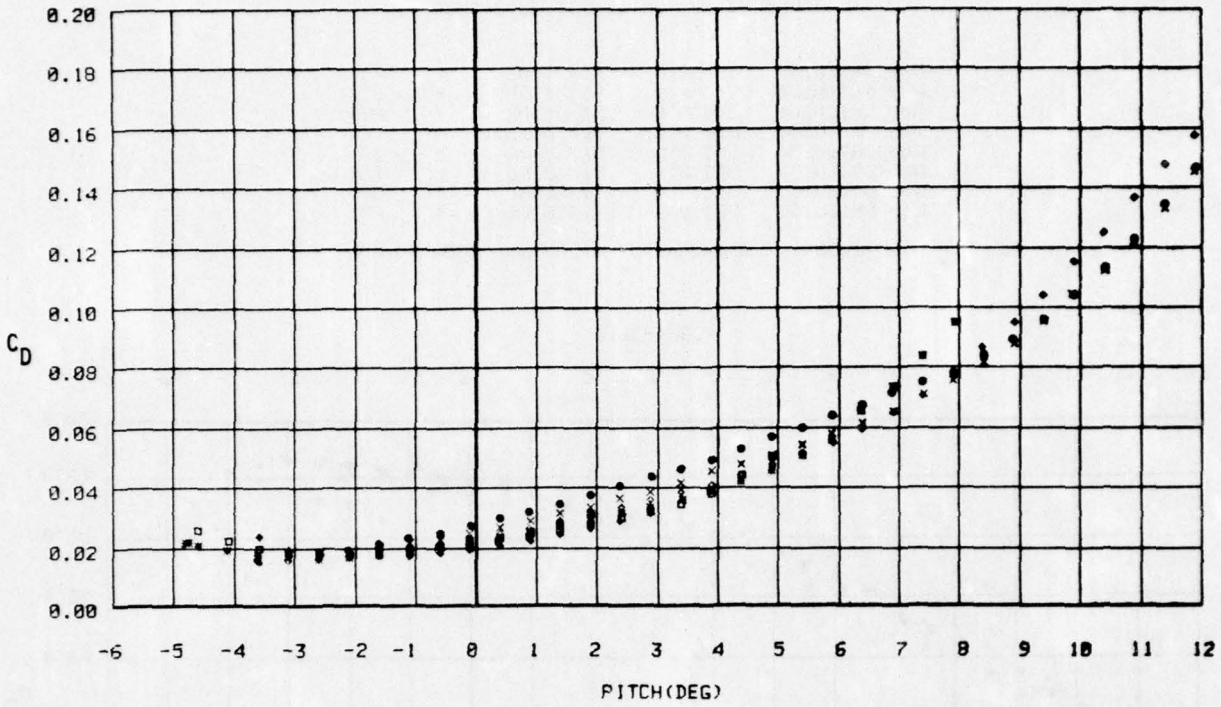

RUN	SYMBOL	VELOCITY	FLAP ANGLE	LOCATION
25	•	15.9 KTS	5.0 DEG	CARRIAGE 5
26	×	20.0 KTS	5.0 DEG	CARRIAGE 5
27	◇	25.1 KTS	5.0 DEG	CARRIAGE 5
28	■	30.0 KTS	5.0 DEG	CARRIAGE 5
29	□	35.0 KTS	5.0 DEG	CARRIAGE 5
30	•	40.1 KTS	5.0 DEG	CARRIAGE 5
31	■	45.4 KTS	5.0 DEG	CARRIAGE 5

DRAG COEFFICIENT VS. PITCH ANGLE

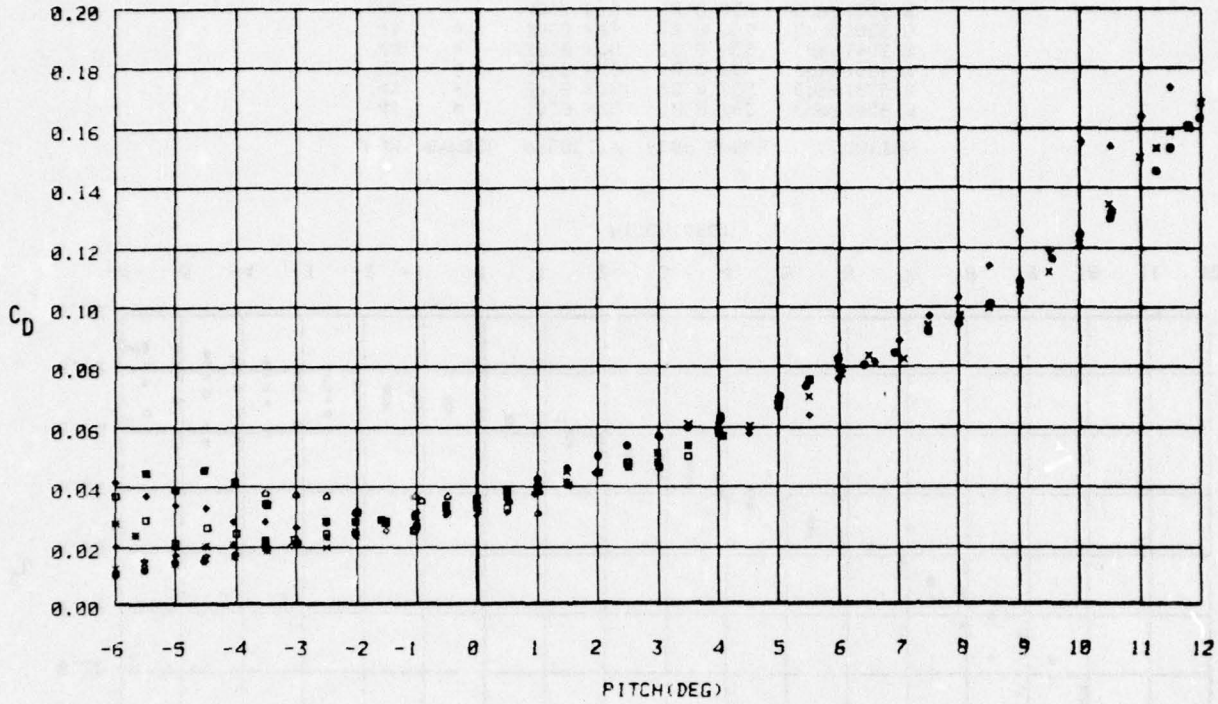

RUN	SYMBOL	VELOCITY	FLAP ANGLE	LOCATION
138	•	16.0 KTS	10.0 DEG	ROTATING ARM
142	×	20.2 KTS	10.0 DEG	ROTATING ARM
139	◦	25.1 KTS	10.0 DEG	ROTATING ARM
143	▪	30.1 KTS	10.0 DEG	ROTATING ARM
140	□	35.1 KTS	10.0 DEG	ROTATING ARM
144	◆	40.1 KTS	10.0 DEG	ROTATING ARM
141	▪	45.1 KTS	10.0 DEG	ROTATING ARM
145	▵	50.2 KTS	10.0 DEG	ROTATING ARM

DRAG COEFFICIENT VS. PITCH ANGLE

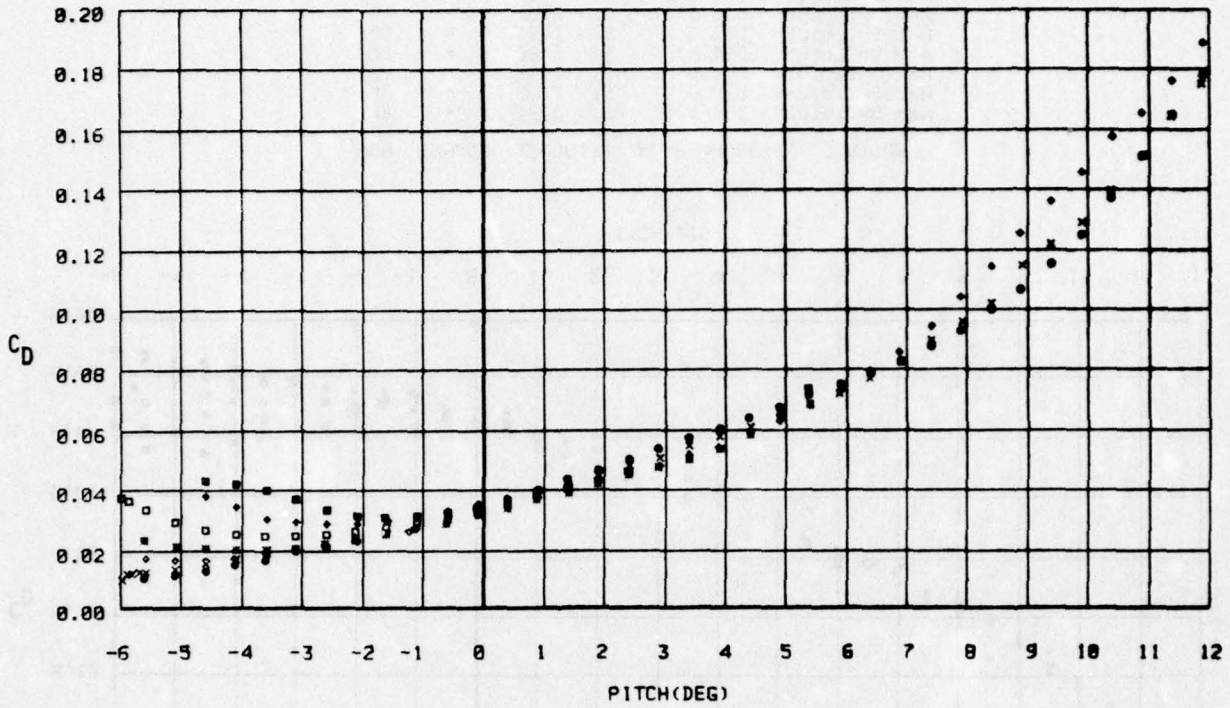

RUN	SYMBOL	VELOCITY	FLAP ANGLE	LOCATION
41	•	15.9 KTS	10.0 DEG	CARRIAGE 5
42	×	20.0 KTS	10.0 DEG	CARRIAGE 5
43	◇	25.0 KTS	10.0 DEG	CARRIAGE 5
44	▪	30.0 KTS	10.0 DEG	CARRIAGE 5
45	□	35.0 KTS	10.0 DEG	CARRIAGE 5
46	◆	40.1 KTS	10.0 DEG	CARRIAGE 5
47	■	45.3 KTS	10.0 DEG	CARRIAGE 5

DRAG COEFFICIENT VS. PITCH ANGLE

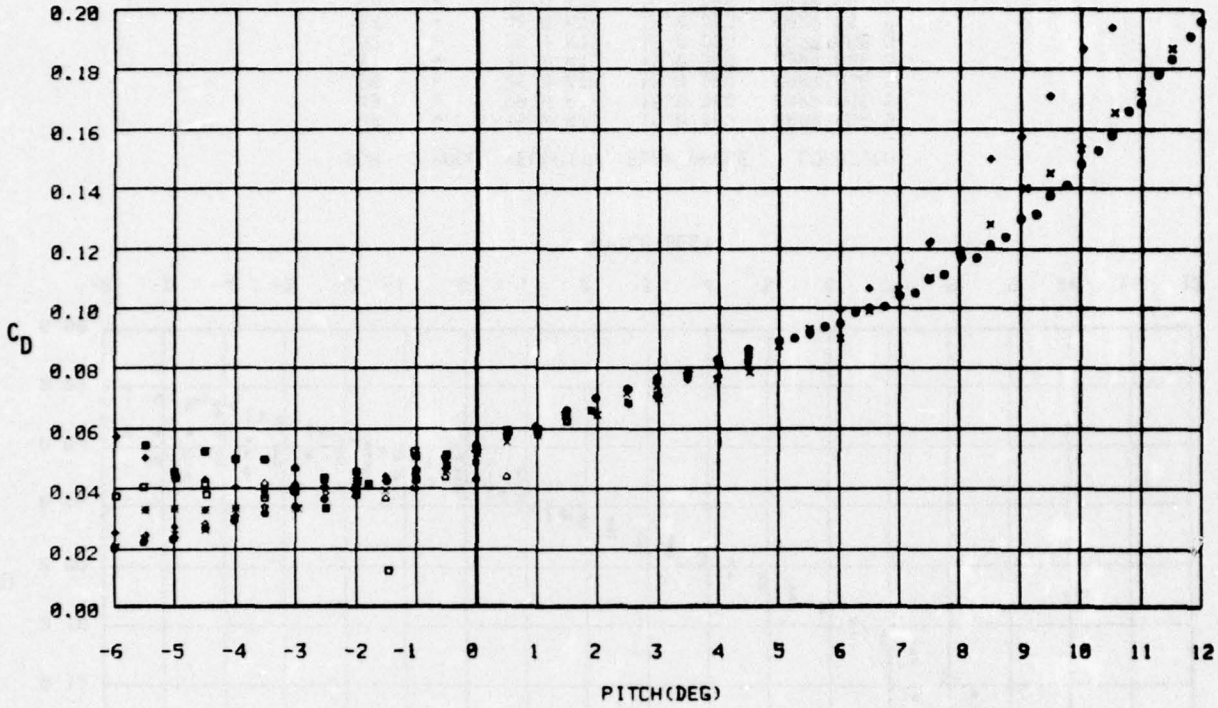

RUN	SYMBOL	VELOCITY	FLAP ANGLE	LOCATION
146	•	15.9 KTS	15.0 DEG	ROTATING ARM
150	×	20.2 KTS	15.0 DEG	ROTATING ARM
147	◇	25.1 KTS	15.0 DEG	ROTATING ARM
151	■	30.1 KTS	15.0 DEG	ROTATING ARM
148	□	35.1 KTS	15.0 DEG	ROTATING ARM
152	◆	40.0 KTS	15.0 DEG	ROTATING ARM
149	■	45.1 KTS	15.0 DEG	ROTATING ARM
153	○	50.2 KTS	15.0 DEG	ROTATING ARM

DRAG COEFFICIENT VS. PITCH ANGLE

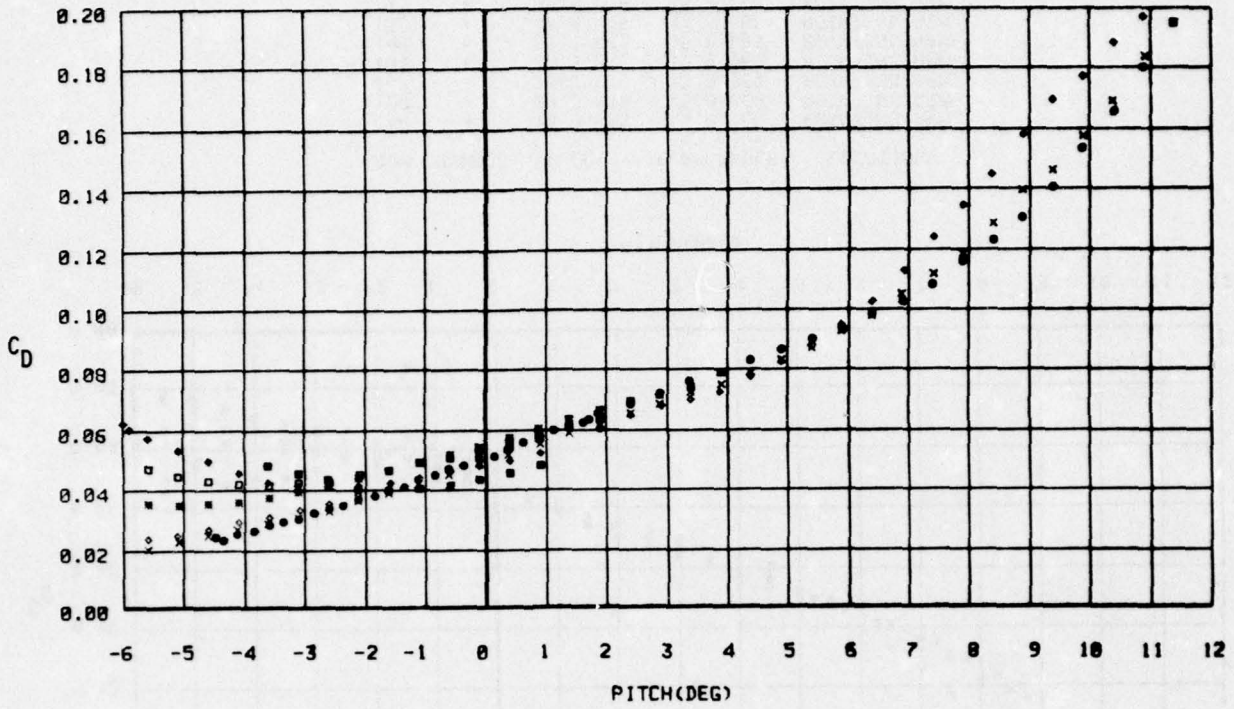

RUN	SYMBOL	VELOCITY	FLAP ANGLE	LOCATION
48	•	15.9 KTS	15.0 DEG	CARRIAGE 5
49	×	20.0 KTS	15.0 DEG	CARRIAGE 5
50	◇	25.0 KTS	15.0 DEG	CARRIAGE 5
51	■	30.0 KTS	15.0 DEG	CARRIAGE 5
52	□	35.1 KTS	15.0 DEG	CARRIAGE 5
53	◆	40.0 KTS	15.0 DEG	CARRIAGE 5
54	▪	45.4 KTS	15.0 DEG	CARRIAGE 5

DRAG COEFFICIENT VS. PITCH ANGLE

APPENDIX B - LIFT, DRAG, AND L/D INFORMATION FOR 16-309 FOIL IN HIGH-SPEED TOW FACILITY

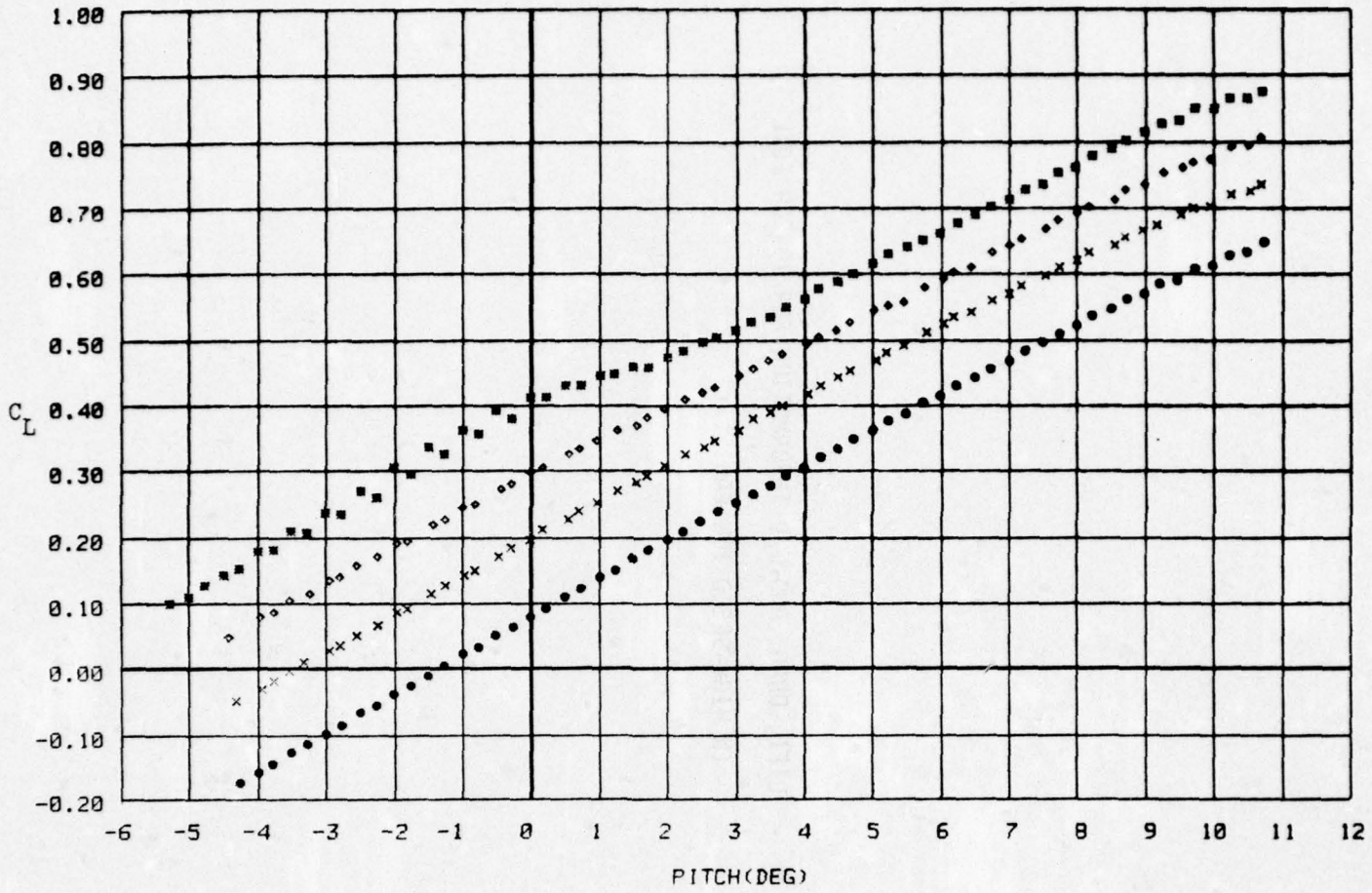

RUN	SYMBOL	VELOCITY	FLAP ANGLE	LOCATION
6	•	15.9 KTS	0.0 DEG	CARRIAGE 5
12	×	16.0 KTS	5.0 DEG	CARRIAGE 5
18	◇	16.0 KTS	10.0 DEG	CARRIAGE 5
23	*	15.9 KTS	15.0 DEG	CARRIAGE 5

LIFT COEFFICIENT VS. PITCH ANGLE

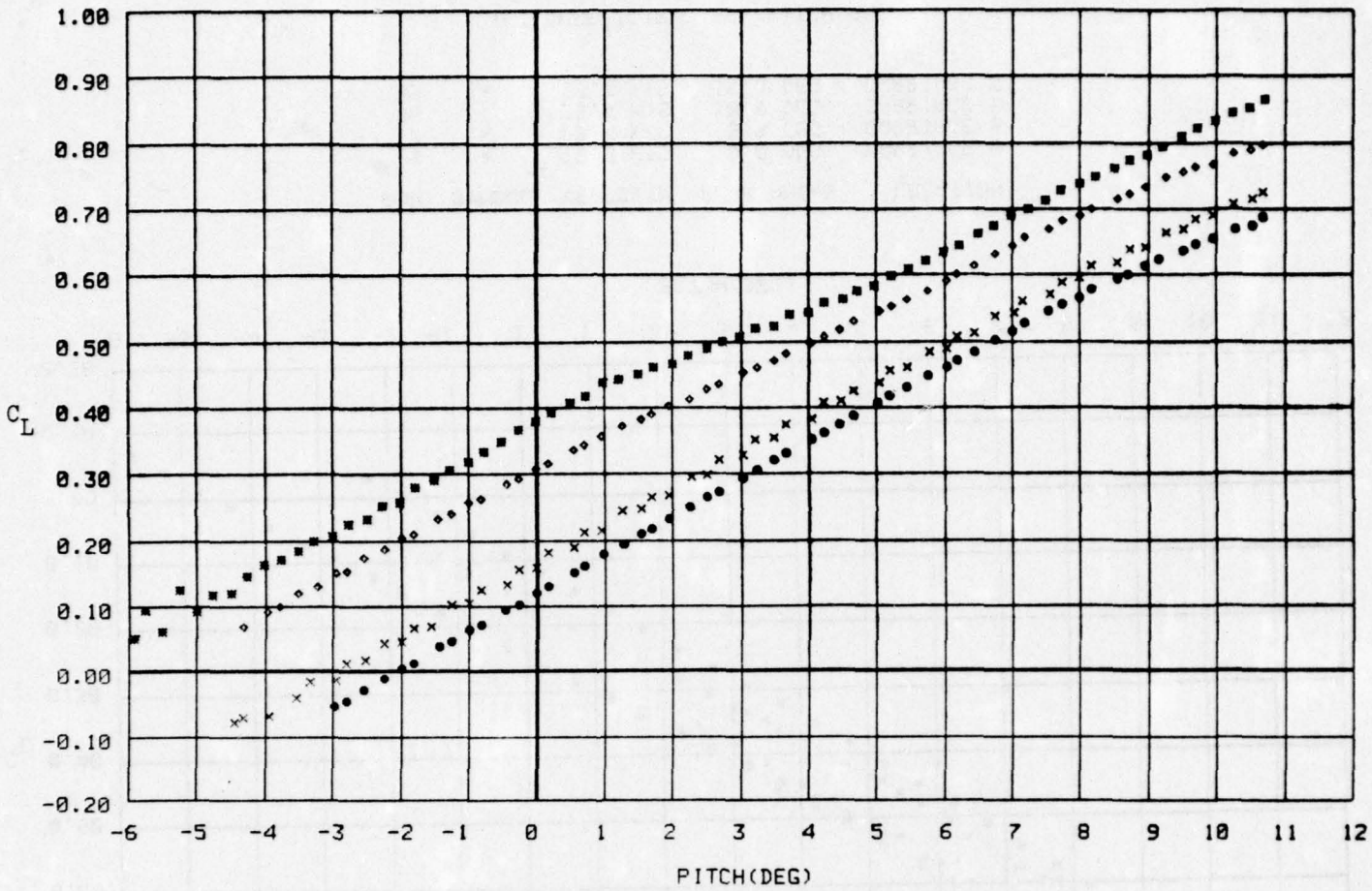

RUN	SYMBOL	VELOCITY	FLAP ANGLE	LOCATION
1	•	19.5 KTS	0.0 DEG	CARRIAGE 5
13	×	19.5 KTS	5.0 DEG	CARRIAGE 5
19	◇	19.5 KTS	10.0 DEG	CARRIAGE 5
24	•	19.4 KTS	15.0 DEG	CARRIAGE 5

LIFT COEFFICIENT VS. PITCH ANGLE

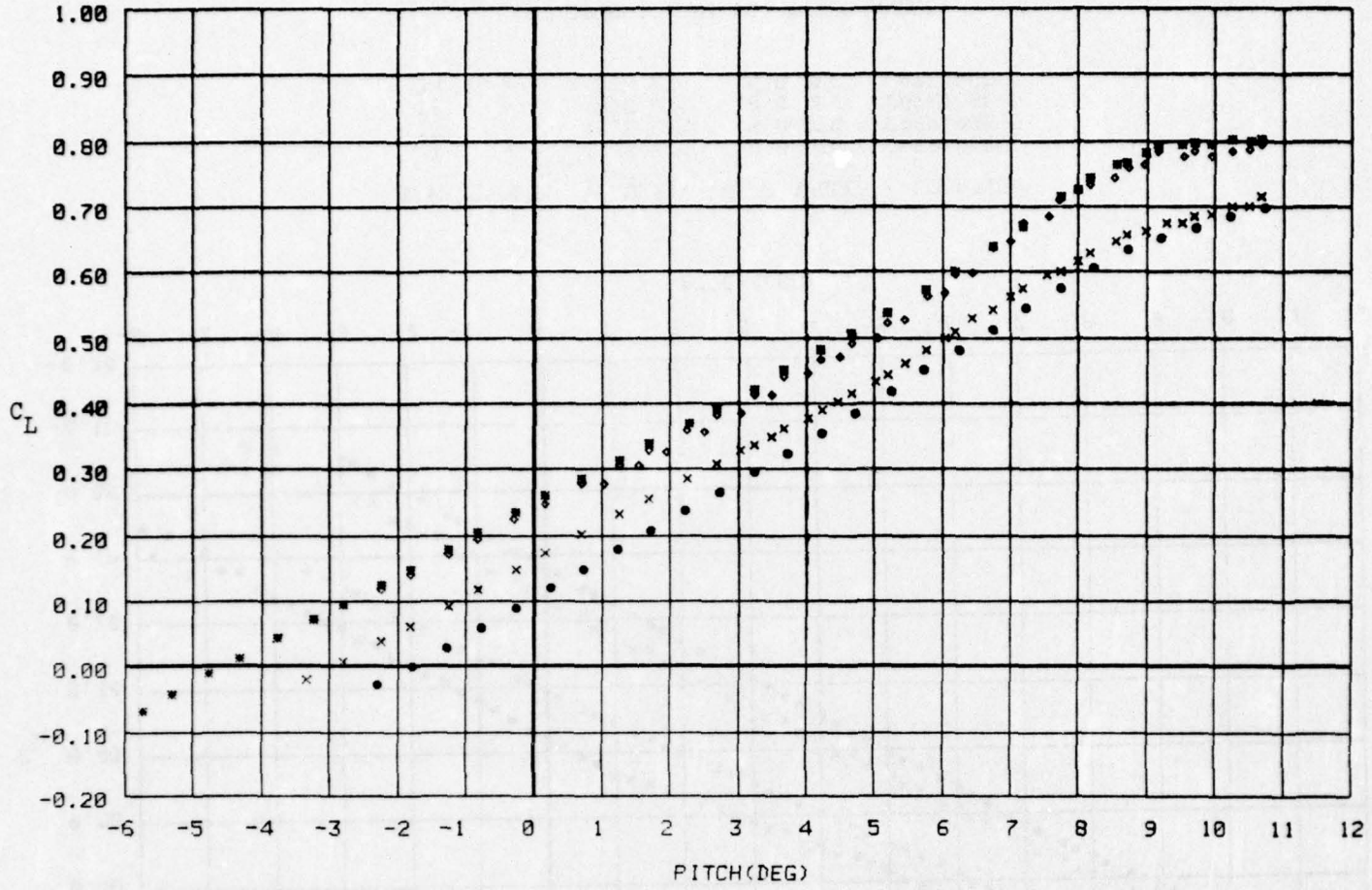

RUN	SYMBOL	VELOCITY	FLAP ANGLE	LOCATION
3	•	29.3 KTS	0.0 DEG	CARRIAGE 5
17	×	29.4 KTS	5.0 DEG	CARRIAGE 5
20	◇	29.4 KTS	10.0 DEG	CARRIAGE 5
25	*	29.3 KTS	15.0 DEG	CARRIAGE 5

LIFT COEFFICIENT VS. PITCH ANGLE

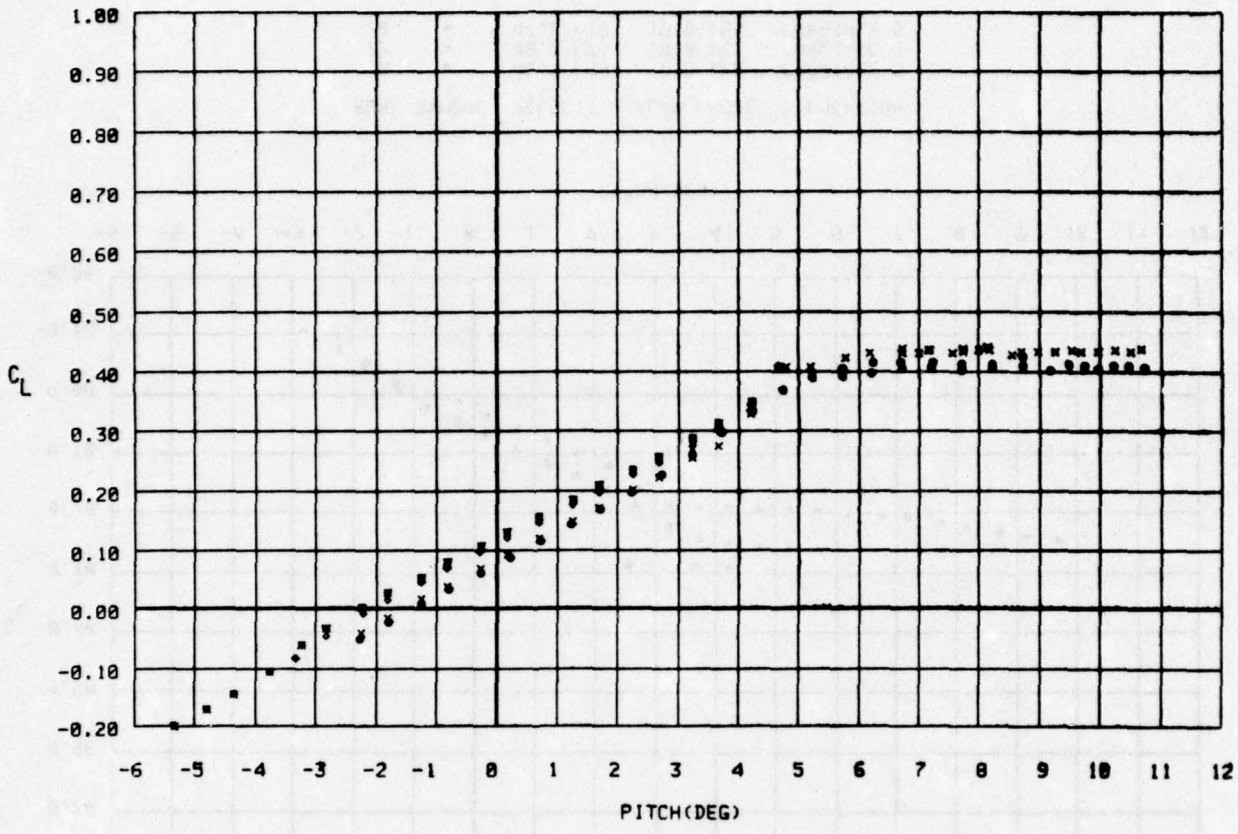

RUN	SYMBOL	VELOCITY	FLAP ANGLE	LOCATION
4	•	38.9 KTS	0.0 DEG	CARRIAGE 5
15	×	39.0 KTS	5.0 DEG	CARRIAGE 5
21	◦	39.1 KTS	10.0 DEG	CARRIAGE 5
26	▪	39.0 KTS	15.0 DEG	CARRIAGE 5

LIFT COEFFICIENT VS. PITCH ANGLE

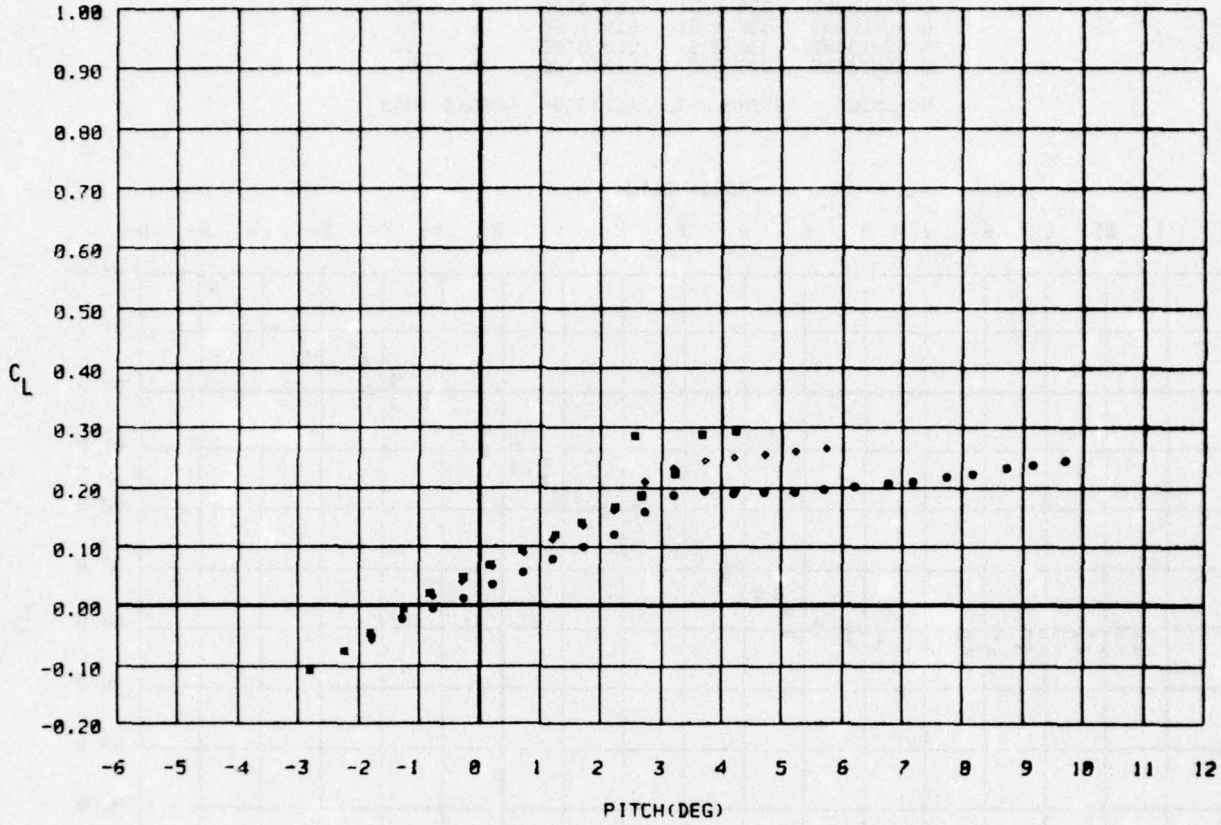

RUN	SYMBOL	VELOCITY	FLAP ANGLE	LOCATION
8	•	48.7 KTS	0.0 DEG	CARRIAGE 5
22	◦	48.7 KTS	10.0 DEG	CARRIAGE 5
28	•	47.2 KTS	15.0 DEG	CARRIAGE 5

LIFT COEFFICIENT VS. PITCH ANGLE

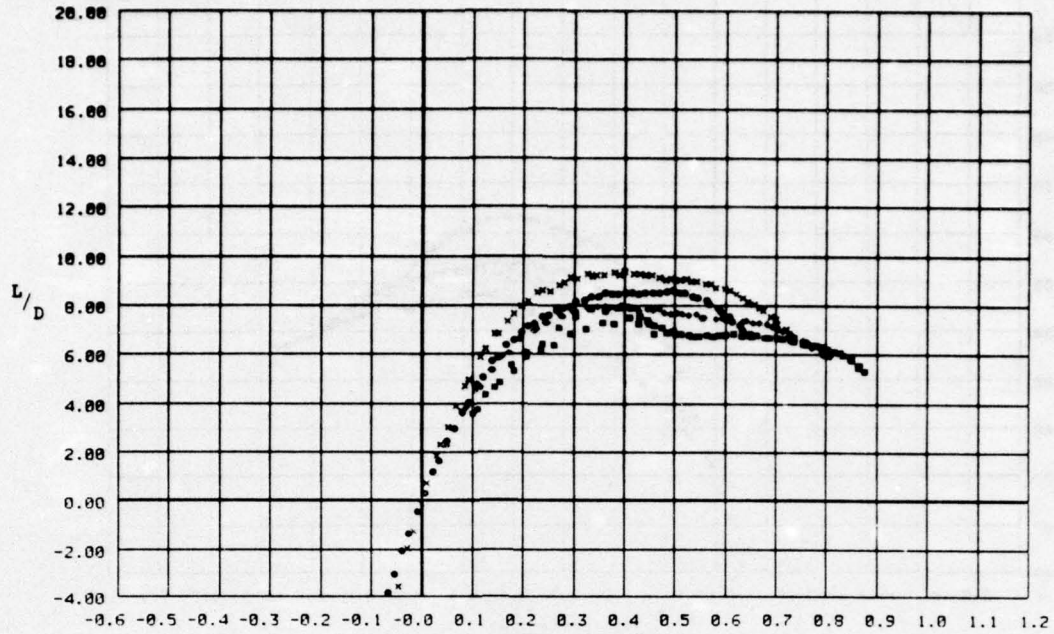

LIFT/DRAG VS. LIFT COEFFICIENT

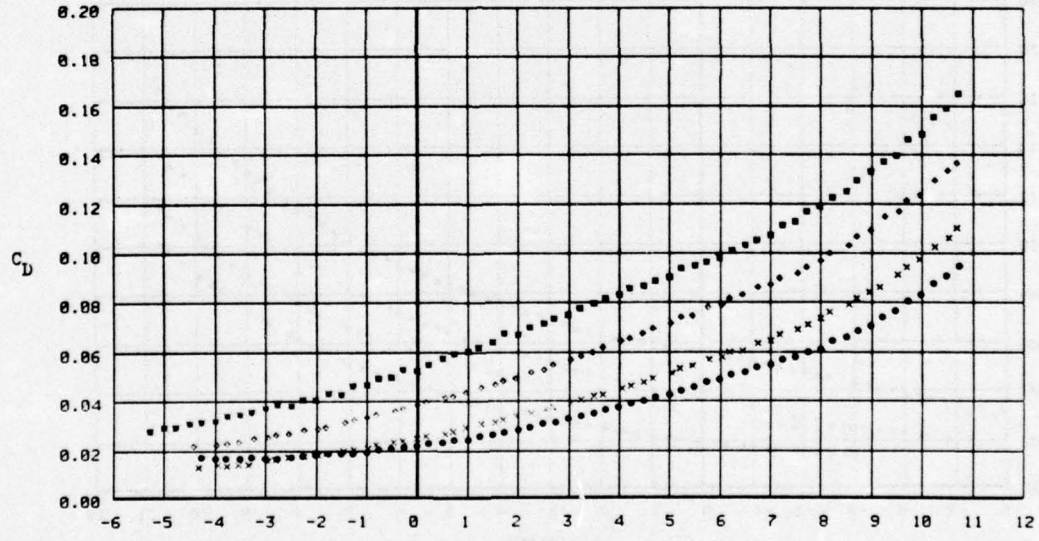

DRAG COEFFICIENT VS PITCH ANGLE

RUN	SYMBOL	VELOCITY	FLAP ANGLE	LOCATION
6	•	15.9 KTS	0.0 DEG	CARRIAGE 5
12	×	16.0 KTS	5.0 DEG	CARRIAGE 5
18	◇	16.0 KTS	10.0 DEG	CARRIAGE 5
23	•	15.9 KTS	15.0 DEG	CARRIAGE 5

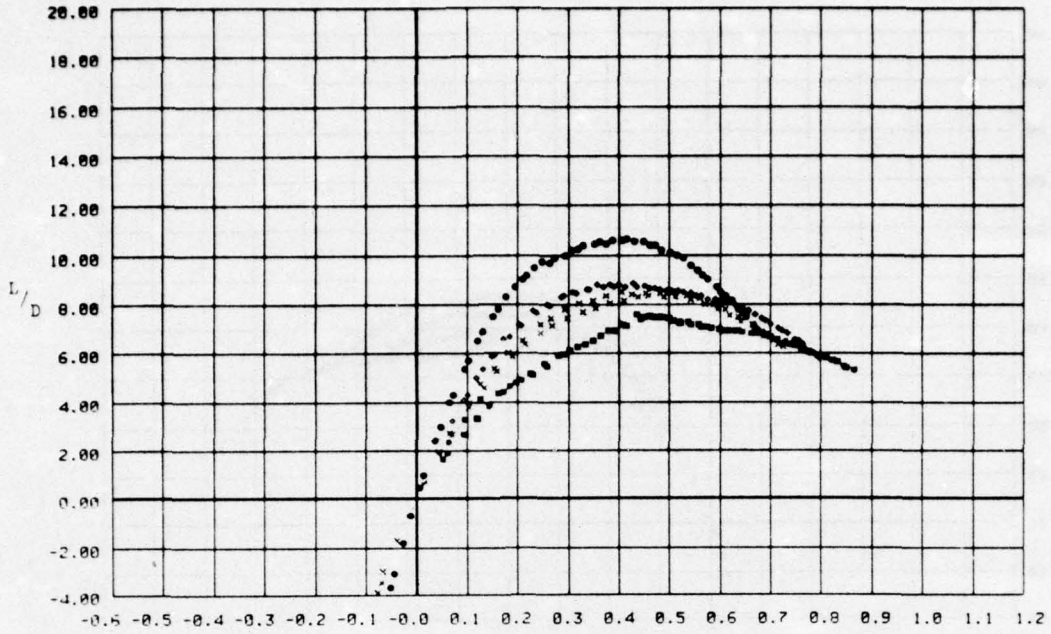

LIFT/DRAG VS. LIFT COEFFICIENT

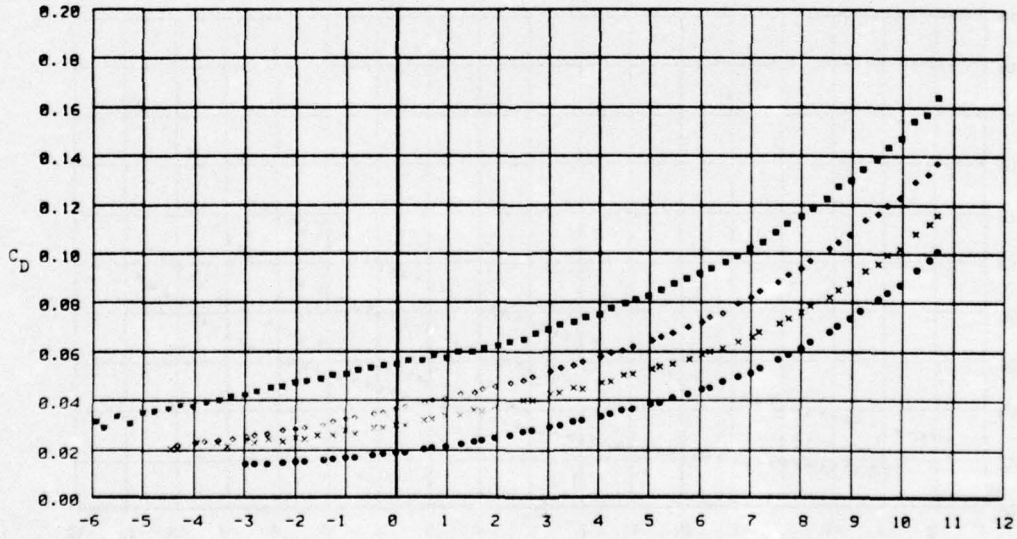

DRAG COEFFICIENT VS. PITCH ANGLE

RUN	SYMBOL	VELOCITY	FLAP ANGLE	LOCATION
1	•	19.5 KTS	0.0 DEG	CARRIAGE 5
13	×	19.5 KTS	5.0 DEG	CARRIAGE 5
19	◦	19.5 KTS	10.0 DEG	CARRIAGE 5
24	•	19.4 KTS	15.0 DEG	CARRIAGE 5

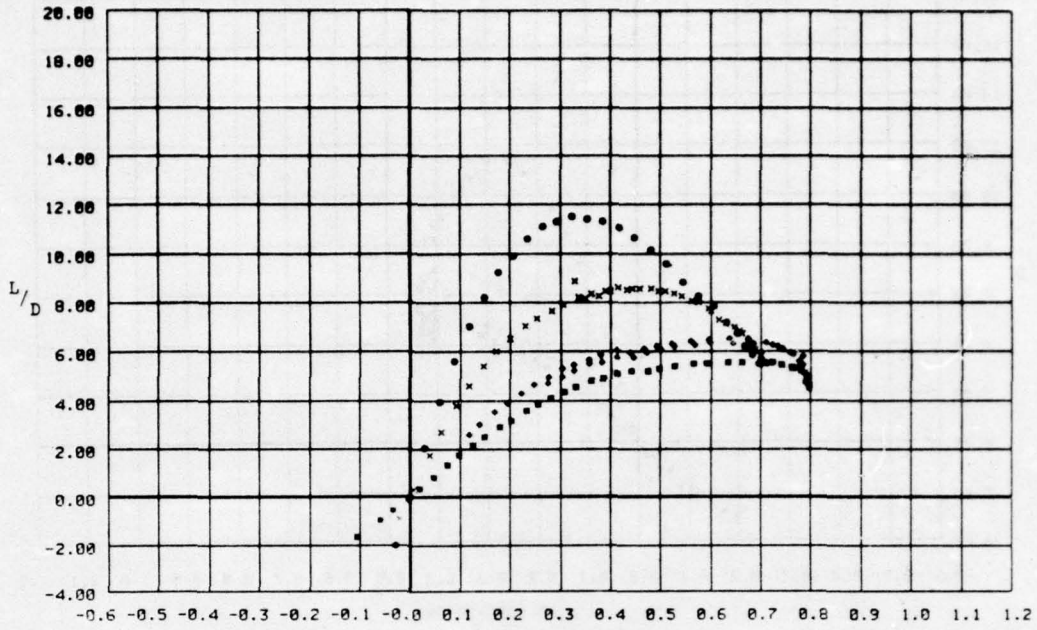

LIFT/DRAG VS. LIFT COEFFICIENT

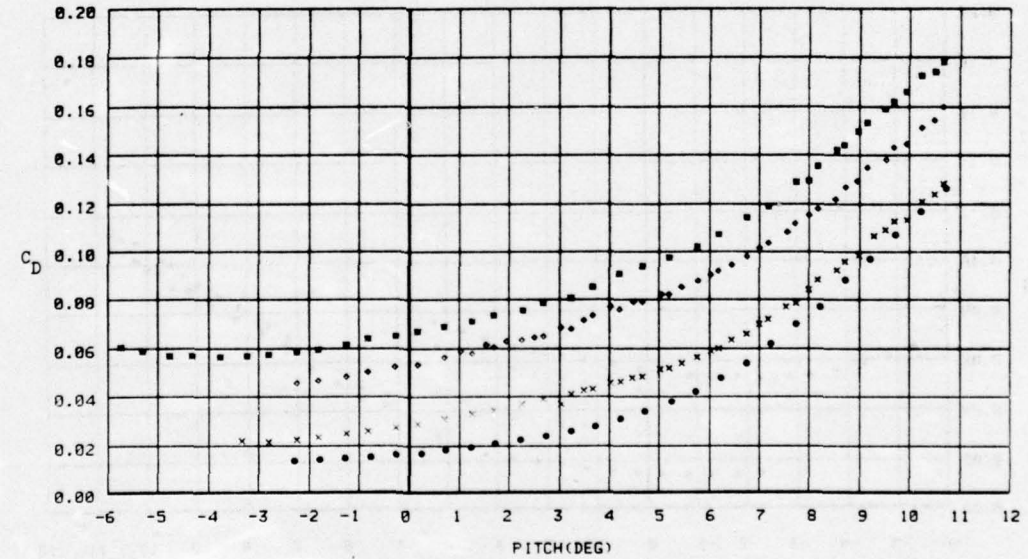

DRAG COEFFICIENT VS. PITCH ANGLE

RUN	SYMBOL	VELOCITY	FLAP ANGLE	LOCATION
3	•	29.3 KTS	0.0 DEG	CARRIAGE 5
17	×	29.4 KTS	5.0 DEG	CARRIAGE 5
20	^	29.4 KTS	10.0 DEG	CARRIAGE 5
25	•	29.3 KTS	15.0 DEG	CARRIAGE 5

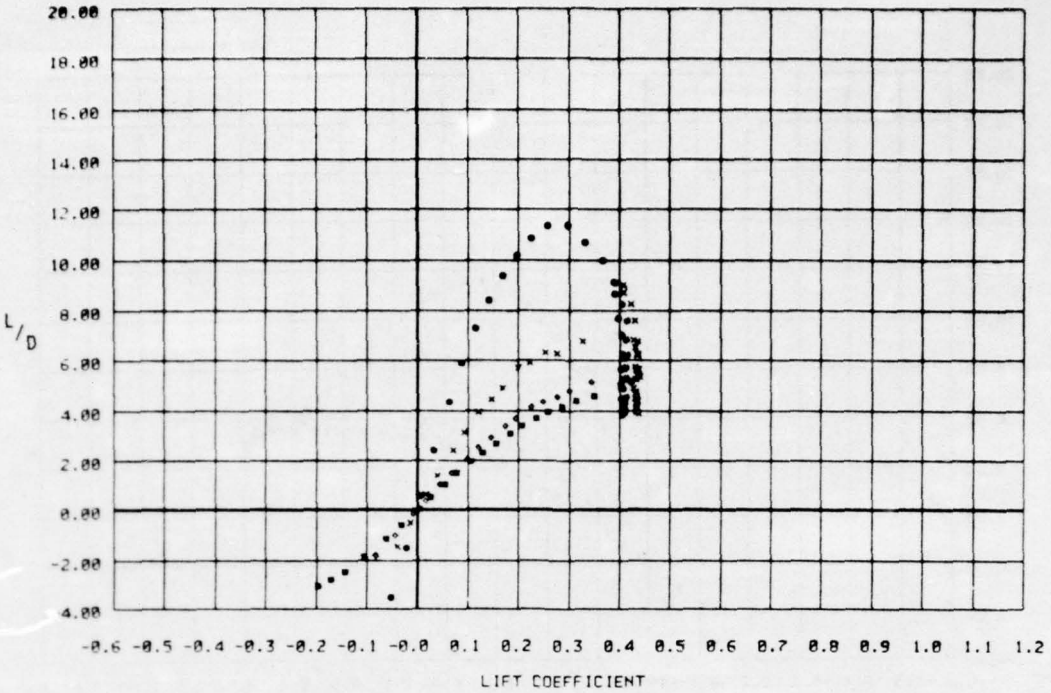

LIFT/DRAG VS. LIFT COEFFICIENT

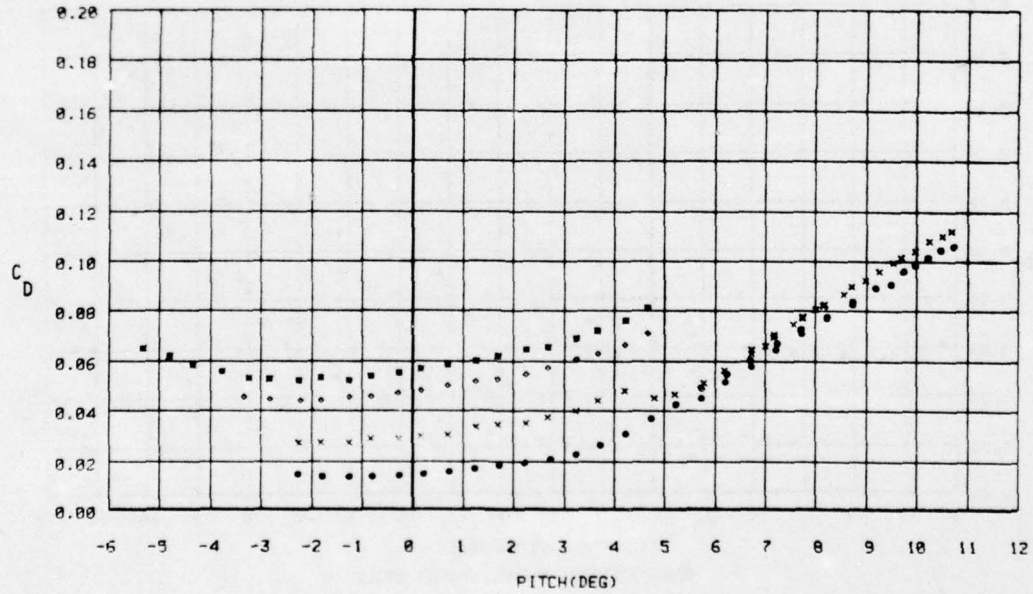

RUN	SYMBOL	VELOCITY	FLAP ANGLE	LOCATION
4	•	38.9 KTS	0.0 DEG	CARRIAGE 5
15	×	39.0 KTS	5.0 DEG	CARRIAGE 5
21	◇	39.1 KTS	10.0 DEG	CARRIAGE 5
26	▪	39.0 KTS	15.0 DEG	CARRIAGE 5

DRAG COEFFICIENT VS. PITCH ANGLE

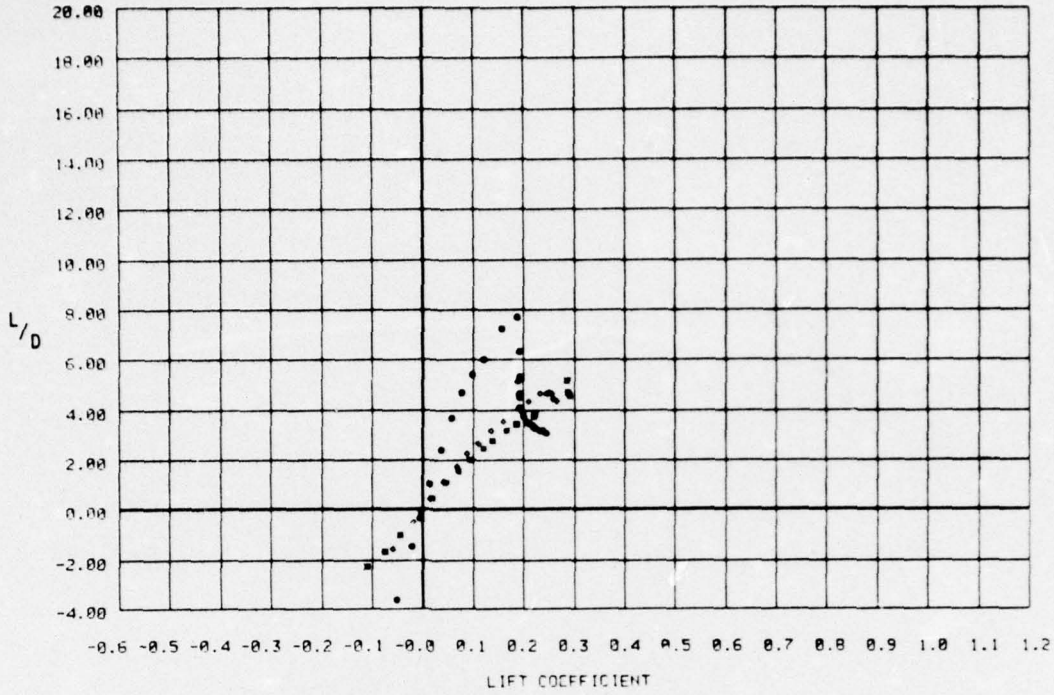

LIFT/DRAG VS. LIFT COEFFICIENT

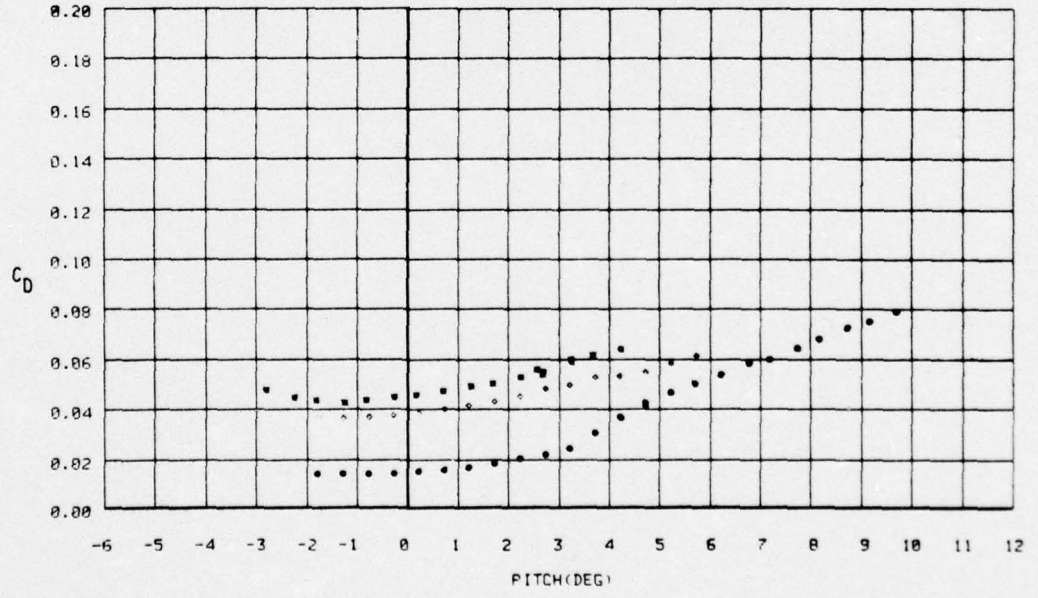

RUN	SYMBOL	VELOCITY	FLAP ANGLE	LOCATION
8	•	48.7 KTS	0.0 DEG	CARRIAGE 5
22	◦	48.7 KTS	10.0 DEG	CARRIAGE 5
28	•	47.2 KTS	15.0 DEG	CARRIAGE 5

DRAG COEFFICIENT VS. PITCH ANGLE

APPENDIX C - LIFT, DRAG, AND L/D INFORMATION FOR 64A309 FOIL IN HIGH-SPEED TOW FACILITY

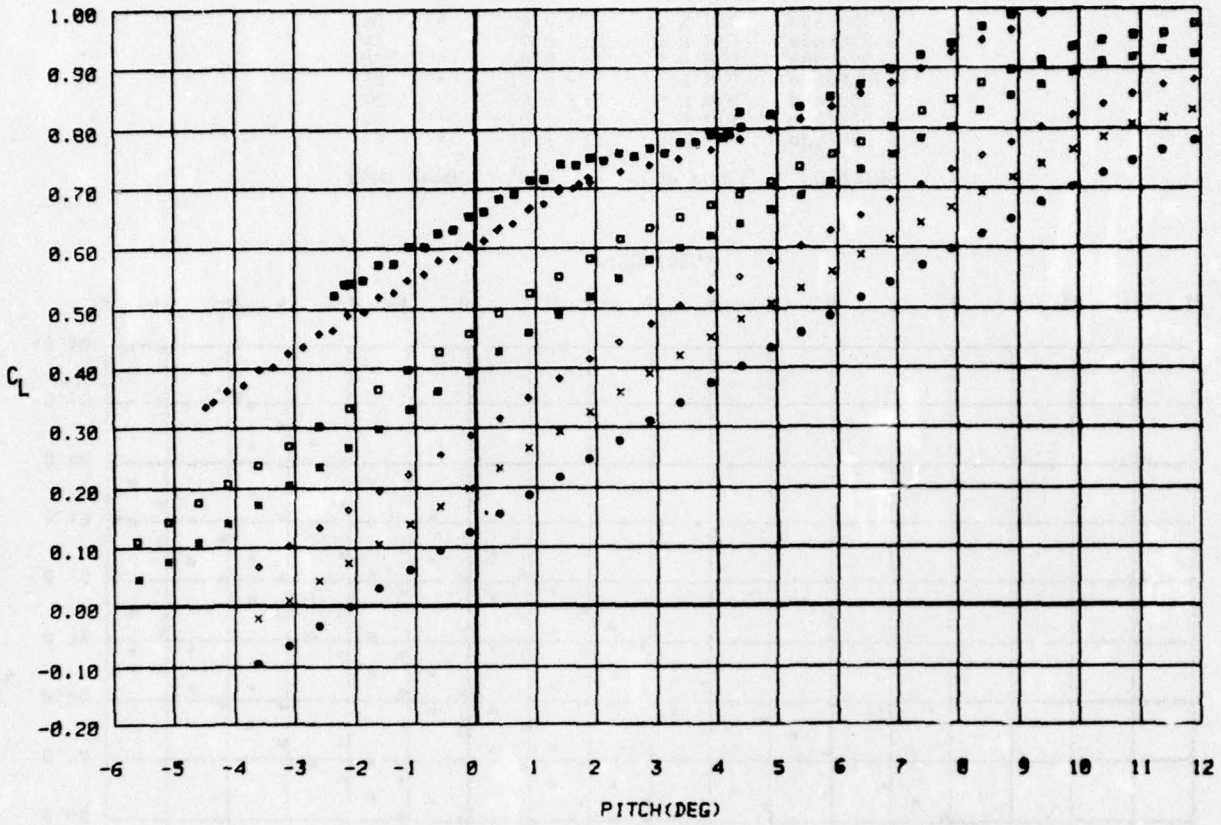

RUN	SYMBOL	VELOCITY	FLAP ANGLE	LOCATION
1	•	15.9 KTS	0.0 DEG	CARRIAGE 5
17	×	15.9 KTS	2.5 DEG	CARRIAGE 5
25	◇	15.9 KTS	5.0 DEG	CARRIAGE 5
33	■	15.8 KTS	7.5 DEG	CARRIAGE 5
41	□	15.9 KTS	10.0 DEG	CARRIAGE 5
48	◆	15.9 KTS	15.0 DEG	CARRIAGE 5
55	■	15.9 KTS	17.5 DEG	CARRIAGE 5

LIFT COEFFICIENT VS. PITCH ANGLE

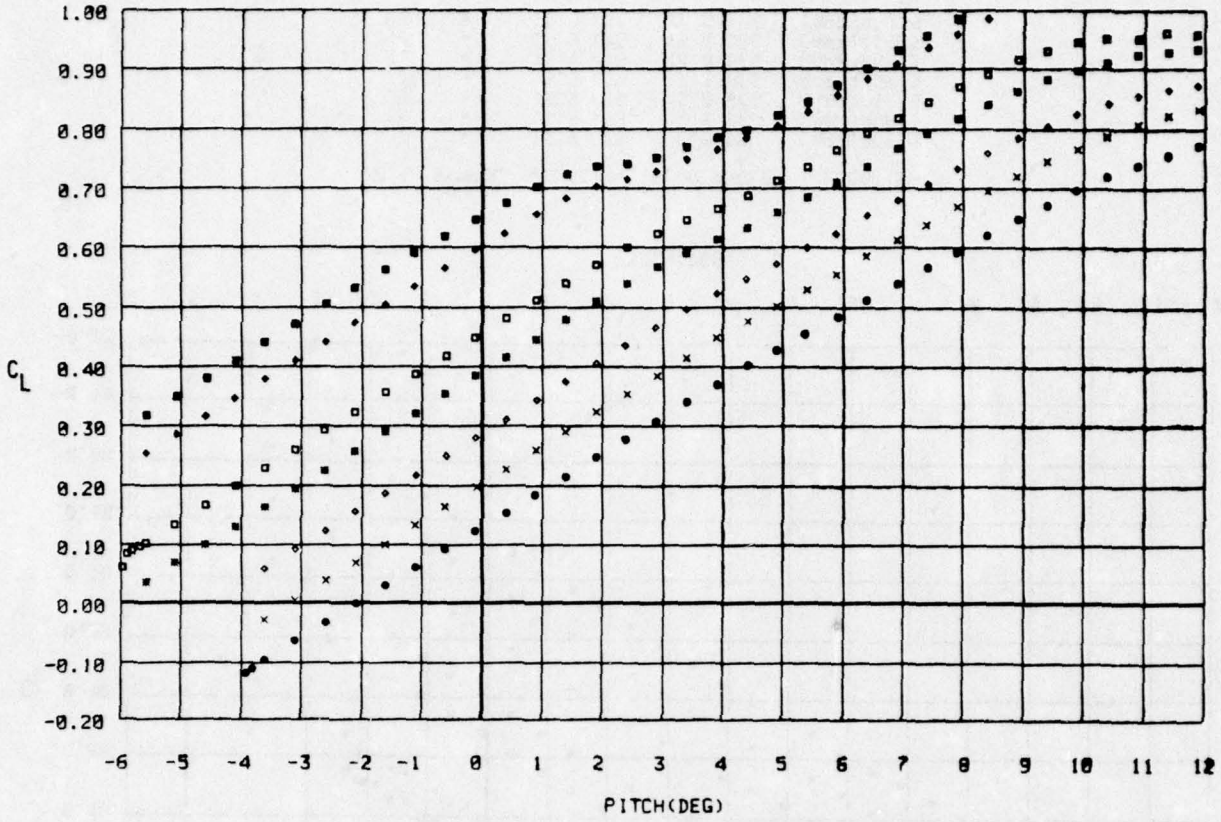

RUN	SYMBOL	VELOCITY	FLAP ANGLE	LOCATION
3	•	19.9 KTS	0.0 DEG	CARRIAGE 5
18	×	20.2 KTS	2.5 DEG	CARRIAGE 5
26	◇	20.0 KTS	5.0 DEG	CARRIAGE 5
34	▪	20.0 KTS	7.5 DEG	CARRIAGE 5
42	□	20.0 KTS	10.0 DEG	CARRIAGE 5
49	◆	20.0 KTS	15.0 DEG	CARRIAGE 5
56	■	20.0 KTS	17.5 DEG	CARRIAGE 5

LIFT COEFFICIENT VS. PITCH ANGLE

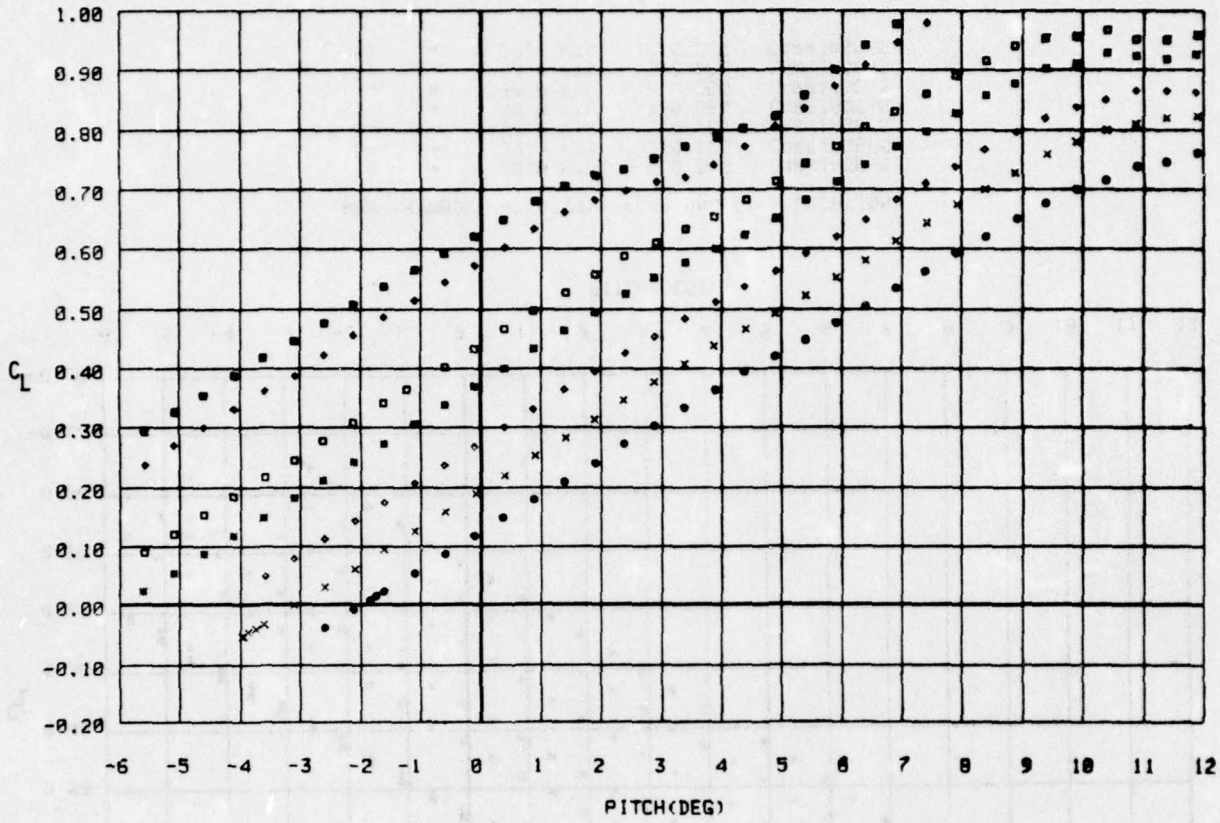

RUN	SYMBOL	VELOCITY	FLAP ANGLE	LOCATION
4	•	25.0 KTS	0.0 DEG	CARRIAGE 5
19	×	25.0 KTS	2.5 DEG	CARRIAGE 5
27	◦	25.1 KTS	5.0 DEG	CARRIAGE 5
35	▪	25.0 KTS	7.5 DEG	CARRIAGE 5
43	□	25.0 KTS	10.0 DEG	CARRIAGE 5
50	◆	25.0 KTS	15.0 DEG	CARRIAGE 5
57	■	25.0 KTS	17.5 DEG	CARRIAGE 5

LIFT COEFFICIENT VS. PITCH ANGLE

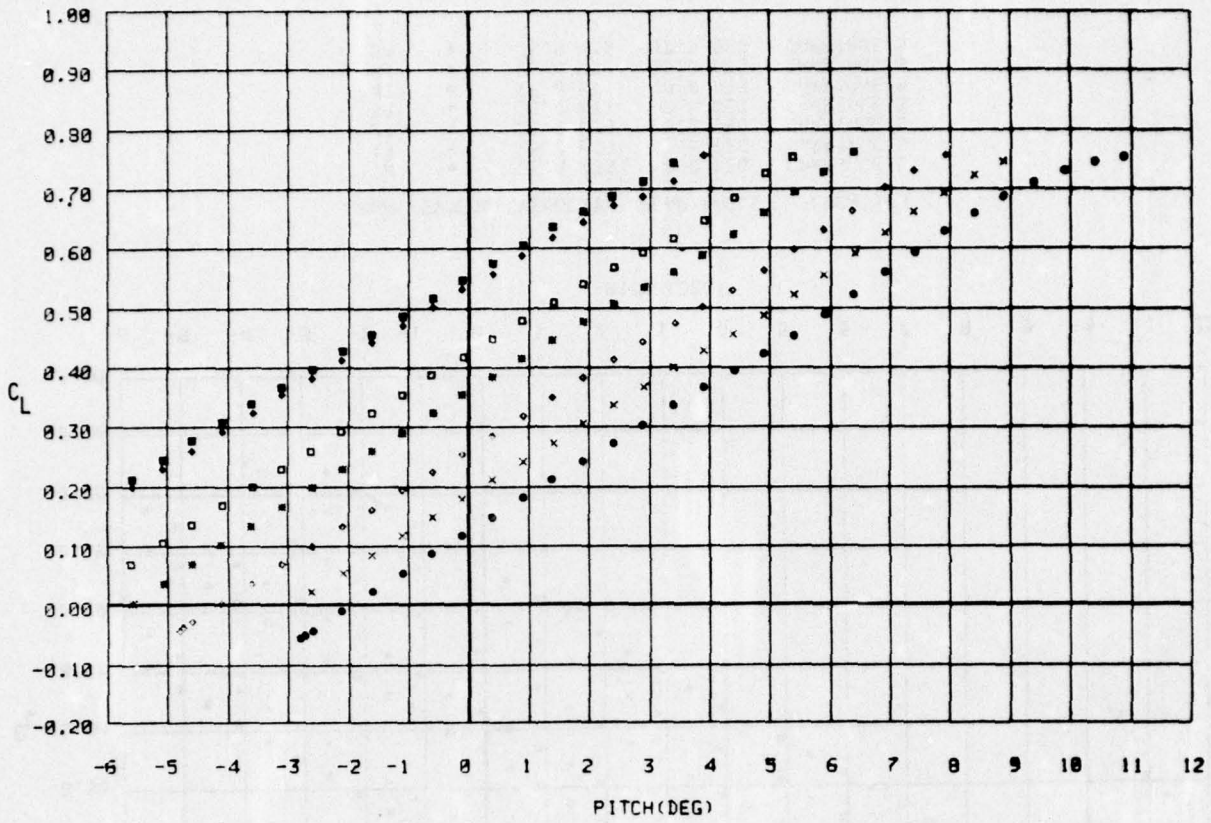

RUN	SYMBOL	VELOCITY	FLAP ANGLE	LOCATION
9	•	30.0 KTS	0.0 DEG	CARRIAGE 5
20	×	29.9 KTS	2.5 DEG	CARRIAGE 5
28	◇	30.0 KTS	5.0 DEG	CARRIAGE 5
36	◆	30.0 KTS	7.5 DEG	CARRIAGE 5
44	□	30.0 KTS	10.0 DEG	CARRIAGE 5
51	◆	30.0 KTS	15.0 DEG	CARRIAGE 5
58	■	30.1 KTS	17.5 DEG	CARRIAGE 5

LIFT COEFFICIENT VS. PITCH ANGLE

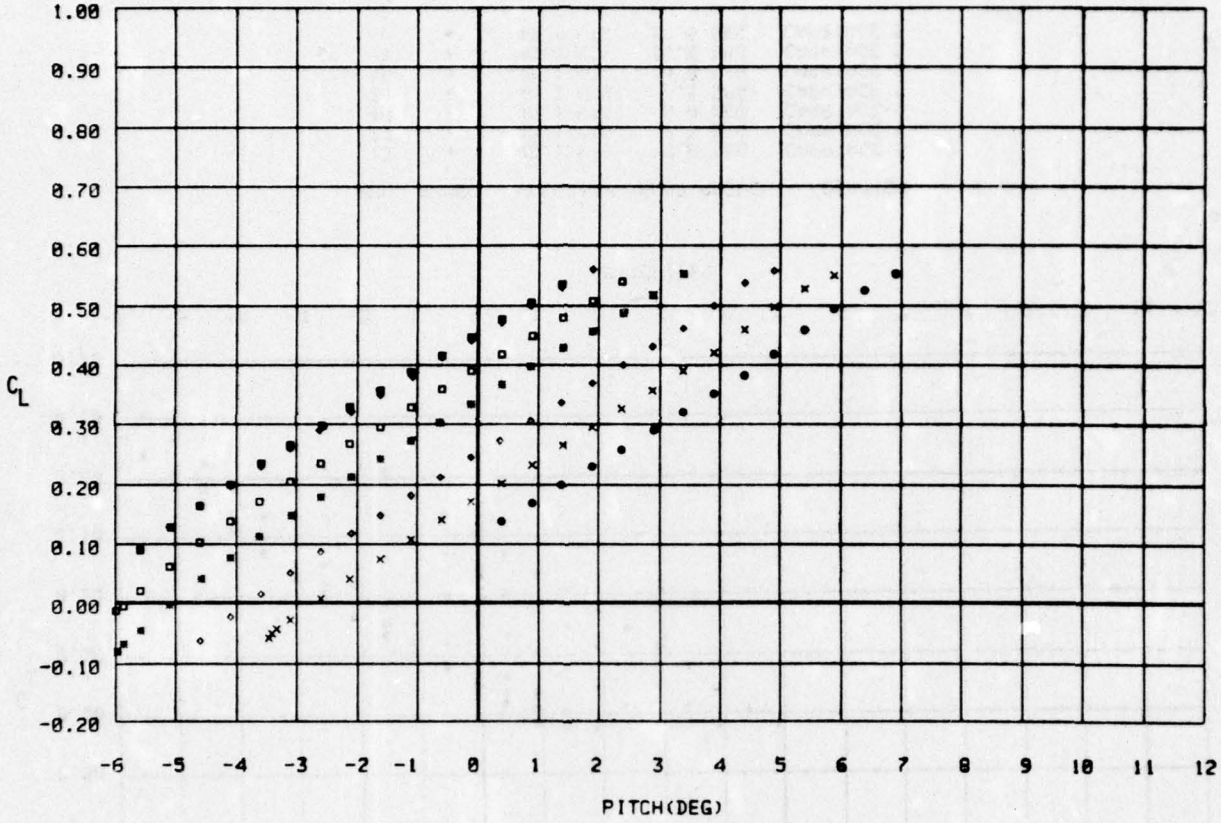

RUN	SYMBOL	VELOCITY	FLAP ANGLE	LOCATION
11	•	35.0 KTS	0.0 DEG	CARRIAGE 5
21	×	35.1 KTS	2.5 DEG	CARRIAGE 5
29	◇	35.0 KTS	5.0 DEG	CARRIAGE 5
37	■	35.0 KTS	7.5 DEG	CARRIAGE 5
45	□	35.0 KTS	10.0 DEG	CARRIAGE 5
52	◆	35.1 KTS	15.0 DEG	CARRIAGE 5
59	■	35.1 KTS	17.5 DEG	CARRIAGE 5

LIFT COEFFICIENT VS. PITCH ANGLE

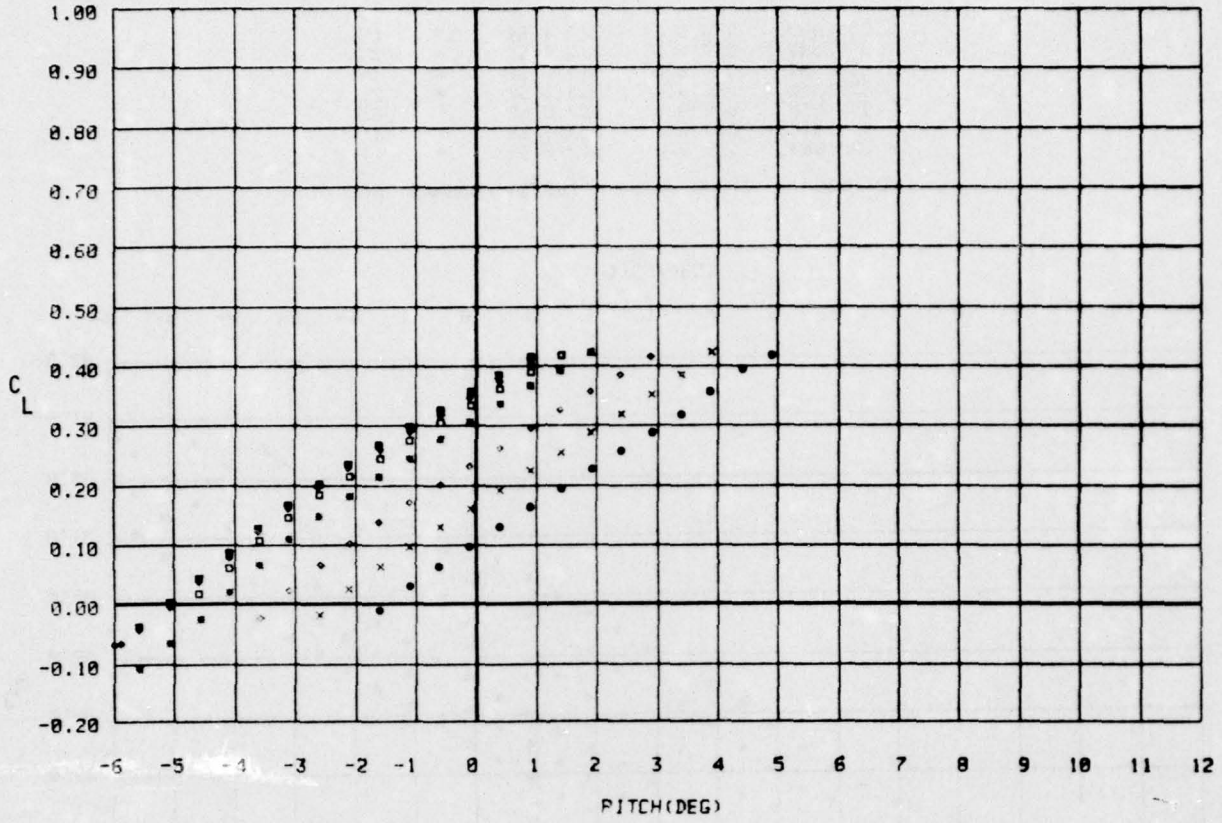

RUN	SYMBOL	VELOCITY	FLAP ANGLE	LOCATION
12	•	40.1 KTS	0.0 DEG	CARRIAGE 5
22	×	40.1 KTS	2.5 DEG	CARRIAGE 5
30	◇	40.1 KTS	5.0 DEG	CARRIAGE 5
38	▪	40.1 KTS	7.5 DEG	CARRIAGE 5
46	□	40.1 KTS	10.0 DEG	CARRIAGE 5
53	◆	40.0 KTS	15.0 DEG	CARRIAGE 5
60	■	40.1 KTS	17.5 DEG	CARRIAGE 5

LIFT COEFFICIENT VS. PITCH ANGLE

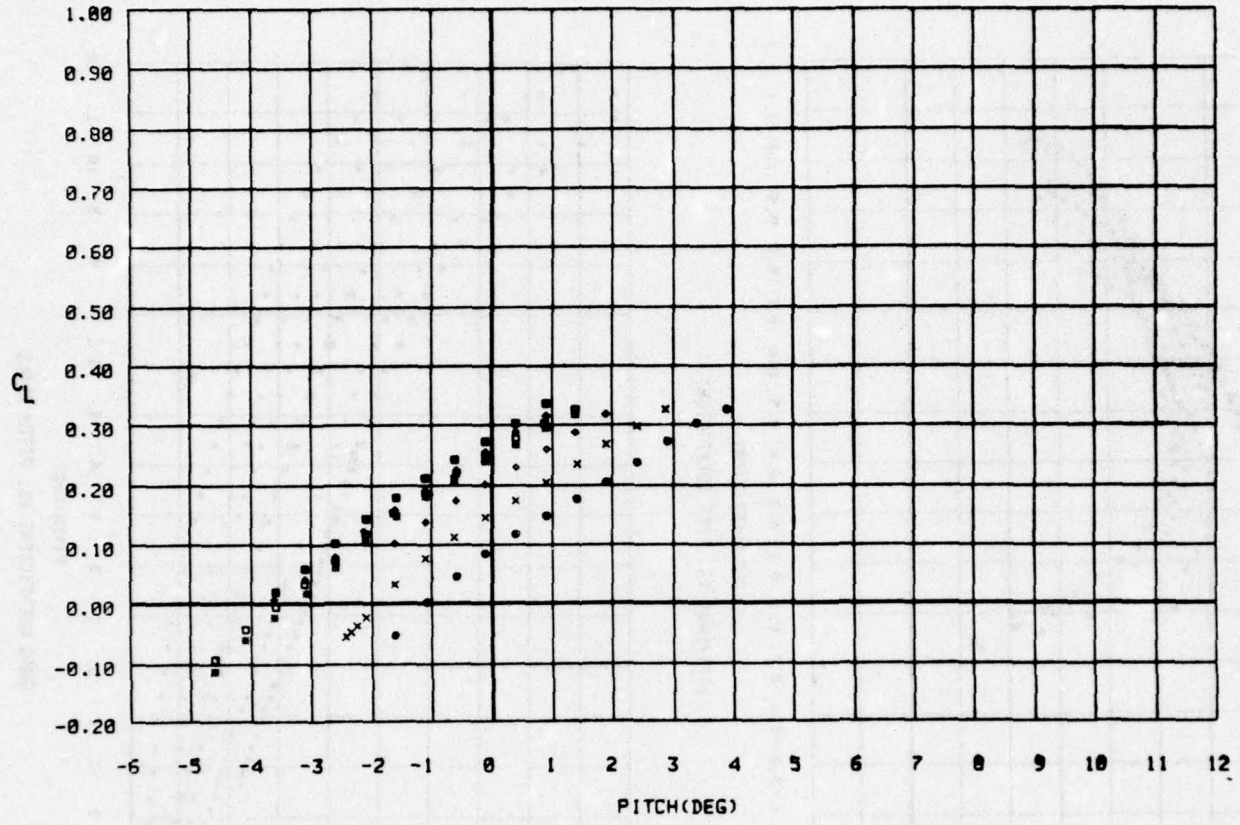

RUN	SYMBOL	VELOCITY	FLAP ANGLE	LOCATION
14	•	45.5 KTS	0.0 DEG	CARRIAGE 5
23	×	45.5 KTS	2.5 DEG	CARRIAGE 5
31	◇	45.4 KTS	5.0 DEG	CARRIAGE 5
39	■	45.4 KTS	7.5 DEG	CARRIAGE 5
47	□	45.3 KTS	10.0 DEG	CARRIAGE 5
54	◆	45.4 KTS	15.0 DEG	CARRIAGE 5
62	■	45.4 KTS	17.5 DEG	CARRIAGE 5

LIFT COEFFICIENT VS. PITCH ANGLE

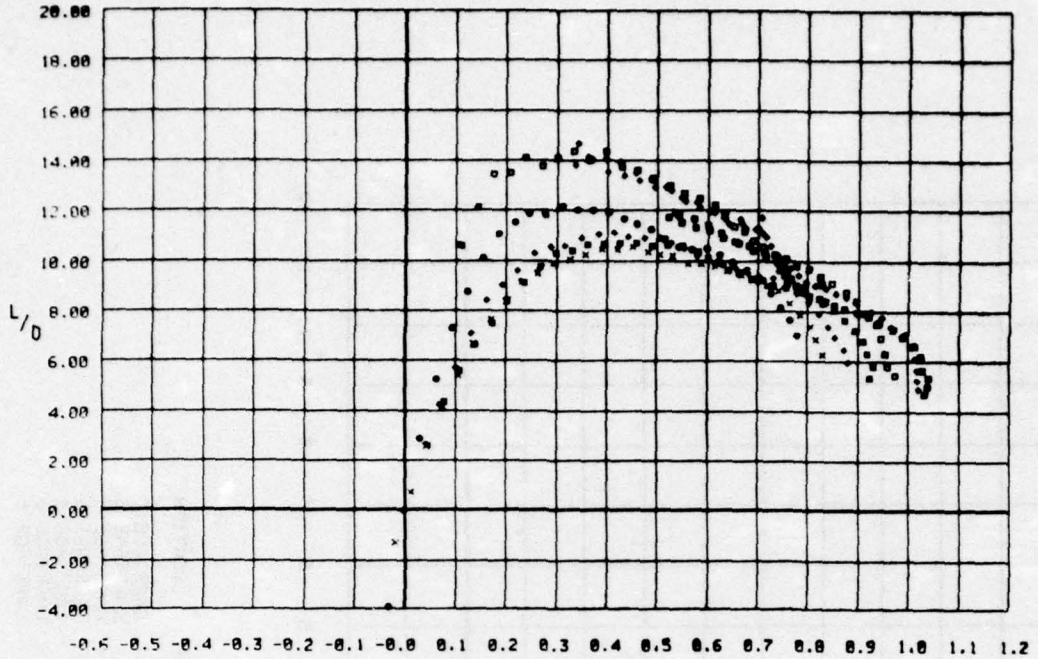

LIFT/DRAG VS. LIFT COEFFICIENT

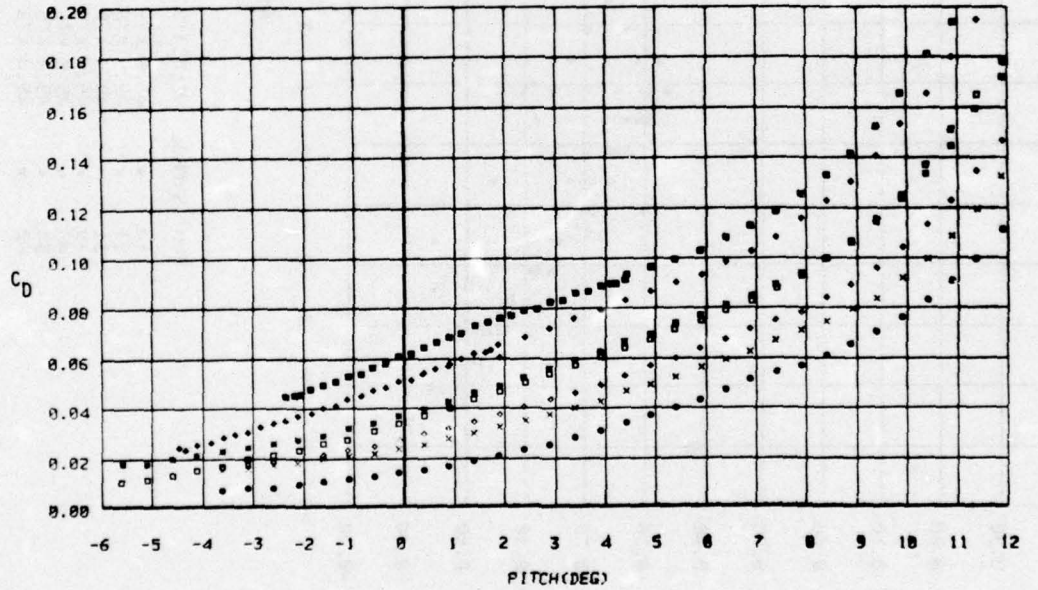

DRAG COEFFICIENT VS. PITCH ANGLE

RUN	SYMBOL	VELOCITY	FLAP ANGLE	LOCATION
1	•	15.9 KTS	0.0 DEG	CARRIAGE 5
17	×	15.9 KTS	2.5 DEG	CARRIAGE 5
25	◆	15.9 KTS	5.0 DEG	CARRIAGE 5
33	*	15.8 KTS	7.5 DEG	CARRIAGE 5
41	□	15.9 KTS	10.0 DEG	CARRIAGE 5
48	+	15.9 KTS	15.0 DEG	CARRIAGE 5
55	●	15.9 KTS	17.5 DEG	CARRIAGE 5

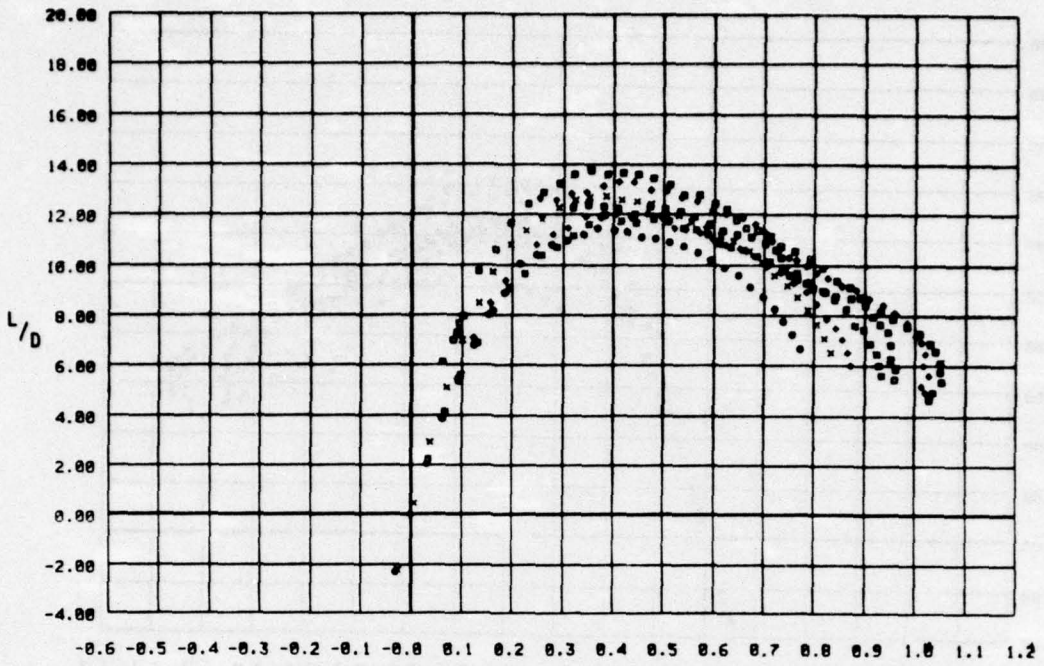

LIFT/DRAG VS. LIFT COEFFICIENT

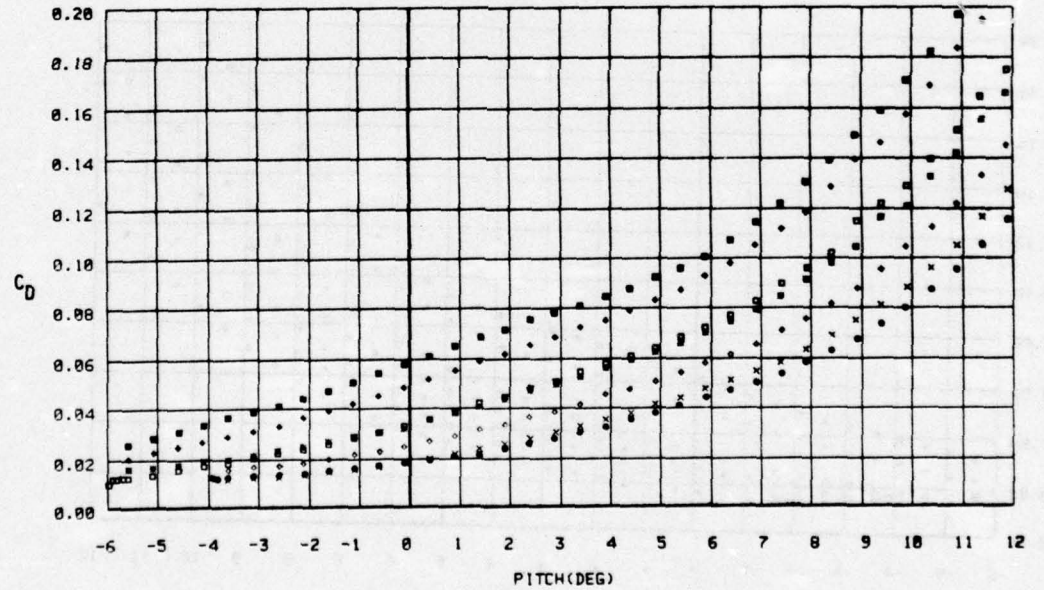

DRAG COEFFICIENT VS. PITCH ANGLE

RUN	SYMBOL	VELOCITY	FLAP ANGLE	LOCATION
3	•	19.9 KTS	0.0 DEG	CARRIAGE 5
18	×	20.2 KTS	2.5 DEG	CARRIAGE 5
26	▵	20.0 KTS	5.0 DEG	CARRIAGE 5
34	▪	20.0 KTS	7.5 DEG	CARRIAGE 5
42	▫	20.0 KTS	10.0 DEG	CARRIAGE 5
49	◆	20.0 KTS	15.0 DEG	CARRIAGE 5
56	◆	20.0 KTS	17.5 DEG	CARRIAGE 5

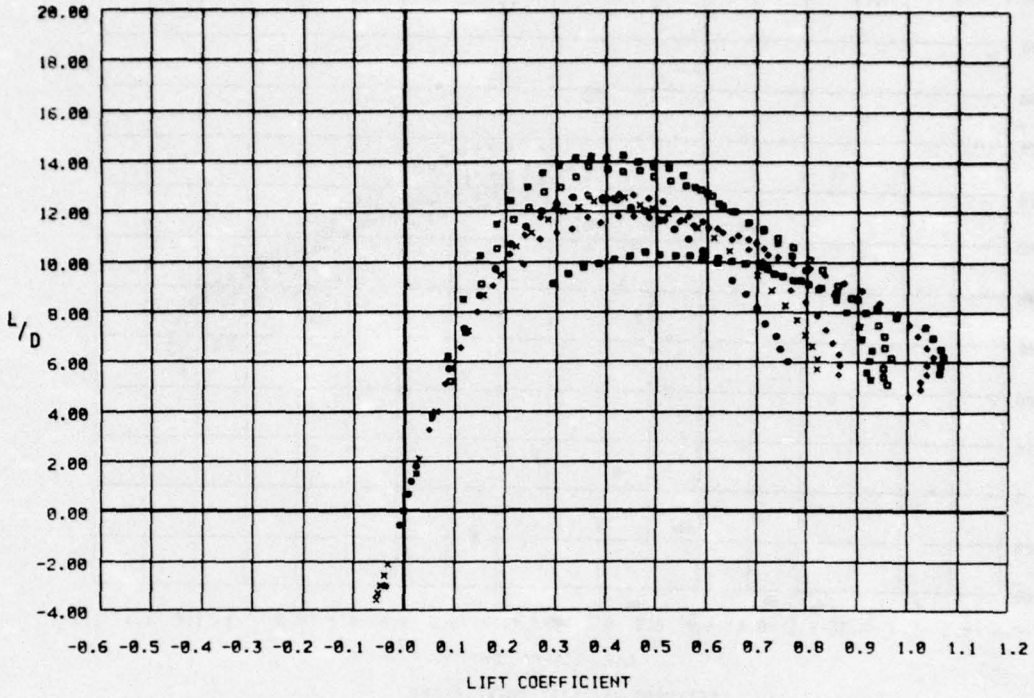

LIFT/DRAG VS. LIFT COEFFICIENT

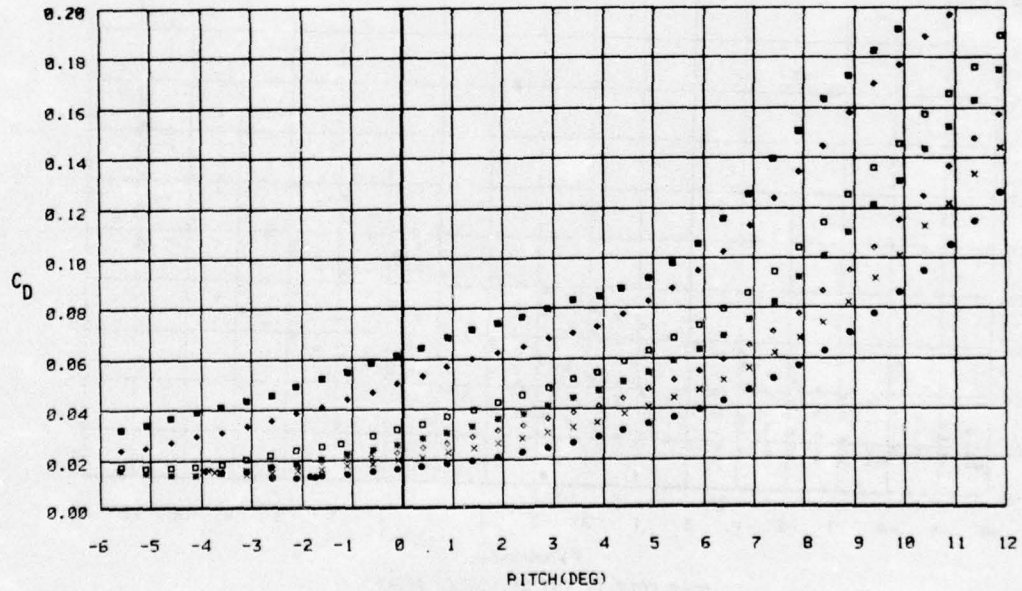

DRAG COEFFICIENT VS. PITCH ANGLE

RUN	SYMBOL	VELOCITY	FLAP ANGLE	LOCATION
4	•	25.0 KTS	0.0 DEG	CARRIAGE 5
19	×	25.0 KTS	2.5 DEG	CARRIAGE 5
27	◇	25.1 KTS	5.0 DEG	CARRIAGE 5
35	■	25.0 KTS	7.5 DEG	CARRIAGE 5
43	□	25.0 KTS	10.0 DEG	CARRIAGE 5
50	◆	25.0 KTS	15.0 DEG	CARRIAGE 5
57	▪	25.0 KTS	17.5 DEG	CARRIAGE 5

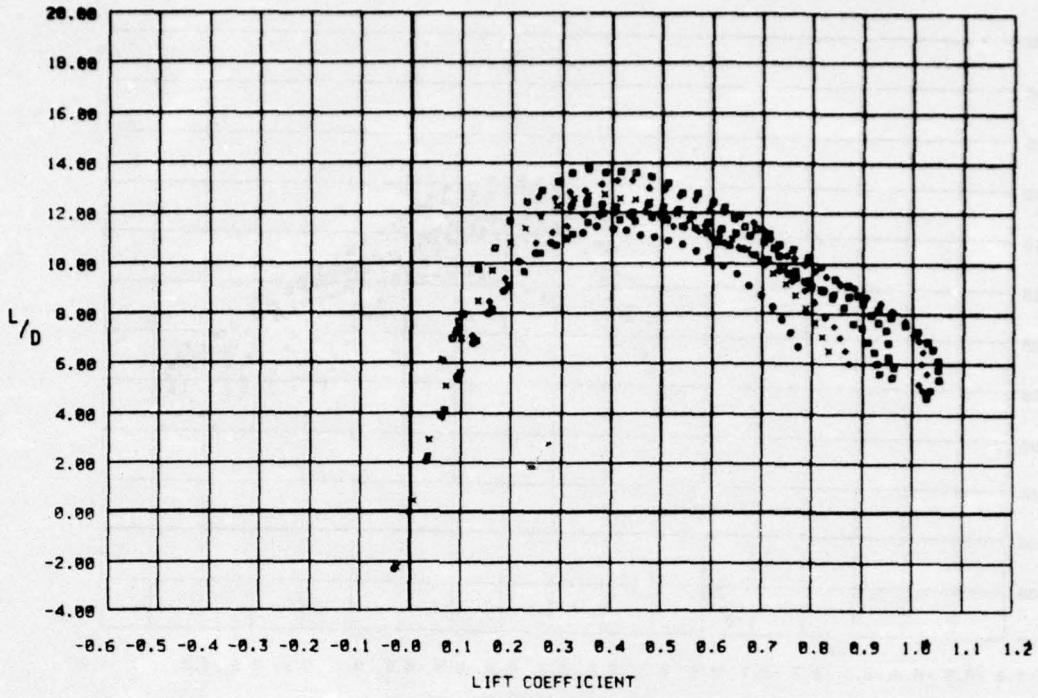

LIFT/DRAG VS. LIFT COEFFICIENT

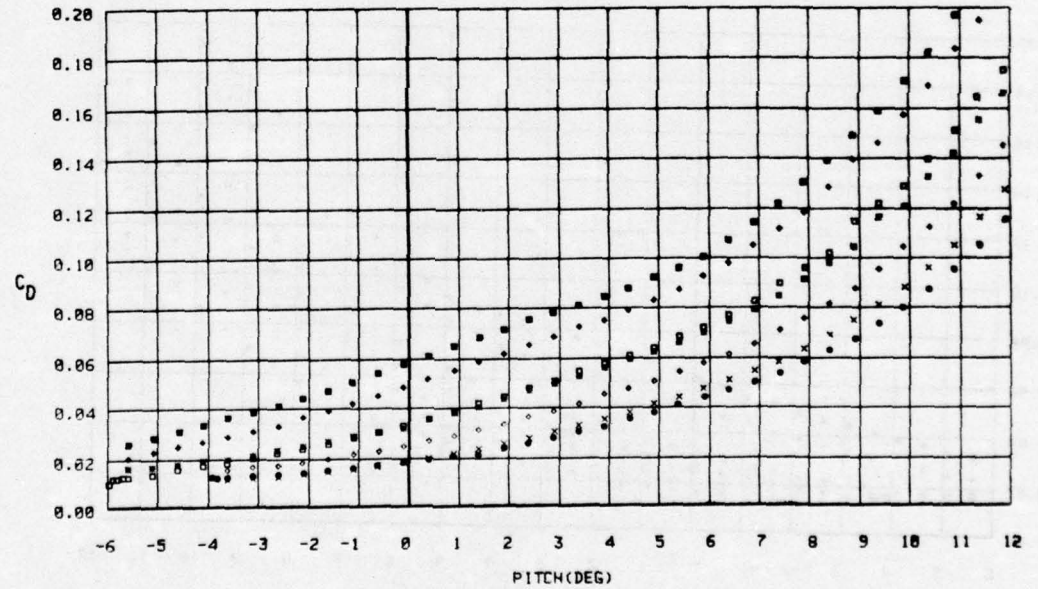

DRAG COEFFICIENT VS. PITCH ANGLE

RUN	SYMBOL	VELOCITY	FLAP ANGLE	LOCATION
3	•	19.9 KTS	0.0 DEG	CARRIAGE 5
18	×	20.2 KTS	2.5 DEG	CARRIAGE 5
26	△	20.0 KTS	5.0 DEG	CARRIAGE 5
34	■	20.0 KTS	7.5 DEG	CARRIAGE 5
42	□	20.0 KTS	10.0 DEG	CARRIAGE 5
49	◆	20.0 KTS	15.0 DEG	CARRIAGE 5
56	●	20.0 KTS	17.5 DEG	CARRIAGE 5

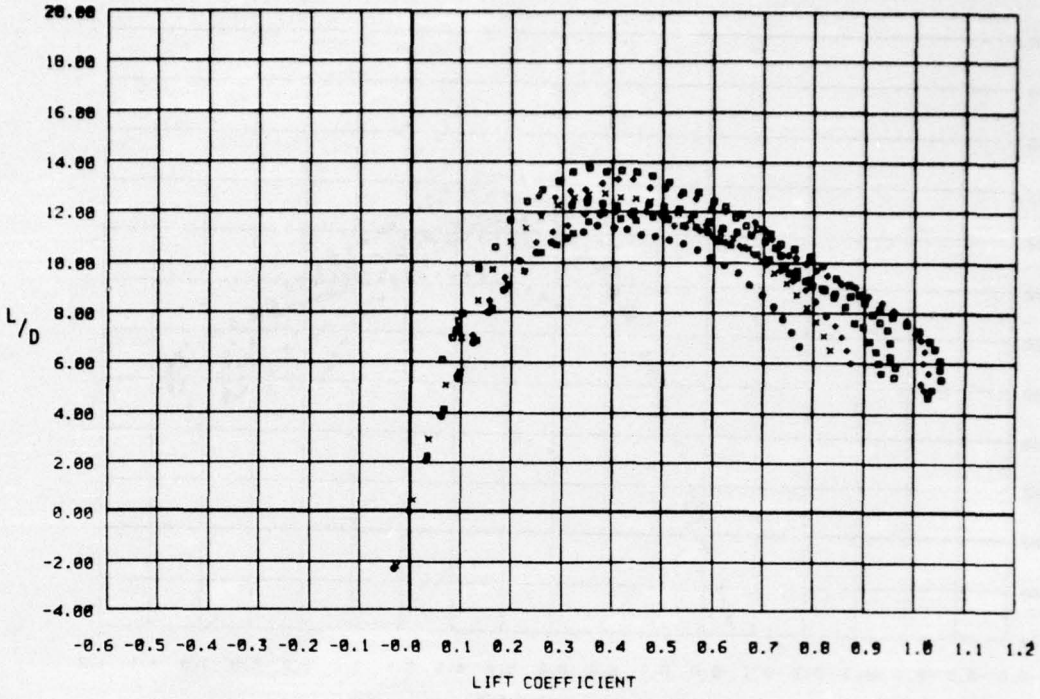

LIFT/DRAG VS. LIFT COEFFICIENT

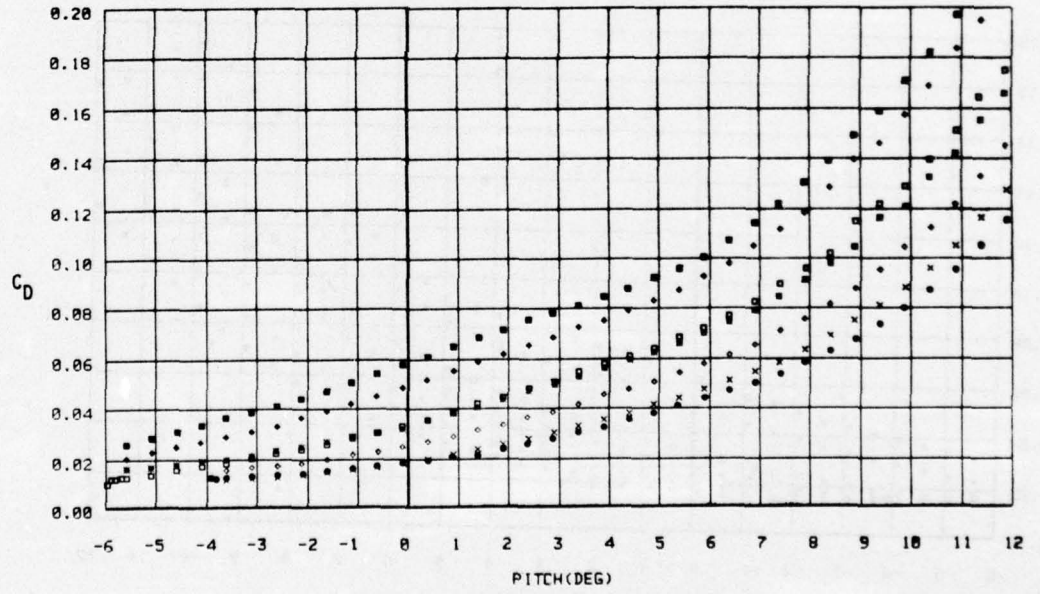

DRAG COEFFICIENT VS. PITCH ANGLE

RUN	SYMBOL	VELOCITY	FLAP ANGLE	LOCATION
3	•	19.9 KTS	0.0 DEG	CARRIAGE 5
18	×	20.2 KTS	2.5 DEG	CARRIAGE 5
26	^	20.0 KTS	5.0 DEG	CARRIAGE 5
34	▪	20.0 KTS	7.5 DEG	CARRIAGE 5
42	▫	20.0 KTS	10.0 DEG	CARRIAGE 5
49	◆	20.0 KTS	15.0 DEG	CARRIAGE 5
56	■	20.0 KTS	17.5 DEG	CARRIAGE 5

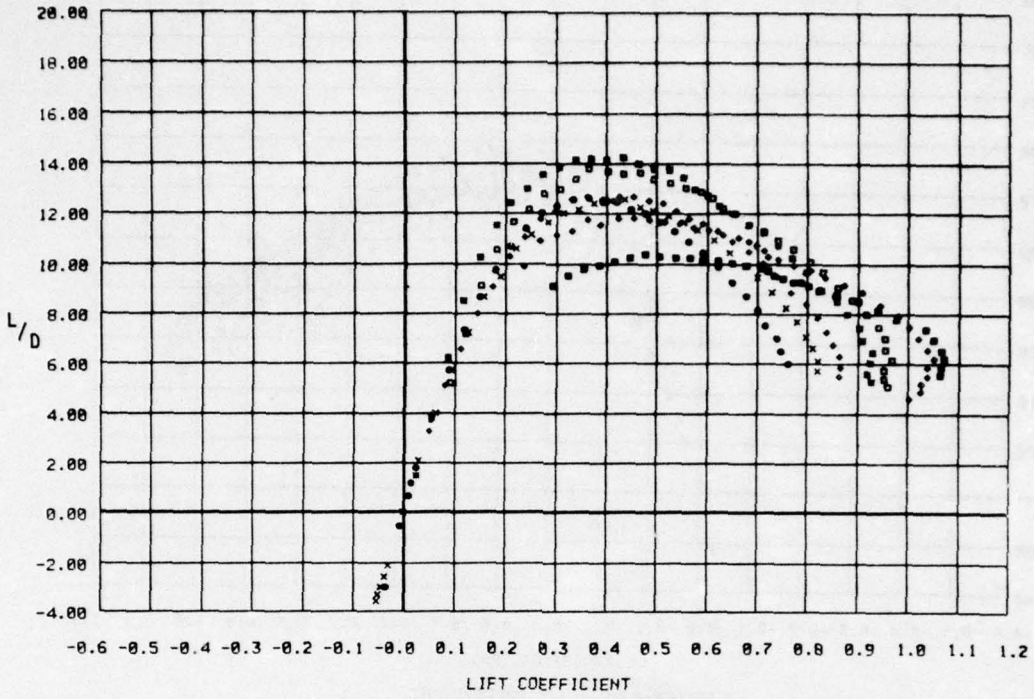

LIFT/DRAG VS. LIFT COEFFICIENT

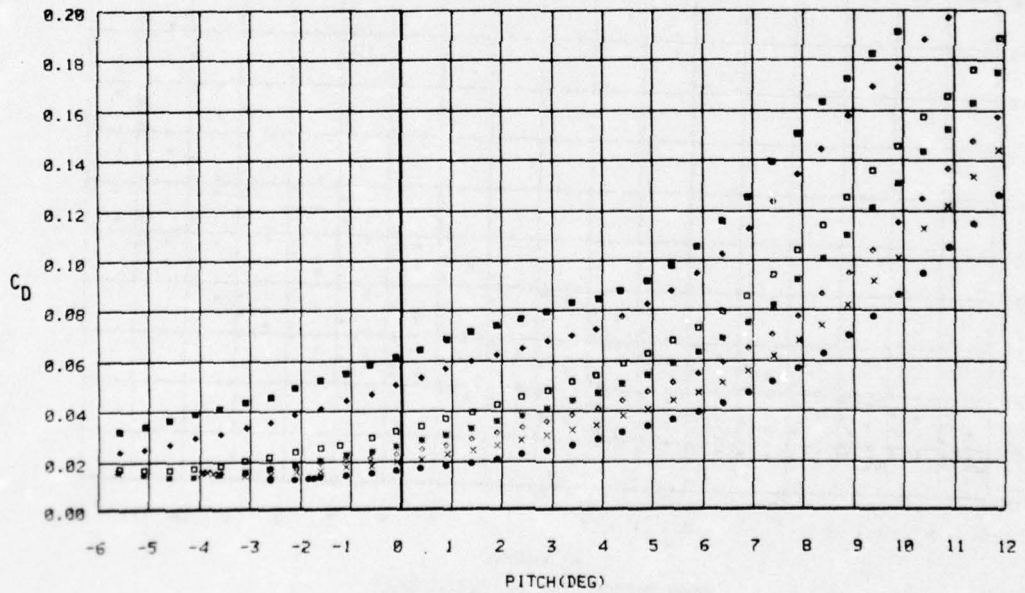

DRAG COEFFICIENT VS. PITCH ANGLE

RUN	SYMBOL	VELOCITY	FLAP ANGLE	LOCATION
4	•	25.0 KTS	0.0 DEG	CARRIAGE 5
19	×	25.0 KTS	2.5 DEG	CARRIAGE 5
27	◦	25.1 KTS	5.0 DEG	CARRIAGE 5
35	▪	25.0 KTS	7.5 DEG	CARRIAGE 5
43	▫	25.0 KTS	10.0 DEG	CARRIAGE 5
50	◆	25.0 KTS	15.0 DEG	CARRIAGE 5
57	◆	25.0 KTS	17.5 DEG	CARRIAGE 5

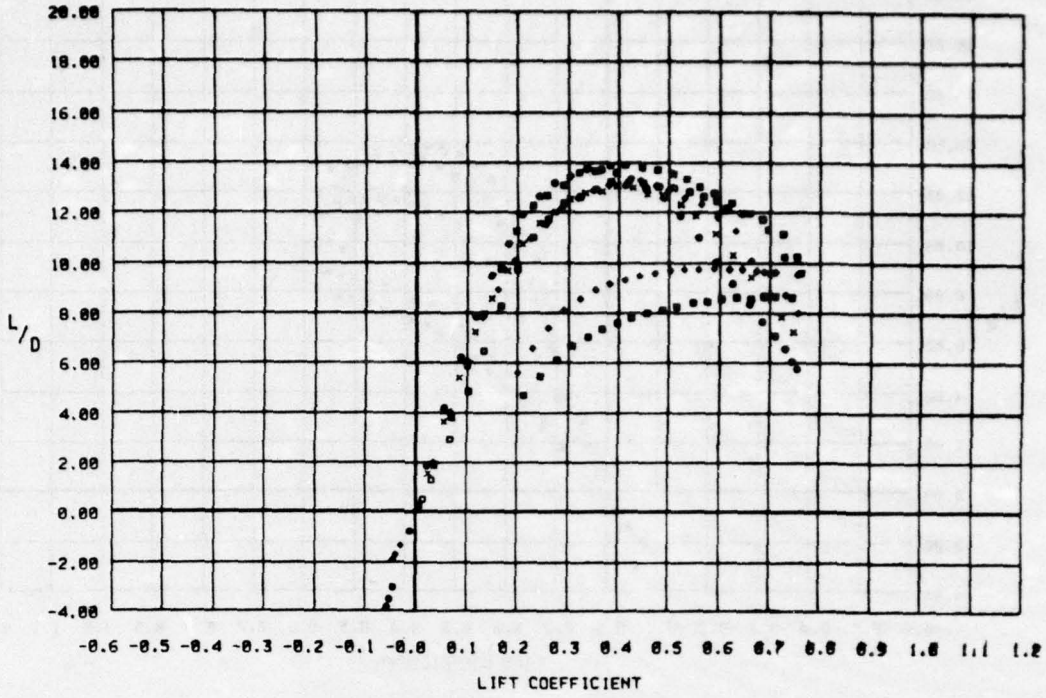

LIFT/DRAG VS. LIFT COEFFICIENT

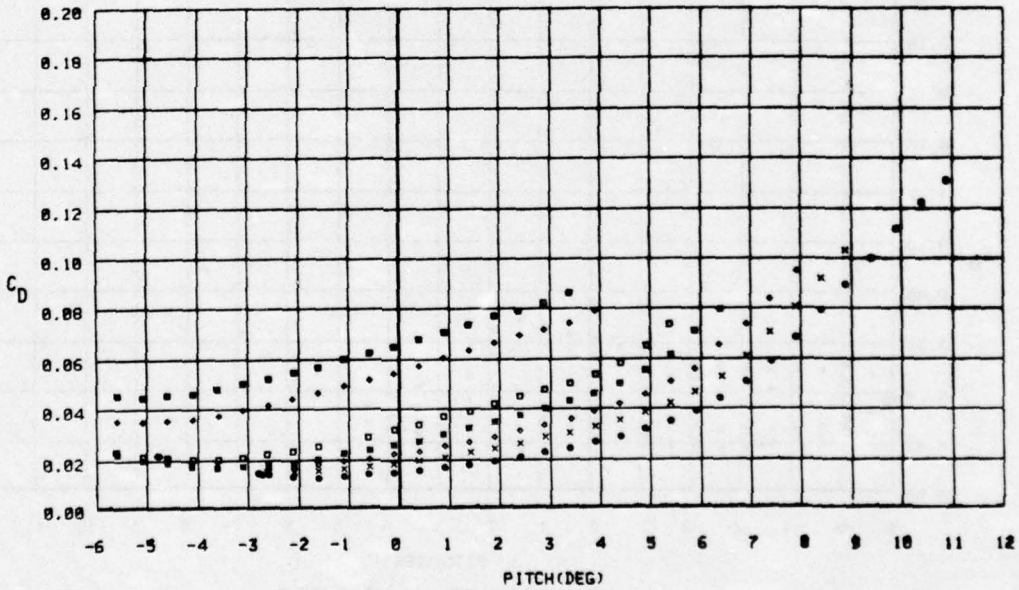

DRAG COEFFICIENT VS. PITCH ANGLE

RUN	SYMBOL	VELOCITY	FLAP ANGLE	LOCATION
9	•	30.0 KTS	0.0 DEG	CARRIAGE 5
20	×	29.9 KTS	2.5 DEG	CARRIAGE 5
28	♦	30.0 KTS	5.0 DEG	CARRIAGE 5
36	■	30.0 KTS	7.5 DEG	CARRIAGE 5
44	□	30.0 KTS	10.0 DEG	CARRIAGE 5
51	◆	30.0 KTS	15.0 DEG	CARRIAGE 5
58	▪	30.1 KTS	17.5 DEG	CARRIAGE 5

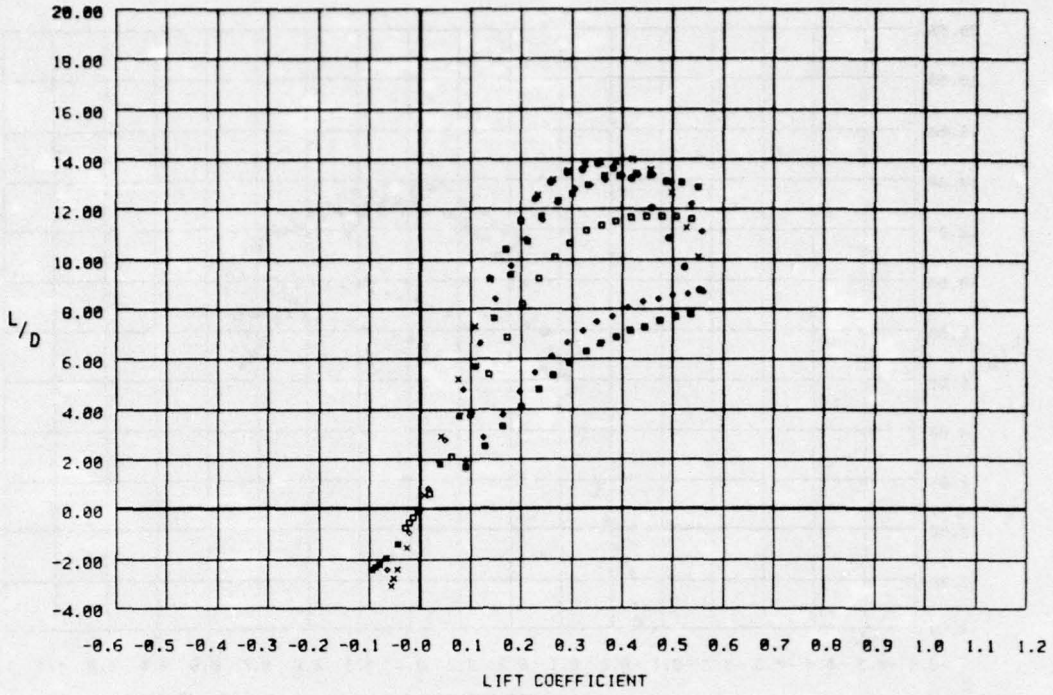

LIFT/DRAG VS. LIFT COEFFICIENT

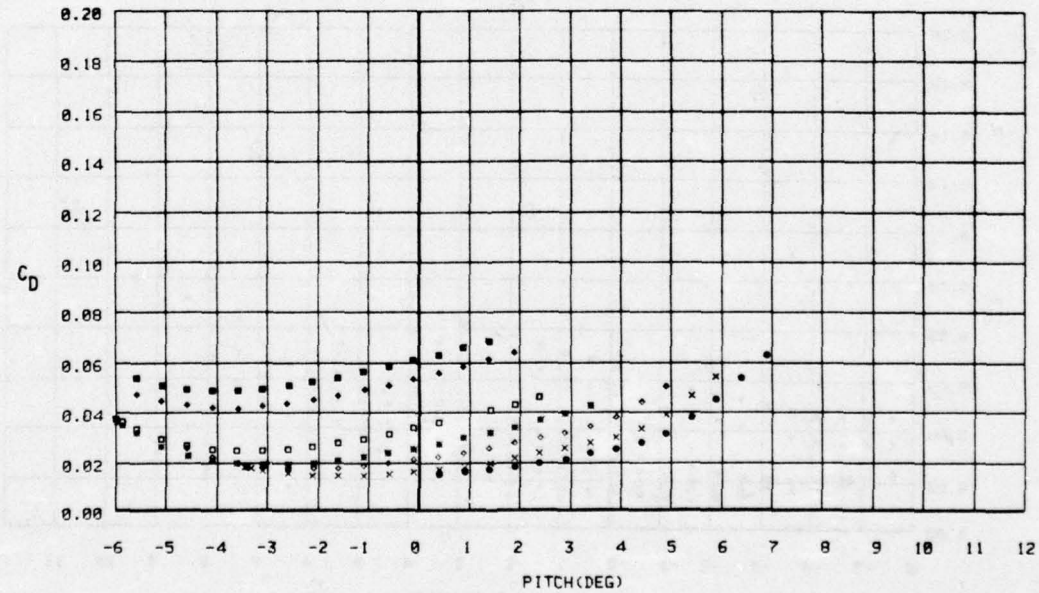

DRAG COEFFICIENT VS. PITCH ANGLE

RUN	SYMBOL	VELOCITY	FLAP ANGLE	LOCATION
11	•	35.0 KTS	0.0 DEG	CARRIAGE 5
21	×	35.1 KTS	2.5 DEG	CARRIAGE 5
29	◆	35.0 KTS	5.0 DEG	CARRIAGE 5
37	■	35.0 KTS	7.5 DEG	CARRIAGE 5
45	□	35.0 KTS	10.0 DEG	CARRIAGE 5
52	◆	35.1 KTS	15.0 DEG	CARRIAGE 5
59	■	35.1 KTS	17.5 DEG	CARRIAGE 5

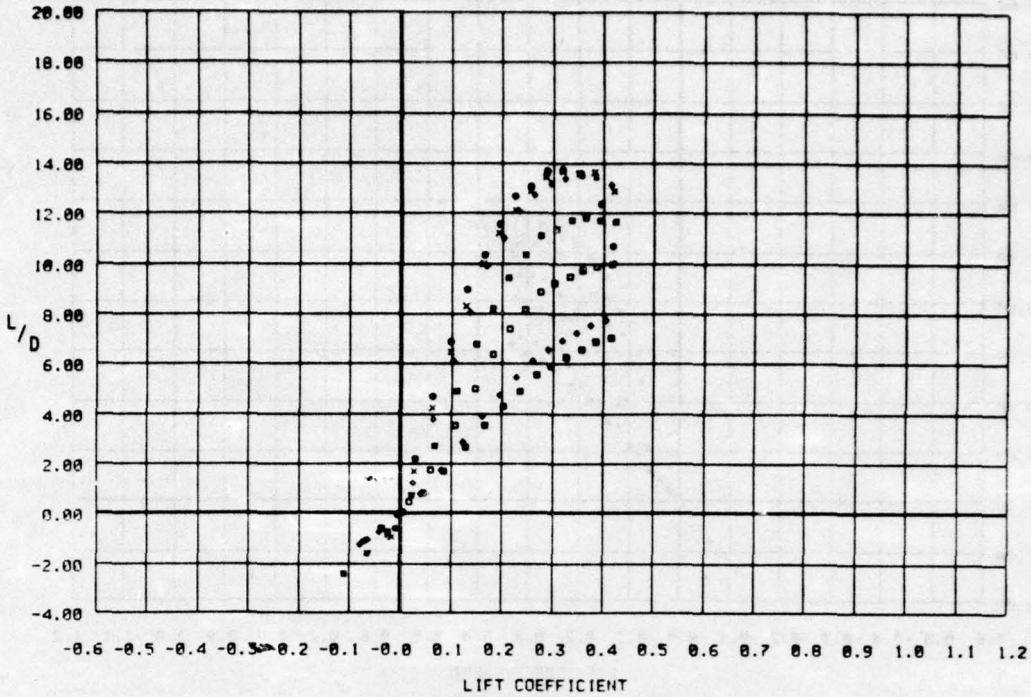

LIFT/DRAG VS. LIFT COEFFICIENT

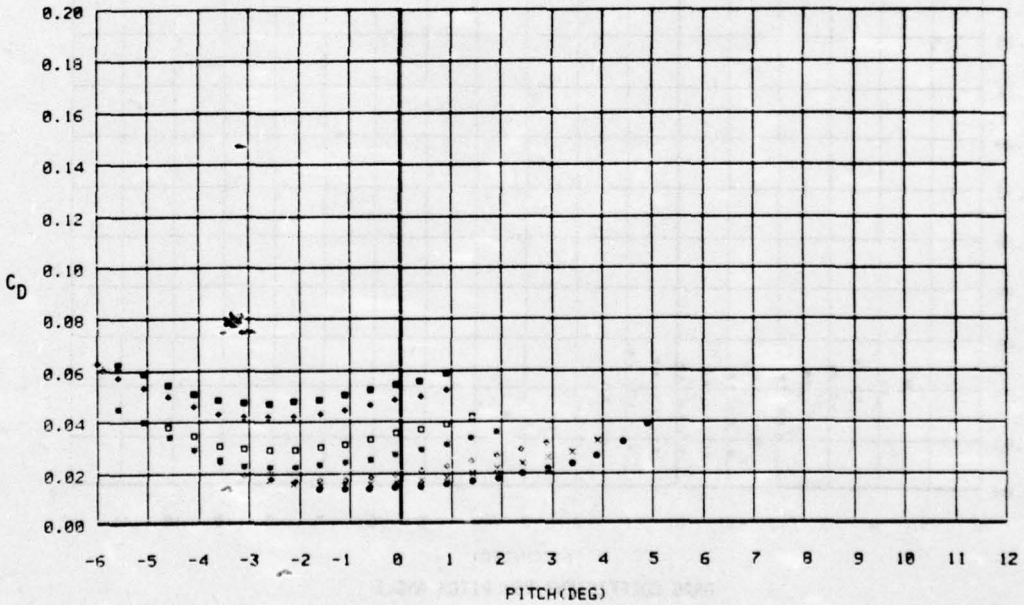

DRAG COEFFICIENT VS. PITCH ANGLE

RUN	SYMBOL	VELOCITY	FLAP ANGLE	LOCATION
12	•	40.1 KTS	0.0 DEG	CARRIAGE 5
22	×	40.1 KTS	2.5 DEG	CARRIAGE 5
30	◇	40.1 KTS	5.0 DEG	CARRIAGE 5
38	▪	40.1 KTS	7.5 DEG	CARRIAGE 5
46	□	40.1 KTS	10.0 DEG	CARRIAGE 5
53	◆	40.0 KTS	15.0 DEG	CARRIAGE 5
60	■	40.1 KTS	17.5 DEG	CARRIAGE 5

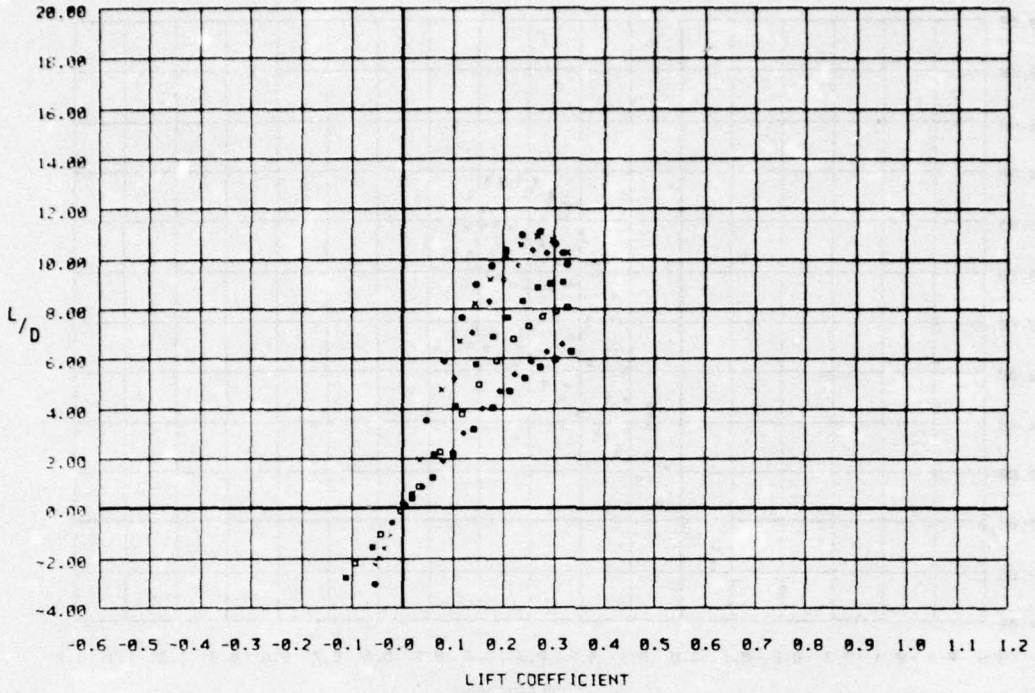

LIFT/DRAG VS. LIFT COEFFICIENT

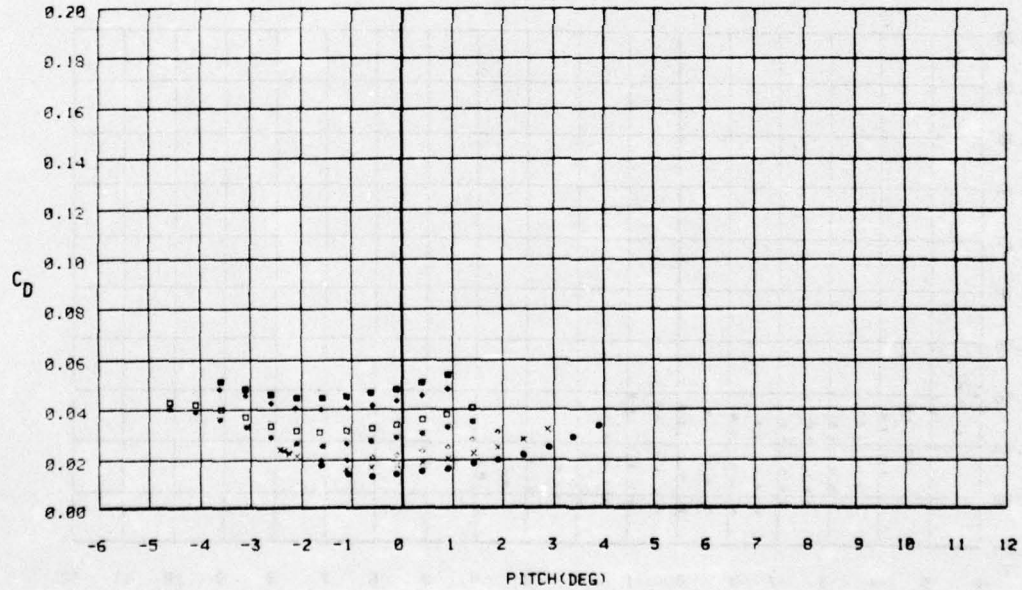

DRAG COEFFICIENT VS. PITCH ANGLE

RUN	SYMBOL	VELOCITY	FLAP ANGLE	LOCATION
14	•	45.5 KTS	0.0 DEG	CARRIAGE 5
23	×	45.5 KTS	2.5 DEG	CARRIAGE 5
31	+	45.4 KTS	5.0 DEG	CARRIAGE 5
39	▪	45.4 KTS	7.5 DEG	CARRIAGE 5
47	□	45.3 KTS	10.0 DEG	CARRIAGE 5
54	◆	45.4 KTS	15.0 DEG	CARRIAGE 5
62	▲	45.4 KTS	17.5 DEG	CARRIAGE 5

APPENDIX D - INFORMATION ON EFFECTS OF LIFT AND DRAG WITH FOIL AT VARIOUS DEPTHS OF SUBMERGENCE

FOR 64A309 FOIL

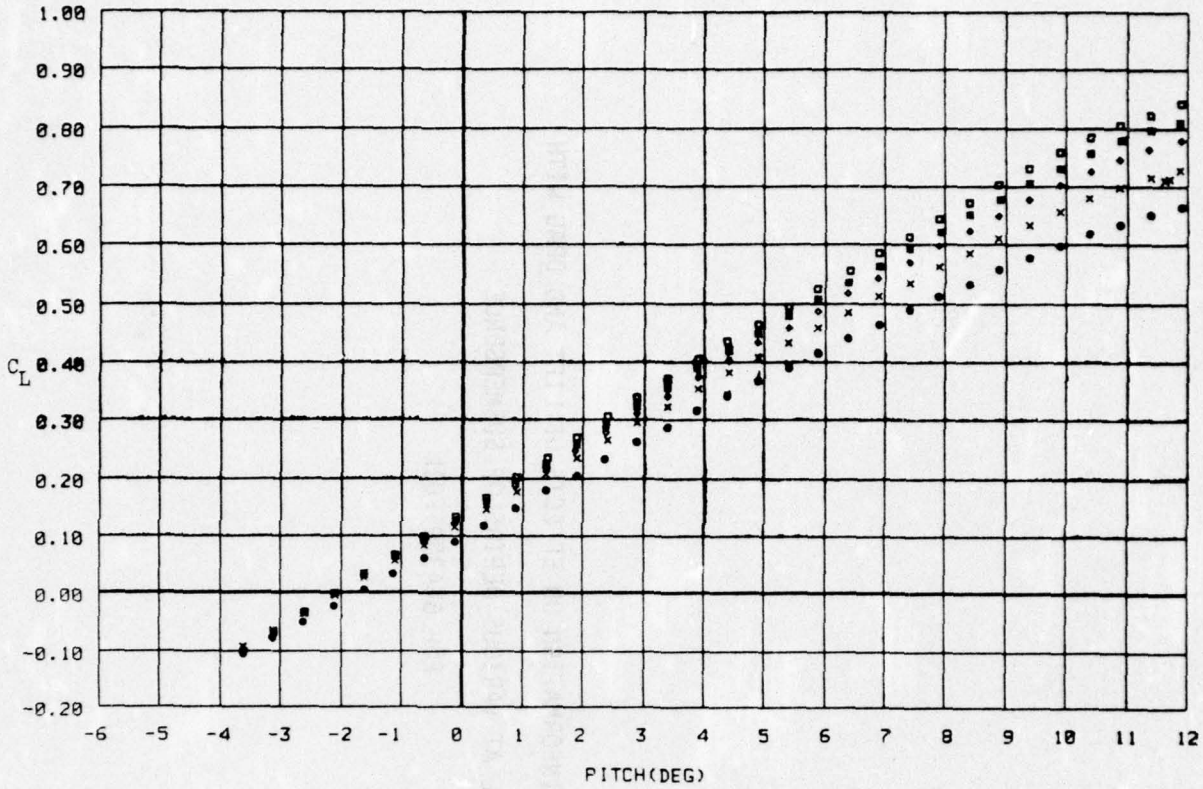

RUN	SYMBOL	VELOCITY	h/c	LOCATION
63	•	15.8 KTS	1/2	CARRIAGE 5
84	×	15.9 KTS	3/4	CARRIAGE 5
1	+	15.9 KTS	1	CARRIAGE 5
70	▪	15.9 KTS	1 1/2	CARRIAGE 5
77	▫	15.9 KTS	2	CARRIAGE 5

LIFT COEFFICIENT VS. PITCH ANGLE

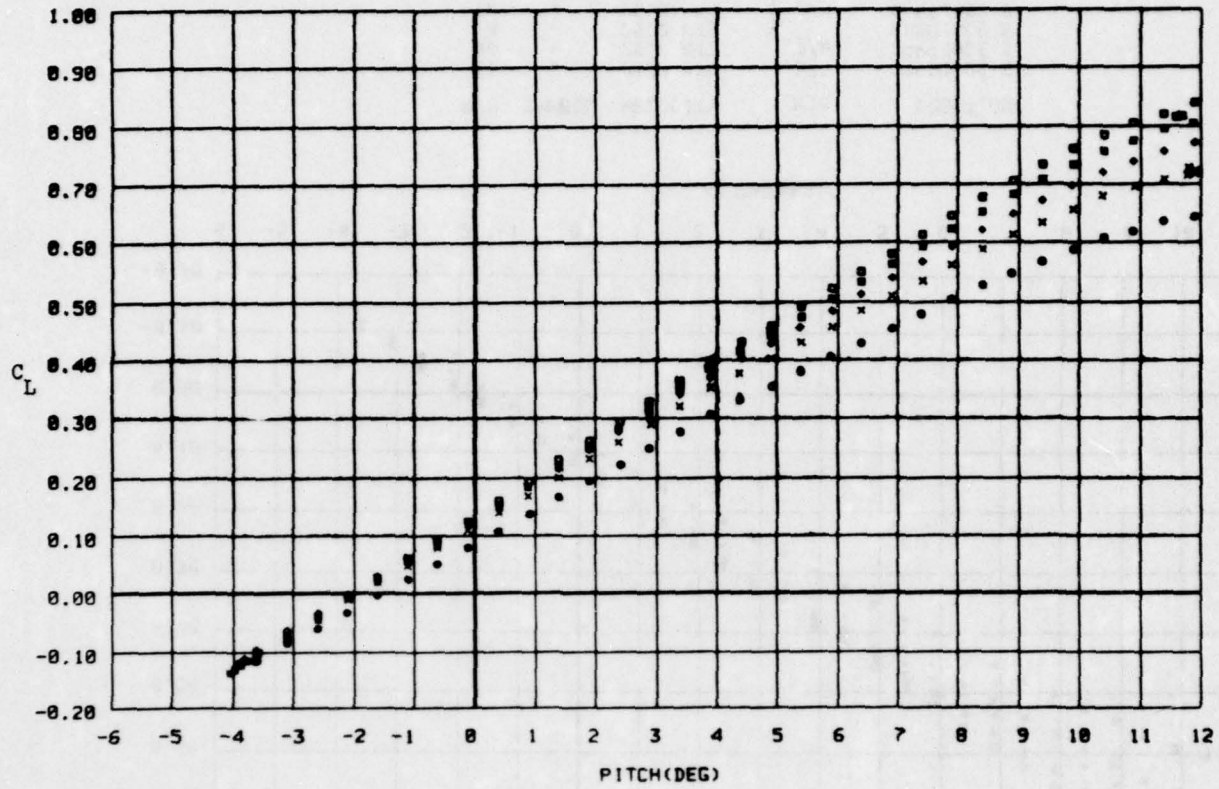

RUN	SYMBOL	VELOCITY	h/c	LOCATION
64	∘	20.0 KTS	1/2	CARRIAGE 5
85	×	20.0 KTS	3/4	CARRIAGE 5
3	◇	19.9 KTS	1	CARRIAGE 5
71	■	20.0 KTS	1 1/2	CARRIAGE 5
78	□	20.0 KTS	2	CARRIAGE 5

LIFT COEFFICIENT VS. PITCH ANGLE

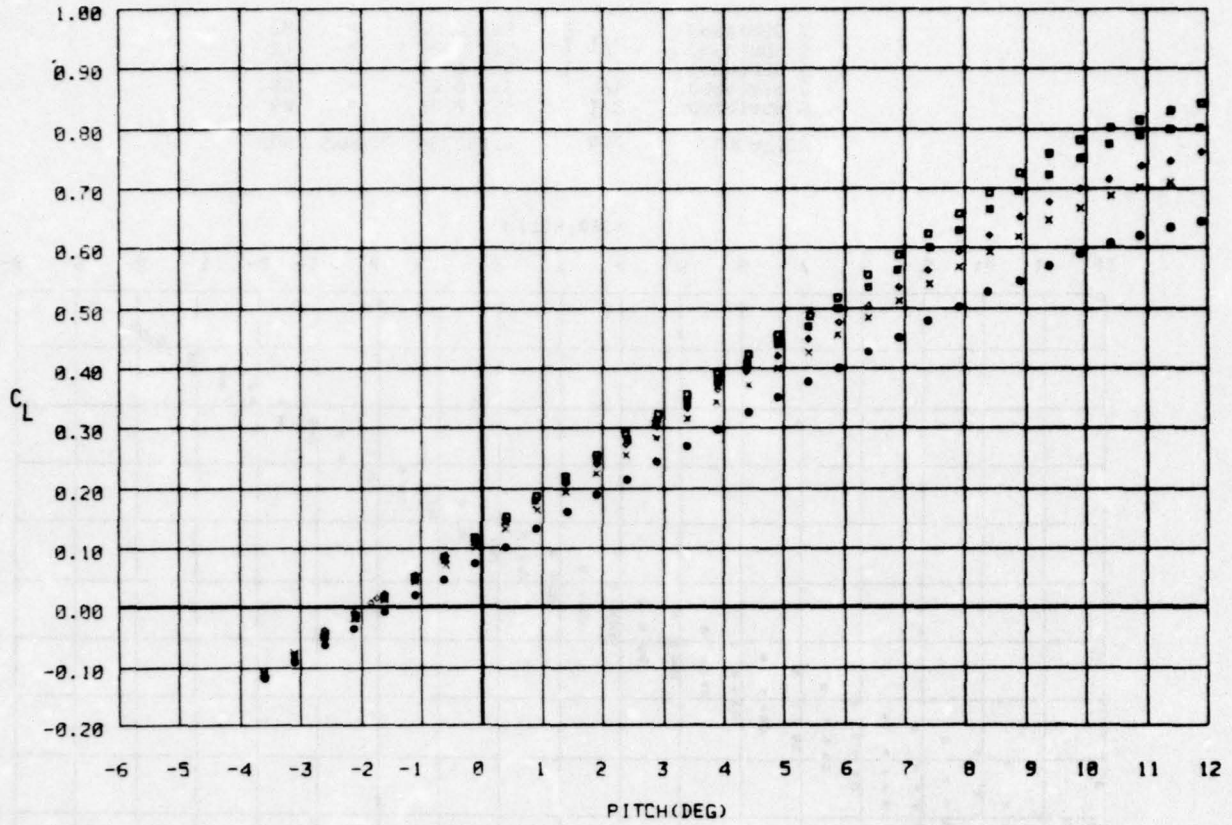

RUN	SYMBOL	VELOCITY	h/c	LOCATION
65	•	25.0 KTS	1/2	CARRIAGE 5
86	×	25.0 KTS	3/4	CARRIAGE 5
4	◇	25.0 KTS	1	CARRIAGE 5
72	■	25.0 KTS	1 1/2	CARRIAGE 5
79	□	25.1 KTS	2	CARRIAGE 5

LIFT COEFFICIENT VS. PITCH ANGLE

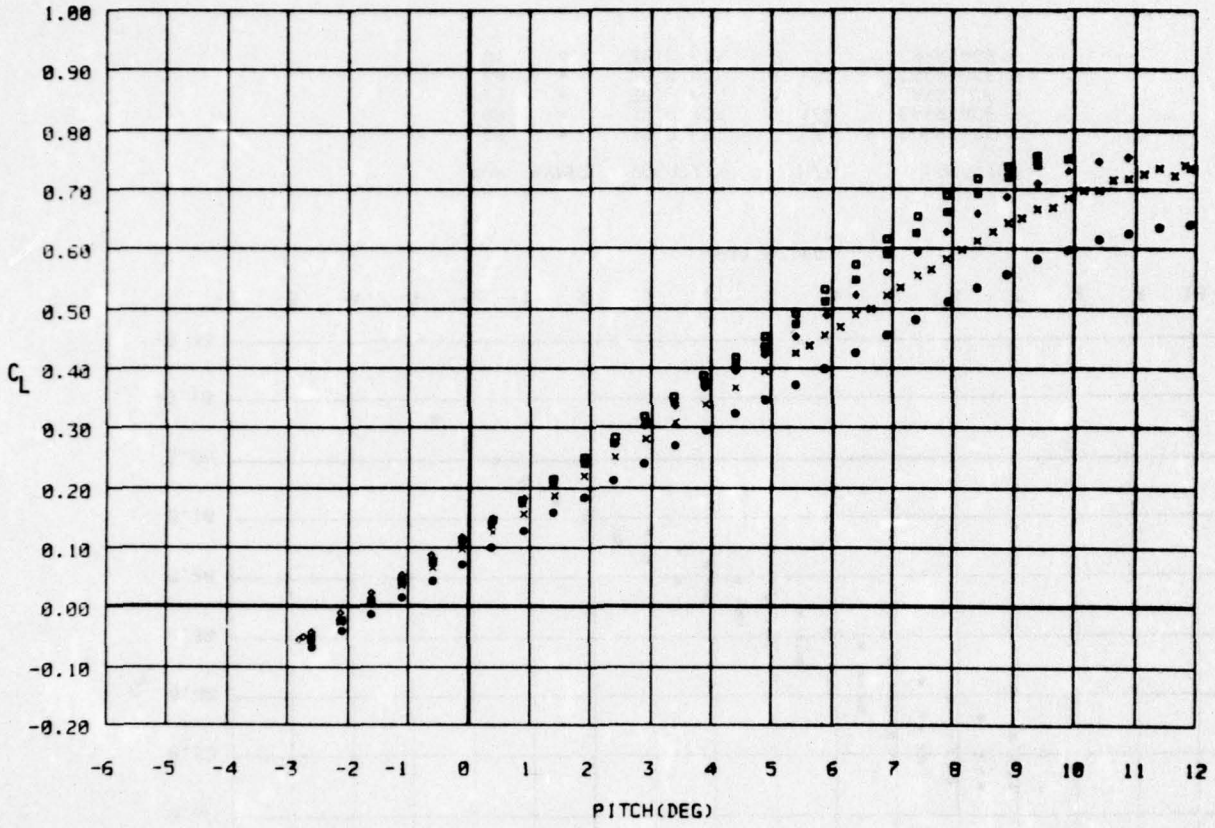

RUN	SYMBOL	VELOCITY	h/c	LOCATION
66	•	30.0 KTS	1/2	CARRIAGE 5
87	×	30.0 KTS	3/4	CARRIAGE 5
9	◇	30.0 KTS	1	CARRIAGE 5
73	■	30.0 KTS	1 1/2	CARRIAGE 5
80	□	30.0 KTS	2	CARRIAGE 5

LIFT COEFFICIENT VS. PITCH ANGLE

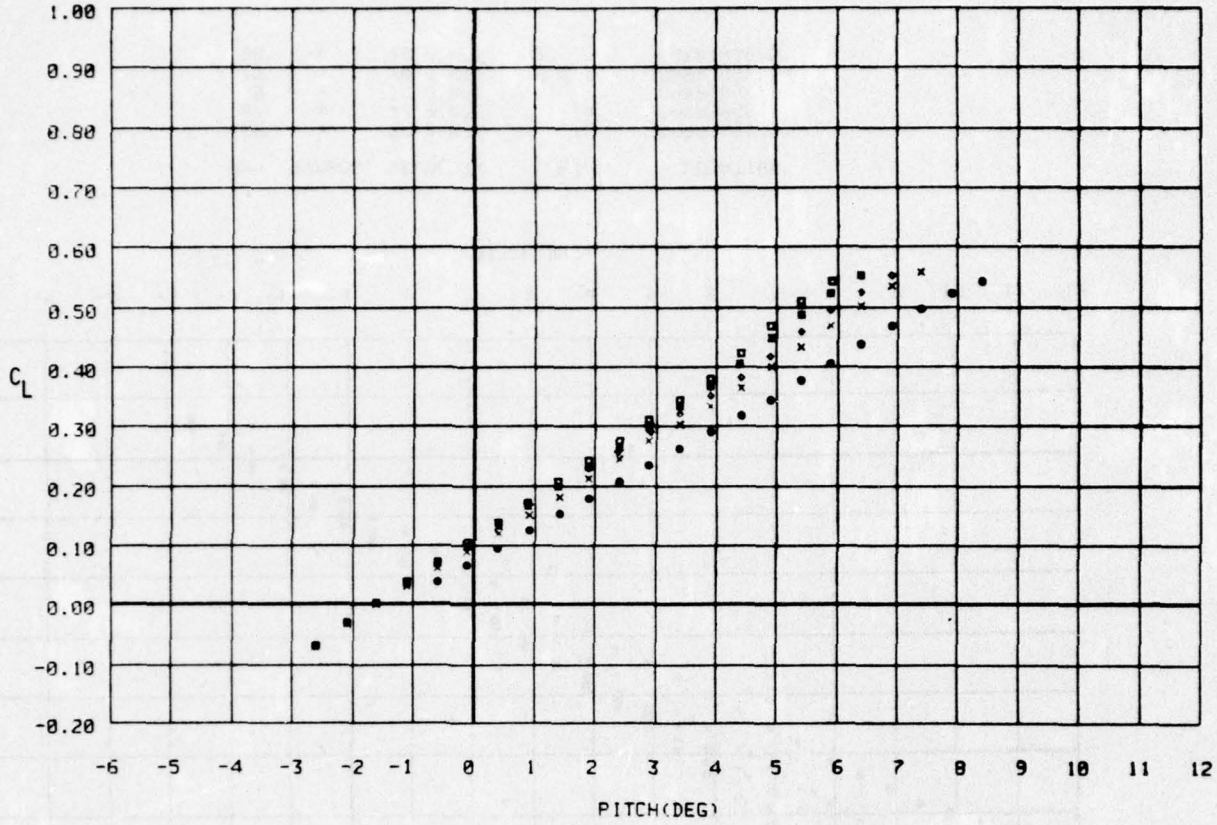

RUN	SYMBOL	VELOCITY	h/c	LOCATION
67	•	35.0 KTS	1/2	CARRIAGE 5
88	×	35.0 KTS	3/4	CARRIAGE 5
11	◇	34.9 KTS	1	CARRIAGE 5
74	■	35.0 KTS	1 1/2	CARRIAGE 5
81	□	35.0 KTS	2	CARRIAGE 5

LIFT COEFFICIENT VS. PITCH ANGLE

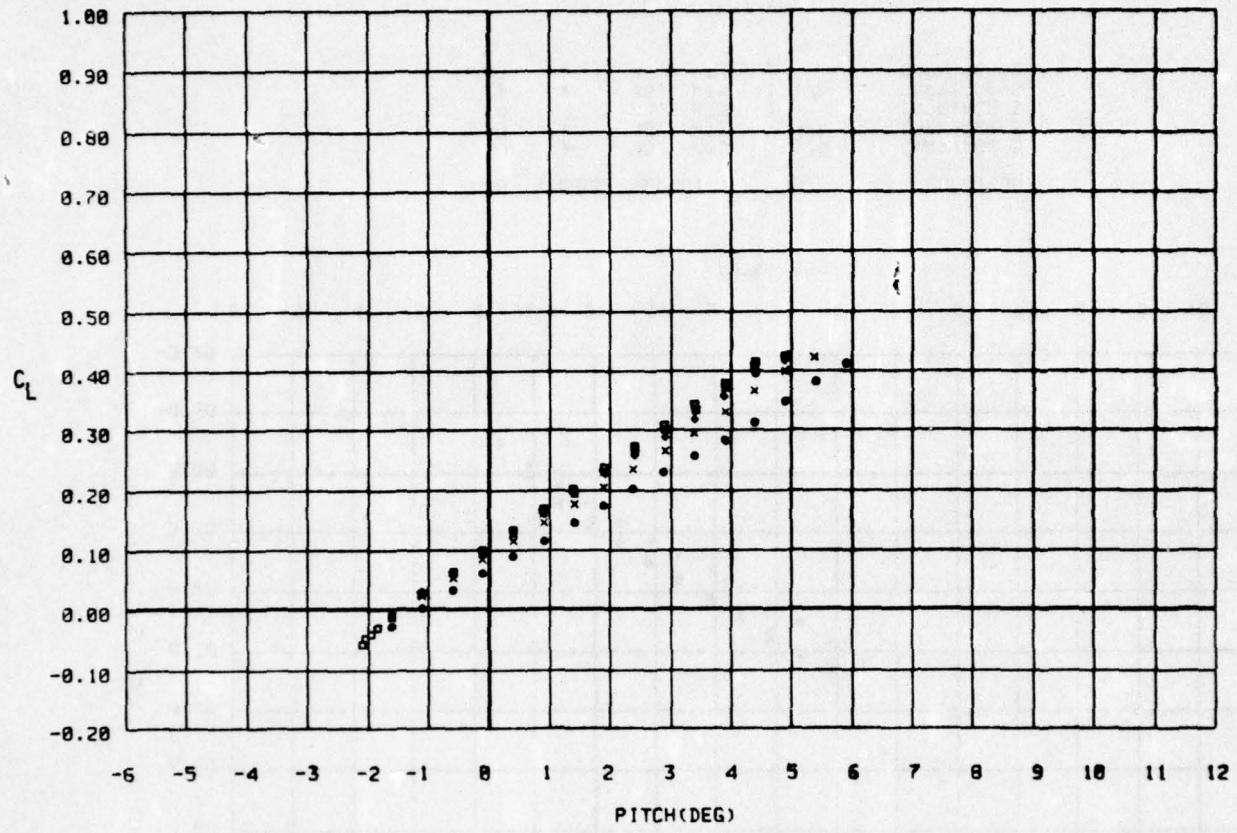

RUN	SYMBOL	VELOCITY	h/c	LOCATION
68	•	40.1 KTS	1/2	CARRIAGE 5
89	×	40.1 KTS	3/4	CARRIAGE 5
12	◆	40.1 KTS	1	CARRIAGE 5
75	■	40.0 KTS	1 1/2	CARRIAGE 5
82	□	40.1 KTS	2	CARRIAGE 5

LIFT COEFFICIENT VS. PITCH ANGLE

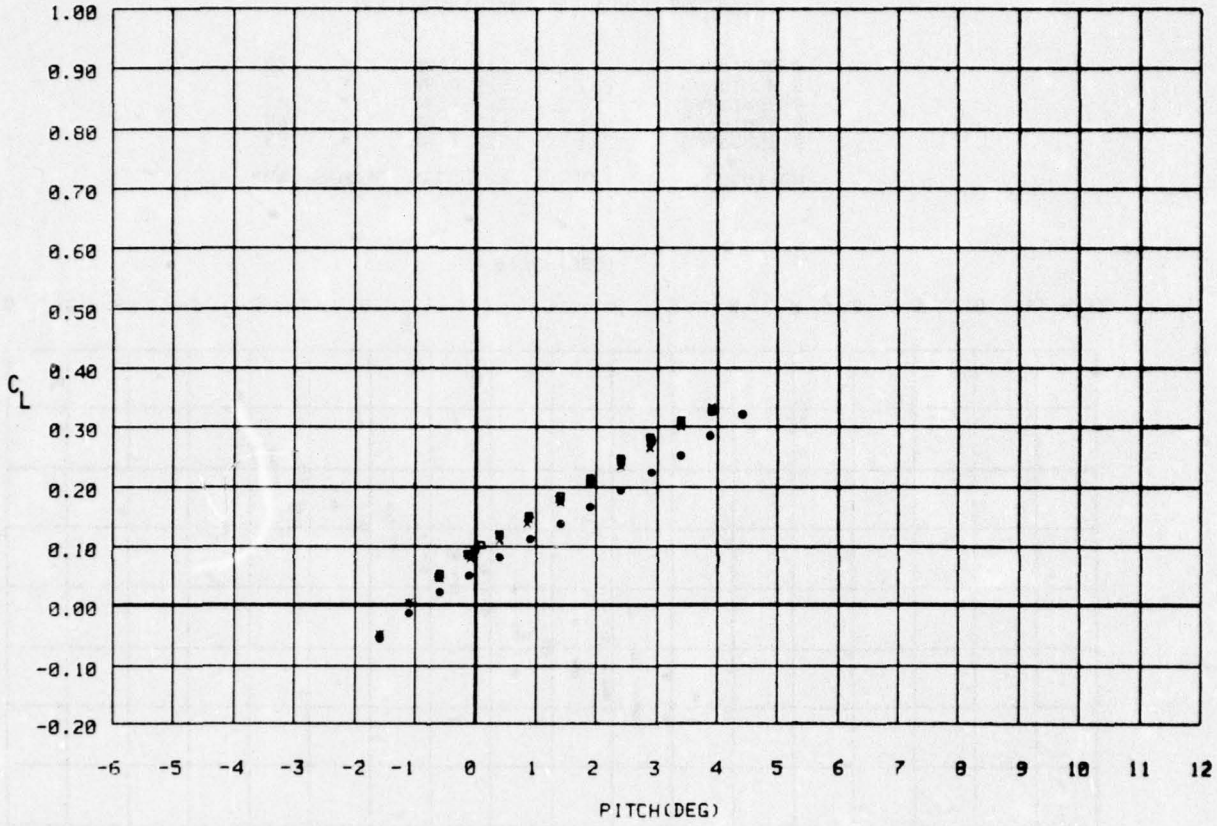

RUN	SYMBOL	VELOCITY	h/c	LOCATION
69	•	45.6 KTS	1/2	CARRIAGE 5
90	×	45.3 KTS	3/4	CARRIAGE 5
14	◇	45.5 KTS	1	CARRIAGE 5
76	■	45.4 KTS	1 1/2	CARRIAGE 5
83	□	45.3 KTS	2	CARRIAGE 5

LIFT COEFFICIENT VS. PITCH ANGLE

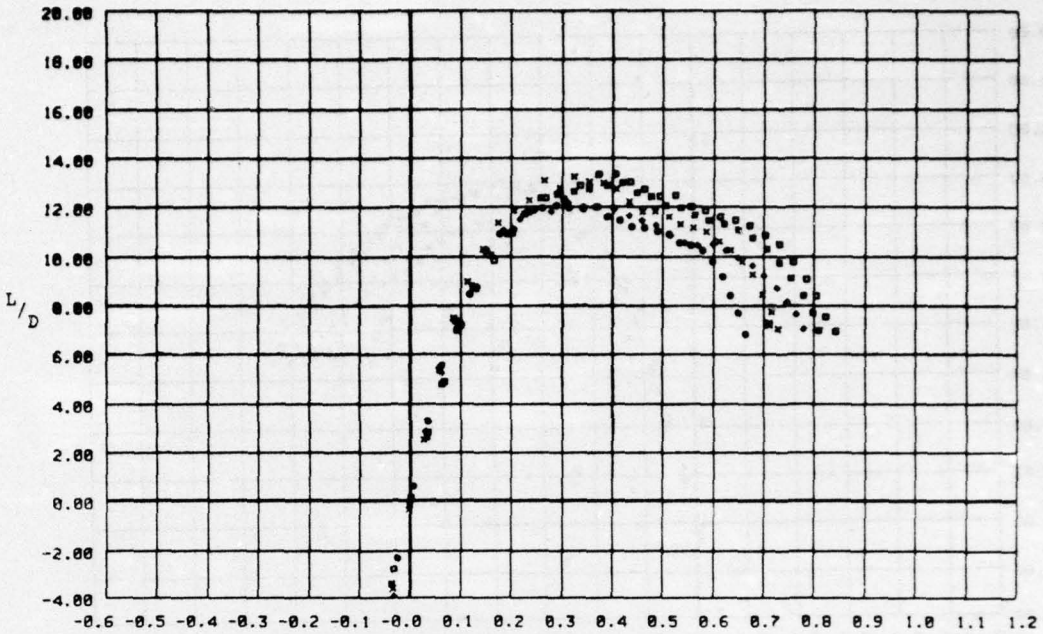

LIFT/DRAG VS. LIFT COEFFICIENT

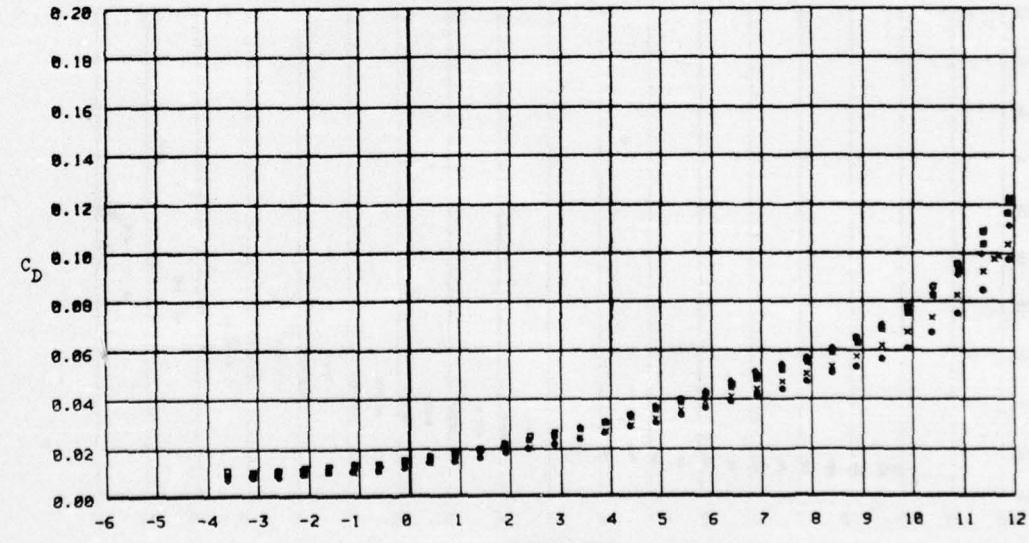

DRAG COEFFICIENT VS. PITCH ANGLE

RUN	SYMBOL	VELOCITY	h/c	LOCATION
63	•	15.8 KTS	1/2	CARRIAGE 5
84	×	15.9 KTS	3/4	CARRIAGE 5
1	◦	15.9 KTS	1	CARRIAGE 5
78	▪	15.9 KTS	1 1/2	CARRIAGE 5
77	▫	15.9 KTS	2	CARRIAGE 5

AD-A032 272 DAVID W TAYLOR NAVAL SHIP RESEARCH AND DEVELOPMENT CE--ETC F/G 13/10
LIFT AND DRAG CHARACTERISTICS OF NACA 16-309 AND NACA 64A309 HY--ETC(U)
OCT 76 D E LAYNE

UNCLASSIFIED SPD-326-07 NL

2 OF 2
AD
A032272

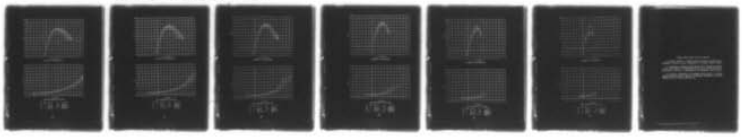

END

DATE
FILMED
1-77

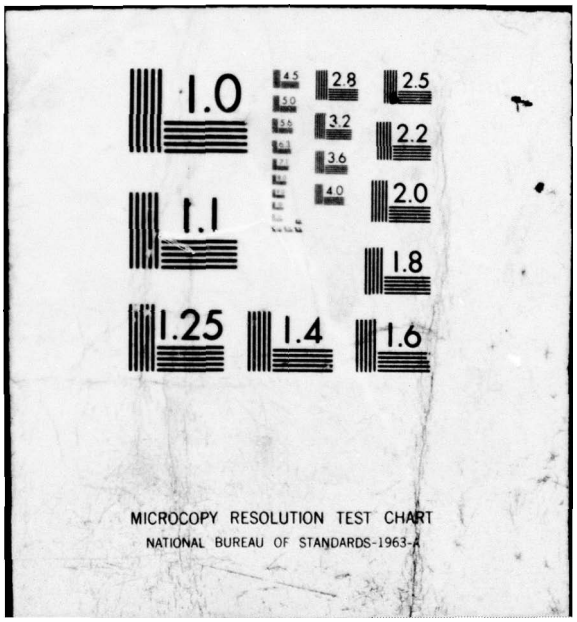
1.0
1.1
1.25
1.4
1.6
1.8
2.0
2.2
2.5
2.8
3.2
3.6
4.0
4.5
5.0
MICROCOPY RESOLUTION TEST CHART
NATIONAL BUREAU OF STANDARDS-1963-A

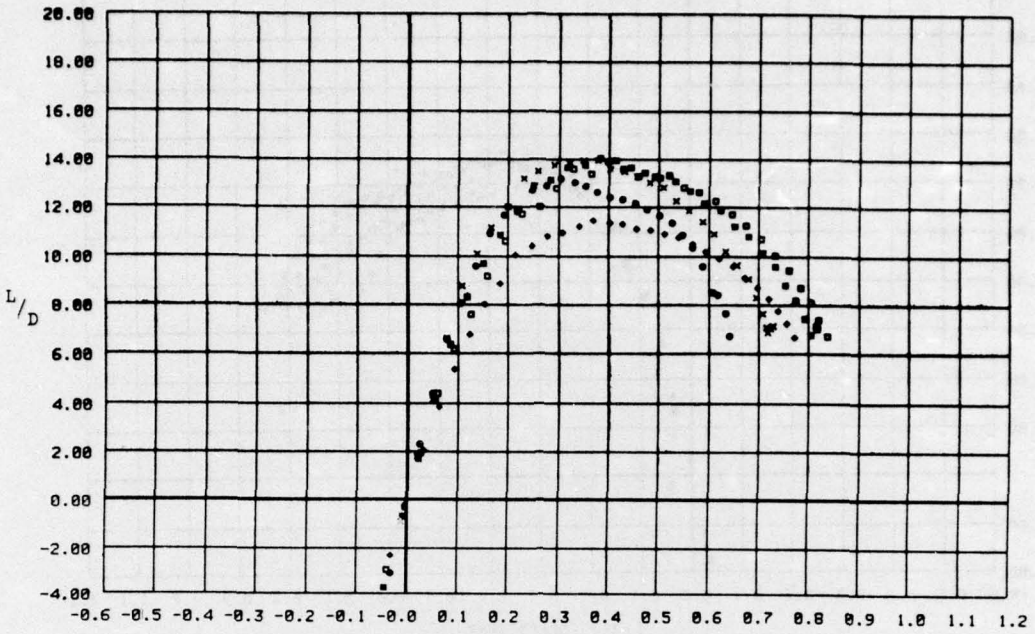

LIFT/DRAG VS. LIFT COEFFICIENT

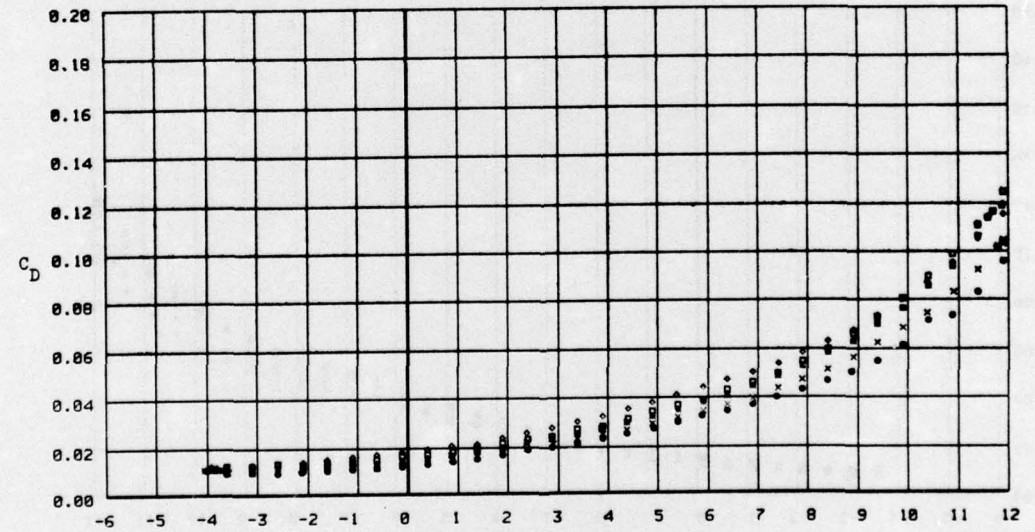

DRAG COEFFICIENT VS. PITCH ANGLE

RUN	SYMBOL	VELOCITY	h/c	LOCATION
64	•	20.0 KTS	1/2	CARRIAGE 5
85	×	20.0 KTS	3/4	CARRIAGE 5
3	◇	19.9 KTS	1	CARRIAGE 5
71	■	20.0 KTS	1 1/2	CARRIAGE 5
78	□	20.0 KTS	2	CARRIAGE 5

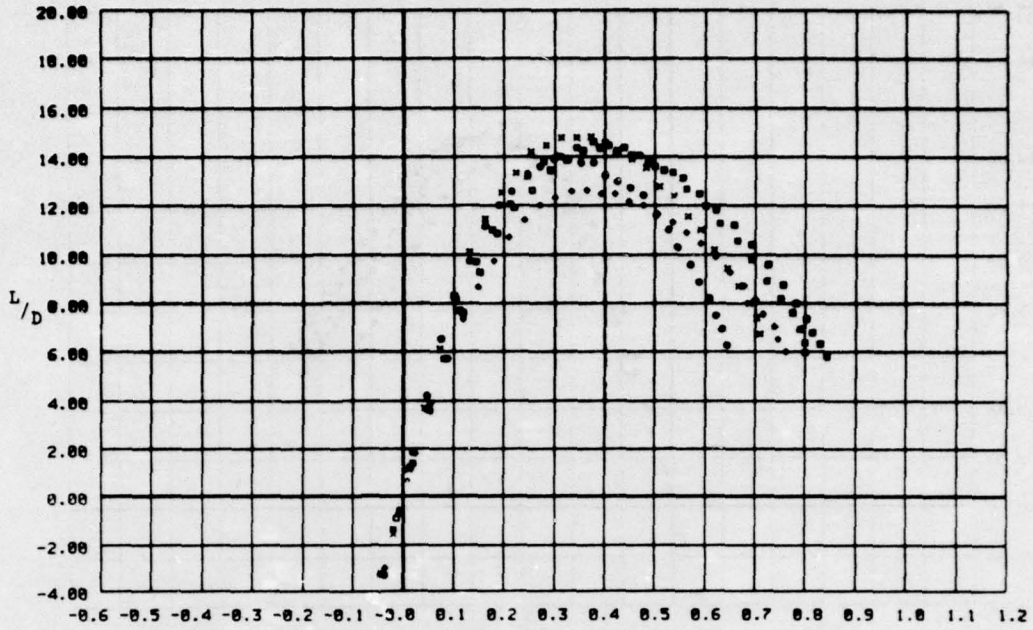

LIFT/DRAG VS. LIFT COEFFICIENT

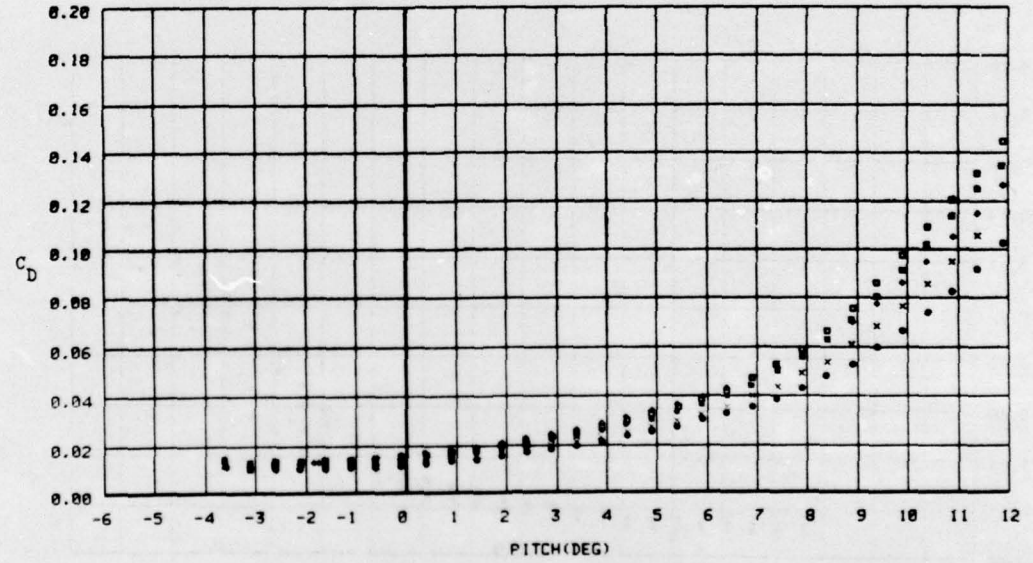

DRAG COEFFICIENT VS. PITCH ANGLE

RUN	SYMBOL	VELOCITY	h/c	LOCATION
65	•	25.0 KTS	1/2	CARRIAGE 5
86	×	25.0 KTS	3/4	CARRIAGE 5
4	◦	25.0 KTS	1	CARRIAGE 5
72	•	25.0 KTS	1 1/2	CARRIAGE 5
79	▫	25.1 KTS	2	CARRIAGE 5

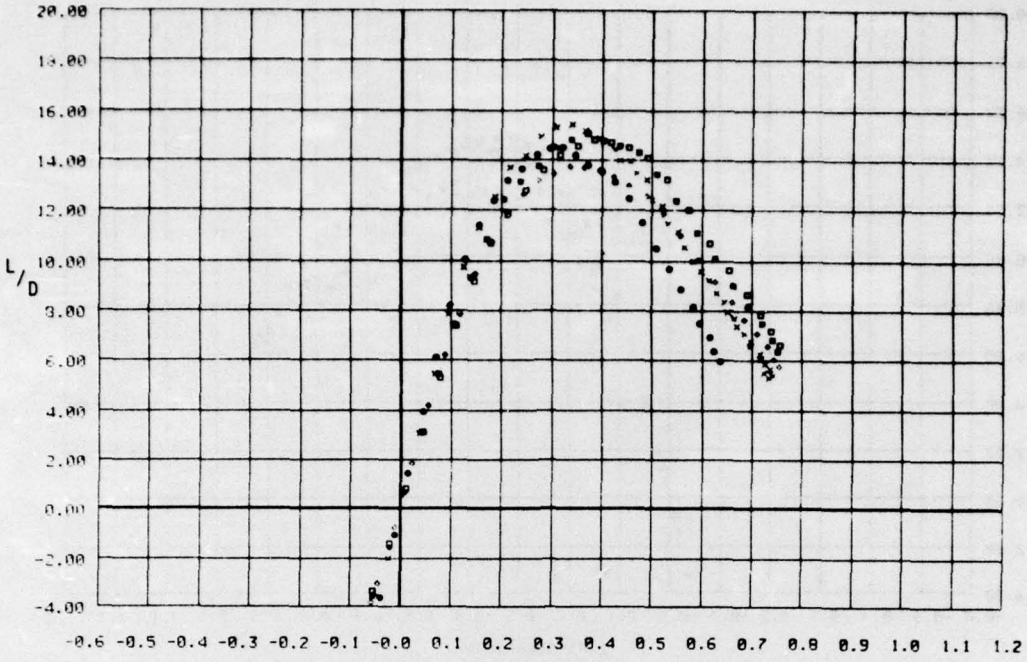

LIFT/DRAG VS. LIFT COEFFICIENT

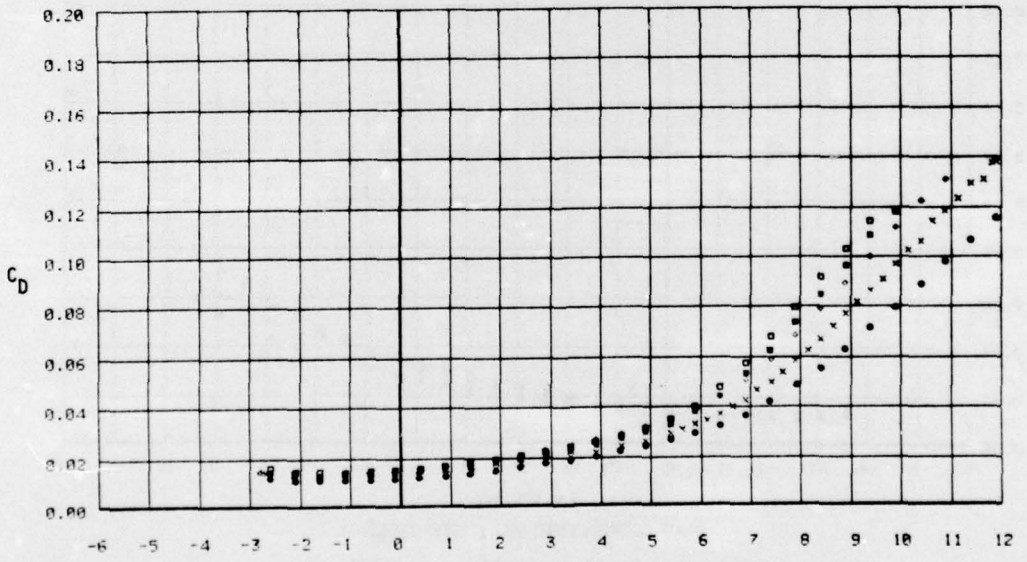

DRAG COEFFICIENT VS. PITCH ANGLE

RUN	SYMBOL	VELOCITY	h/c	LOCATION
66	•	30.0 KTS	1/2	CARRIAGE 5
87	×	30.0 KTS	3/4	CARRIAGE 5
9	◦	30.0 KTS	1	CARRIAGE 5
73	•	30.0 KTS	1 1/2	CARRIAGE 5
80	□	30.0 KTS	2	CARRIAGE 5

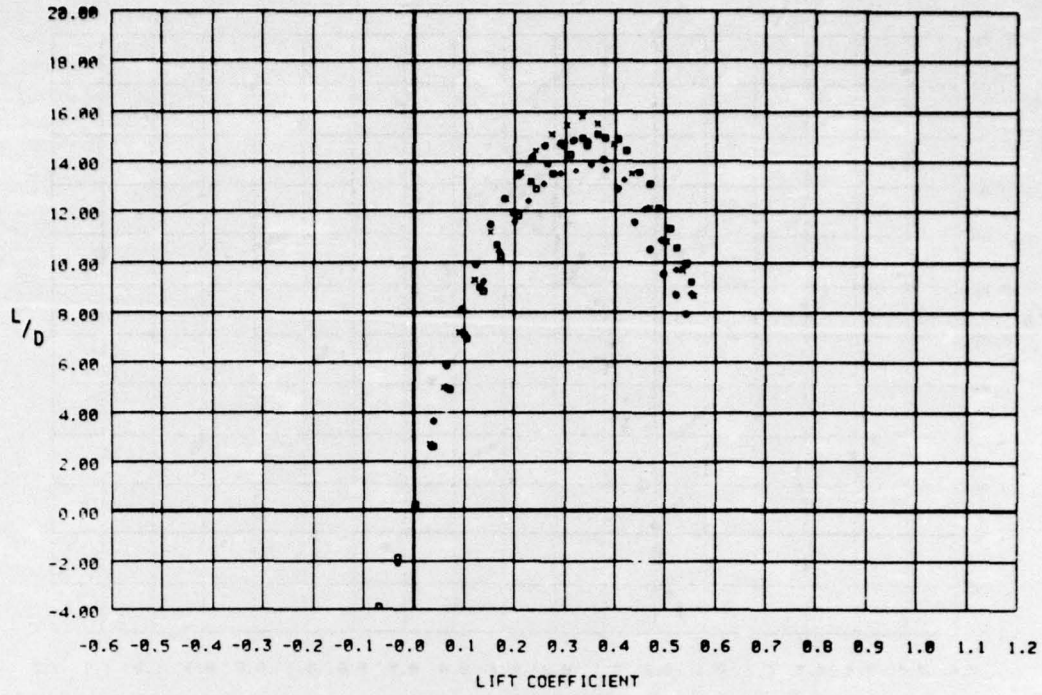

LIFT/DRAG VS. LIFT COEFFICIENT

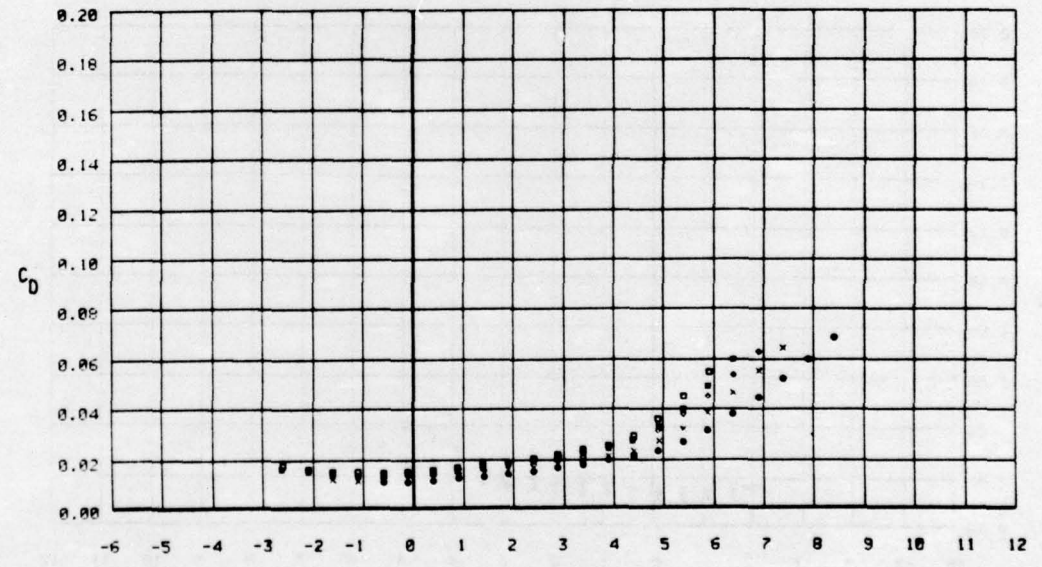

DRAG COEFFICIENT VS. PITCH ANGLE

RUN	SYMBOL	VELOCITY	h/c	LOCATION
67	•	35.0 KTS	1/2	CARRIAGE 5
88	×	35.0 KTS	3/4	CARRIAGE 5
11	◦	34.9 KTS	1	CARRIAGE 5
74	▪	35.0 KTS	1 1/2	CARRIAGE 5
81	▫	35.0 KTS	2	CARRIAGE 5

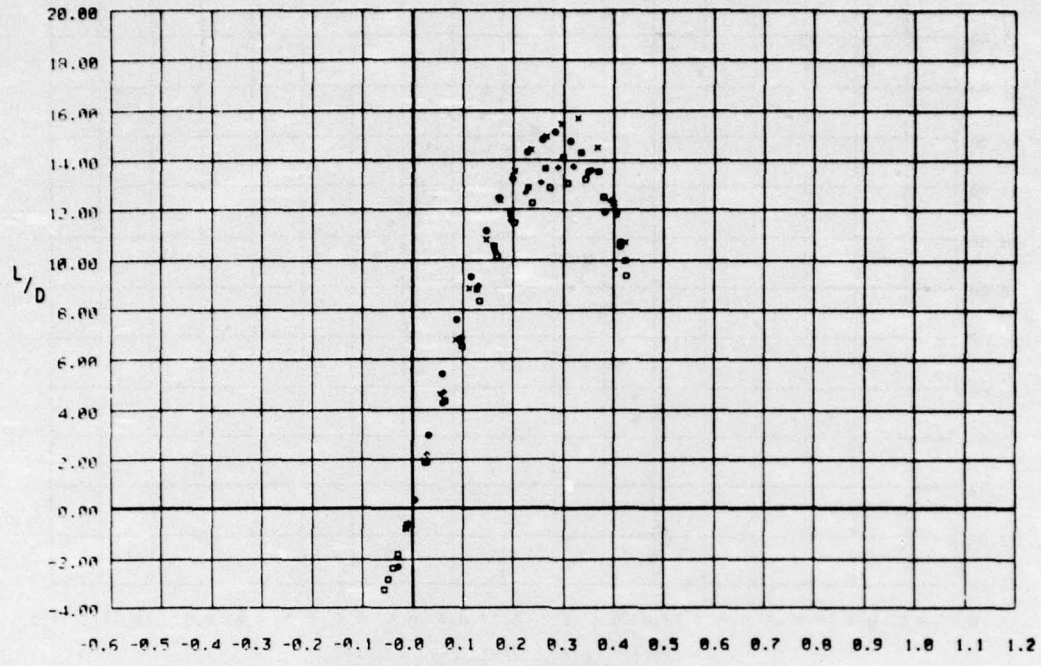

LIFT/DRAG VS. LIFT COEFFICIENT

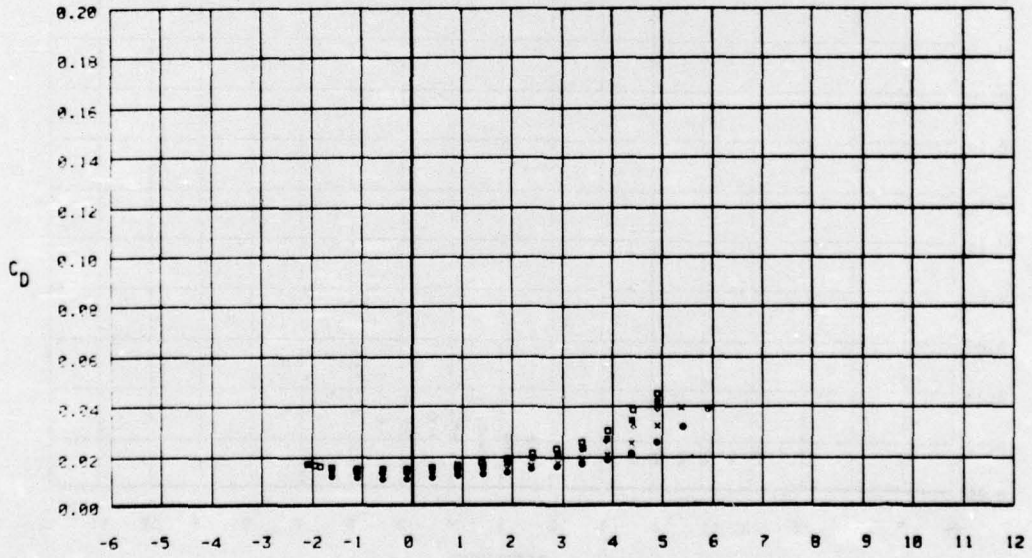

DRAG COEFFICIENT VS. PITCH ANGLE

RUN	SYMBOL	VELOCITY	h/c	LOCATION
68	•	40.1 KTS	1/2	CARRIAGE 5
89	×	40.1 KTS	3/4	CARRIAGE 5
12	◇	40.1 KTS	1	CARRIAGE 5
75	■	40.0 KTS	1 1/2	CARRIAGE 5
82	□	40.1 KTS	2	CARRIAGE 5

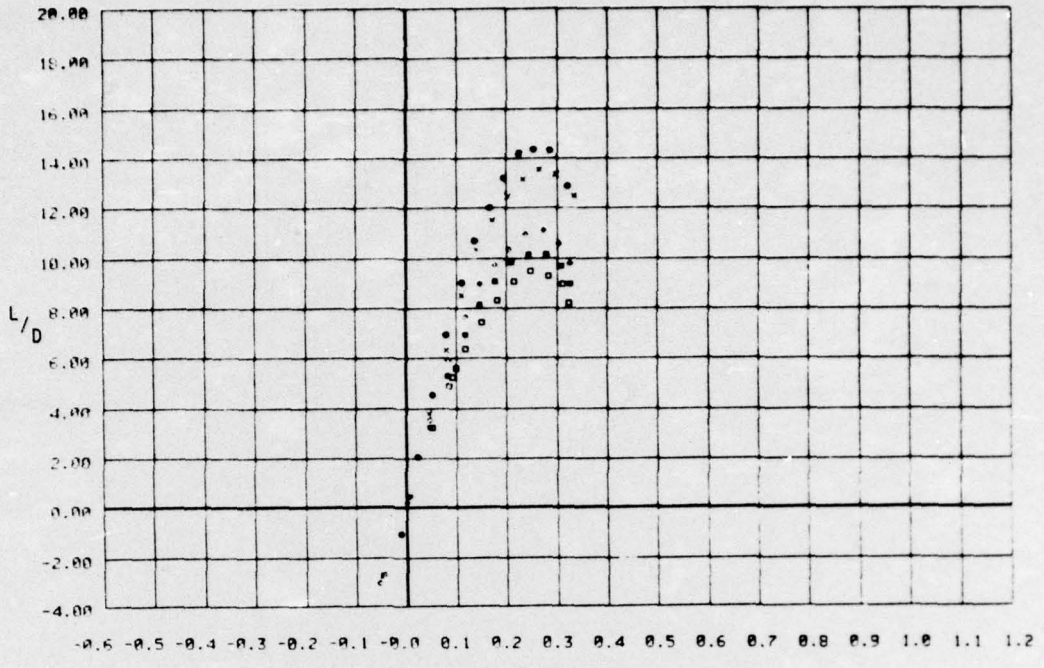

LIFT/DRAG VS. LIFT COEFFICIENT

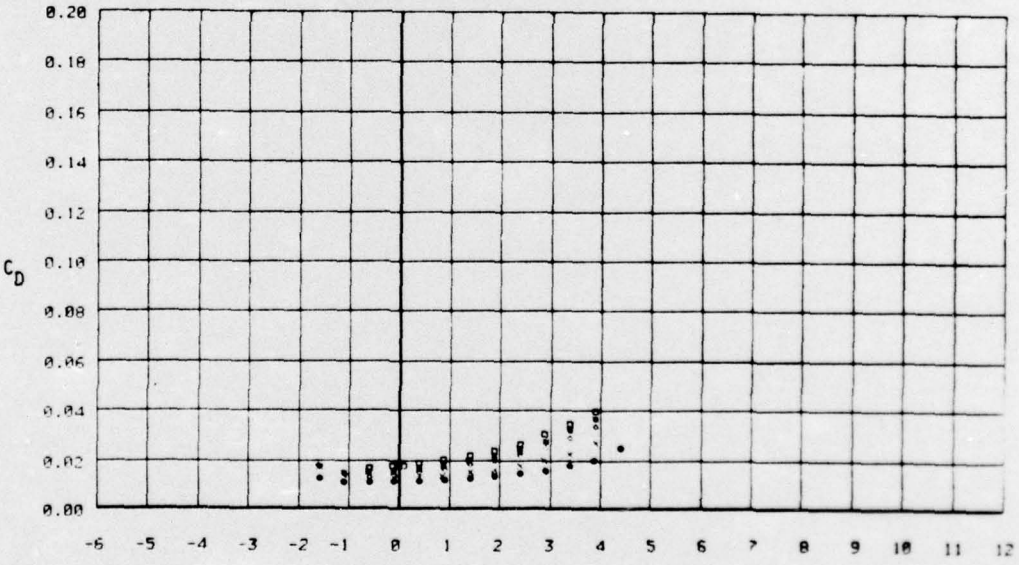

DRAG COEFFICIENT VS. PITCH ANGLE

RUN	SYMBOL	VELOCITY	h/c	LOCATION
69	•	45.6 KTS	1/2	CARRIAGE 5
90	×	45.3 KTS	3/4	CARRIAGE 5
14	◇	45.5 KTS	1	CARRIAGE 5
76	■	45.4 KTS	1 1/2	CARRIAGE 5
83	□	45.3 KTS	2	CARRIAGE 5

DTNSRDC ISSUES THREE TYPES OF REPORTS

(1) DTNSRDC REPORTS, A FORMAL SERIES PUBLISHING INFORMATION OF PERMANENT TECHNICAL VALUE, DESIGNATED BY A SERIAL REPORT NUMBER

(2) DEPARTMENTAL REPORTS, A SEMIFORMAL SERIES, RECORDING INFORMATION OF A PRELIMINARY OR TEMPORARY NATURE, OR OF LIMITED INTEREST OR SIGNIFICANCE, CARRYING A DEPARTMENTAL ALPHANUMERIC IDENTIFICATION

(3) TECHNICAL MEMORANDA, AN INFORMAL SERIES, USUALLY INTERNAL WORKING PAPERS OR DIRECT REPORTS TO SPONSORS, NUMBERED AS TM SERIES REPORTS; NOT FOR GENERAL DISTRIBUTION.